The Dissertation Committee for Christopher James Wilson Certifies that this is the approved version of the following dissertation:

The Acoustic Ecology of Submerged Macrophytes

Committee:

Kenneth H. Dunton, Supervisor

Preston S. Wilson, Co-Supervisor

Lee A. Fuiman

James W. McClelland

G. Christopher Shank

The Acoustic Ecology of Submerged Macrophytes

by

Christopher James Wilson, B.S.

Dissertation

Presented to the Faculty of the Graduate School of

The University of Texas at Austin

in Partial Fulfillment

of the Requirements

for the Degree of

Doctor of Philosophy

The University of Texas at Austin

December 2011

Acknowledgements

The completion of this dissertation was not possible without the help from family, friends and colleagues. I would like to thank Kim Jackson, Chad Greene, Kevin Lee, Nathan Mctigue, Travis Bartholomew, Joseph Stachelek, Susan Schonberg, Kelly Darnell and Dana Sjostrom for all of their help with field and laboratory experiments. My committee members each improved the quality of this dissertation and I am truly appreciative of the time spent by Christopher Shank, Jim McClelland and Lee Fuiman reviewing this body of work. Finally, I would like to express my sincere appreciation for Ken Dunton and Preston Wilson for their advice and patience while acting as my supervisors.

The Acoustic Ecology of Submerged Macrophytes

Christopher James Wilson, Ph.D.

The University of Texas at Austin, 2011

Supervisors: Kenneth H. Dunton and Preston S. Wilson

Underwater acoustics has recently emerged as a viable tool for assessing ecosystem health and exploring the estuarine soundscape. Recent acoustic surveys have mapped distributions of both seagrass meadows and kelp forests, and scientists are currently developing remote sensing capabilities to improve ecological assessments of these communities. Furthermore, researchers are beginning to focus on the propagation and ecological significance of bioacoustic signals within estuarine landscapes. The research presented here includes a thorough examination of the interaction of acoustic energy and macrophyte tissue as it pertains to habitat assessment and ecosystem function. Modeling experiments investigated the interaction of acoustic energy and submerged macrophyte tissue. Both seagrasses and kelp exhibited a similar acoustic response by increasing the acoustic compressibility of a seawater medium. The increase in acoustic compressibility was driven by free-gas volumes contained within the macrophyte tissue. Interestingly, the tissue served to limit the acoustic compressibility of the gas volume below the magnitude predicted by effective medium models. Separate inquiries of high-frequency sound propagation and the seagrass canopy revealed a significant temporal

component to acoustic transmission. Specifically, sound transmission throughout a seagrass canopy was altered by the formation of free gas bubbles and the pressurization of aerenchyma channels, which was mediated by photosynthesis. The photosynthetic controls on sound propagation were species-specific, and patterns of acoustic transmission provided a reasonable proxy for gross primary production in *Syringodium filiforme* plants. Finally, the interaction of sound energy and submerged macrophytes appears to have important ecological implications. This research suggests that seagrass meadows scatter high-frequency sound energy and provide an acoustic refuge to fish from marine mammal predators. This refuge is highly seasonal, specific to different seagrass species and dependent on the abundance of above-ground biomass. Seagrasses also may influence the transmission of low-frequency sounds used by soniferous fish. Propagation characteristics of low-frequency sounds are highly dependent on frequency and result in differential transmission distances among individual fish species. It is clear from this body of work that submerged macrophytes are an important feature of the underwater soundscape. Future research should continue to exploit this feature for remote sensing purposes and examine its ecological significance.

Table of Contents

List of Tables

List of Figures

Introduction

The interaction of sound energy and submerged vegetation has become an emergent trend in the field of underwater acoustics. Most recent work has focused on improving our knowledge of the acoustic characteristics of submerged macrophytes in order to advance underwater mapping and remote sensing capabilities. Although remotely assessing the health of macrophyte communities is clearly an important application, there has been little emphasis on the emerging ecological significance of sound attenuation by macrophytes in the estuarine soundscape. The research presented here attempts to address the unique acoustic characteristics of submerged macrophytes in relation to their functional importance as estuarine habitat.

Acoustic mapping studies have repeatedly demonstrated that submerged macrophytes scatter and absorb acoustic energy. However, the physical mechanisms responsible for attenuating sound energy are poorly understood. To address this deficiency, the first two chapters of this dissertation attempt to model the acoustic response of seagrass leaves and kelp fronds in a one-dimensional acoustic resonator. Results of these chapters indicate that the air contained within seagrass leaves and kelp fronds increases the acoustic compressibility of a seawater medium, which is modified by the macrophyte tissue. The information derived in each of these two chapters will help guide future acoustic modeling efforts of seagrass meadows and kelp forests.

The third chapter of this dissertation describes the importance of photosynthesis and respiration on sound transmission throughout a seagrass leaf canopy. Unlike the controlled laboratory conditions implemented in the first two chapters, the third chapter used an outdoor experimental tank, which introduced natural variation in the form of sunlight. Results from this chapter indicate that sound transmission throughout a seagrass canopy varies on circadian cycles

mediated by plant photosynthesis and respiration. Patterns in acoustic transmission differ between seagrass species and both leaf pressurization and bubble formation appear to modify this response.

The final chapter of this dissertation examined the influence of seagrass meadows on the propagation of biologically-relevant segments of the acoustic spectrum. The research in this chapter focused entirely on empirical relationships obtained in seasonal field surveys of acoustic transmission in bare and vegetated substrates. Seagrass meadows altered the transmission of acoustic energy in frequencies relevant to both dolphin echolocation and fish communication. Transmission characteristics differed by acoustic frequency, substrate type and by season. The results of this study suggest that seagrasses may provide a seasonal acoustic refuge to fish from marine mammal predators.

The underwater soundscape has only recently gained popularity as a prominent ecological feature of submerged habitats. While research on the perception and utilization of sound by marine organisms is becoming more common, there is a current lack of knowledge about how biological sounds interact with physical features of the environment. The following dissertation demonstrates that submerged macrophytes provide both a physical and biological element that interacts with sound energy. Furthermore, these communities represent a dominant feature of the estuarine soundscape.

Chapter 1

Seagrass leaves in 3-D: Using computed tomography and low-frequency acoustics to investigate the material properties of seagrass tissue.

Abstract

As a preliminary step toward development of a predictive model of sound speed in water containing seagrass, the acoustic and material properties of leaf tissue for *Thalassia testudinum*, *Syringodium filiforme* and *Halodule wrightii* were assessed using a one-dimensional acoustic resonator and computed tomography imagery. The high-resolution three-dimensional imagery provided valuable information about leaf morphology and produced precise estimates for plant tissue volume and the volume of air contained within the aerenchyma of the plant tissue, which in turn yielded measurements of the plant tissue density (*Thalassia* = 1032.34 ± 115.42 kg·m^{-3}; *Syringodium* = 664.17 ± 10.38 kg·m^{-3}; *Halodule* = 964.96 ± 21.72 kg·m^{-3}). The acoustic resonator technique was used to investigate the species-specific and biomass-dependent differences in the propagation of sound through seawater containing seagrass leaves in the 0.2 kHz to10 kHz frequency band. The three species each caused a unique decrease in sound speed with an increase in biomass. The values for leaf air volume, tissue volume and tissue density were then combined with the results of the acoustic experiments and an effective medium acoustic model to determine the acoustic compressibility of the leaves. Further implementation of two effective medium models failed to yield measurements of leaf tissue compressibility. Failure of these models indicates that tissue elasticity and structure must be considered for a complete understanding of acoustic propagation in seagrass meadows.

Introduction

Seagrasses are vascular plants that form extensive meadows through both vegetative lateral growth and sexual reproduction (Olesen et al. 2004). These meadows provide a suite of ecosystem functions including valuable nursery habitats, sediment stabilization, and shoreline protection through wave attenuation (Heck and Thoman 1984; Fonseca and Cahalan 1992). Current models predict that worldwide distributions of seagrass meadows are in a state of decline and that the future of these ecosystems is further affected by global climate change (Short 1999; Duarte 2002). Recent studies have exploited satellite and aerial imagery in an effort to document changes in the areal coverage of seagrass meadows over time (Ferwerda 2007; Fletcher 2009). Similarly, a study by Kutser et al. (2007) attempted to further the capability of underwater photography by exploring the relationship between the coverage of seagrasses observed in photographs and plant biomass. Despite advancements in the photographic interpretation of seagrass coverage, it is advantageous to continue to develop novel methods for remotely assessing the health and condition of seagrass meadows over time.

Numerous studies utilizing side scan sonar in shallow waters have shown that seagrasses provide a high degree of acoustic backscatter when compared to other benthic substrates (Pasqualini et al. 2000; Mulhearn 2001). This backscatter can provide the means to map a seagrass bed similar to the way that aerial photography is used to plot the presence of areal seagrass cover. The use of multi-beam sonar further improves these mapping capabilities through the quantification of plant canopy height and plant occupied volume obtained from three-dimensional imagery (Komatsu et al. 2003). The same acoustic signal that provides a means for mapping vegetation also serves to hinder mine hunting efforts. Mine hunting studies have shown that when a target mine is placed within a seagrass bed, the location of the mine is acoustically

undetectable from the backscatter provided by the submerged vegetation (McCarthy and Sabol 2000). It is currently hypothesized that the acoustic backscatter observed over seagrasses is largely attributed to the free gas bubbles located on the surface of the plants as well air found within the tissues (Hermand et al. 1998; Hermand 2004).

The gas created by seagrasses during photosynthesis can either dissolve directly into the water column or form numerous bubbles that remain attached to the surface of the plant (Philips and Menez 1988). In addition to the export of oxygen to the outside of the plant, seagrasses also have the ability to transport gases within their tissues (Caffrey and Kemp 1991). Leaf and rhizome tissues are imbedded with large air-filled canals called aerenchyma, which aid in the transport of these gases and allow for the diffusion of oxygen into surrounding sediments. By oxygenating the sediments, the plants limit concentrations of sulfides that are toxic to the plant tissue (Kemp and Murray 1986).

In order to provide a better means for remotely assessing the health of a seagrass ecosystem and to improve mine hunting capabilities, there is clearly a need to better understand the propagation of sound through a seagrass bed. Wilson and Dunton (2009) compared the results of a set of low-frequency acoustic experiments on seagrass tissue to predictions based on Wood's equation for a two-phase medium (Wood 1930). Because the air within the aerenchyma is hypothesized to create the acoustic backscatter observed over seagrass beds, this model only considered the gas content within the plant. A one-dimensional acoustic resonator technique was utilized in the frequency range of 0.5 kHz to 2.5 kHz to assess the acoustic properties of leaf and rhizome tissue for *Halodule wrightii*, *Thalassia testudinum*, and *Syringodium filiforme*. Independent measurements of biomass and gas content estimates were obtained from microscopic imagery and then compared to the results of the acoustic experiments. Wilson and

Dunton (2009) were able to show that the acoustic response of the plant tissue was dependent on species, tissue type, and amount of biomass contained within the resonator. However, Wood's equation based on gas content alone was not sufficient in explaining the acoustic behavior of the plants.

Since gas content alone cannot predict the acoustic behavior of seagrasses, it is important to address the acoustic properties of the plant tissue itself. To investigate the interaction between leaf tissue and the volume of gas within a leaf, a one-dimensional acoustic resonator was used in combination with high-resolution three-dimensional imagery to identify the effect of plant tissue and leaf gas volume on sound propagation. Measured sound speeds were used along with a two-component effective medium model to determine the acoustic compressibility of the leaves of *T. testudinum*, *S. filiforme* and *H. wrightii*. Two different implementations of a three-component effective medium model failed to determine the acoustic compressibilty of the leaf tissue itself.

Materials and Methods

All tissue samples for these experiments were collected from estuaries local to the University of Texas Marine Science Institute (UTMSI) in Port Aransas, Texas. Seagrass samples were collected by hand and brought back to UTMSI in seawater obtained *in situ*. Samples were then stored at the institute in buckets of filtered and aerated seawater from the Gulf of Mexico for no longer than 48 hours prior to the experiments.

All acoustic measurements utilized a one-dimensional acoustic resonator made from glass tubing of circular cross section 64.0 mm outer diameter and 4.9 mm wall thickness with a length of 454 mm. The frequency range of interest in these experiments was 0.2 kHz to 10 kHz. Acoustic excitation was generated with an electromechanical shaker fitted with an aluminum

piston (Figure.1.1). Gaussian white noise was produced by a vector signal analyzer (VSA) in the frequency range of interest. This noise created standing acoustic waves within the resonator, with the air-water interface at the top of the resonator and a block of closed-cell of foam at the bottom of the resonator serving as pressure-release boundaries. Acoustic pressure spectra were obtained using a miniature hydrophone, with signal conditioning provided by a charge amplifier and digitization by the VSA, as described by Wilson and Dunton (2009). The system's resonance frequencies coincide with the peaks of the pressure spectra, and these were used to calculate the sound speed c within the resonator using Eq. (1), where L is the water column length and f_n is the n-th resonance peak of the spectra:

$$f_n = \left[\frac{c}{2L}\right] n. \tag{1}$$

The term in brackets is the slope of a linear function relating the measured resonance frequencies f_n to the mode number n. A least-squares linear fit of the measured resonance frequencies yields the slope, from which the sound speed c was calculated. This method was used because it minimizes the effect of sample inhomogeniety, which tends to perturb the resonance frequencies from the values they would take in a perfectly homogeneous system. The acoustic velocity inside a pipe is reduced relative to its velocity in an unconfined space, as shown by Lafleur and Shields (1995). The measured acoustic velocities reported here were corrected for this effect using the technique described in Wilson and Dunton (2009) and all reported sound speeds, referred to as c_{exp} , correspond to the sound speed that would be observed in nature.

For all species, the length and mass of each leaf was obtained before it was added to the resonator. First, a seawater spectra was obtained with no leaves present, and the sound speed of seawater within the resonator was determined. Next, leaves were added one at a time for all species until there was a noticeable shift in resonance frequencies within the resonator, which in

turn indicated a change in sound speed. For *Thalassia* and *Syringodium*, three leaves were sufficient to produce a noticeable shift in resonance frequencies compared to seawater. However, *Halodule* required a total of nine leaves within the resonator in order to provide an analogous shift in resonance frequencies. Replicate resonator experiments were not completed as the focus of this study was to pair acoustic experiments with high resolution imagery of leaf tissue samples. Following the resonator measurements, the three *Syringodium* and *Thalassia* leaves and nine *Halodule* leaves were immediately brought to a computed tomography (CT) scanner and were scanned within 24 hours.

Seagrass leaf samples for each species were coiled and placed into a vial prior to the CT scan. The coiling of the seagrass leaves reduced the overall scanning volume, which reduced the scanning time and increased the resolution of the scan. Since this study was concerned only with the overall volumes of internal gas and leaf tissue, the coiling and subsequent orientation of the leaves within the vial was not important. The CT scanner produced a series of sequential two-dimensional 16-bit JPEG images that each represented a three-dimensional "slice" of the plant specimen. The height of this slice corresponded to the predetermined distance between two consecutive images. Each of these image slices resembled and was treated as a microscopic cross section during image analysis (Figure 1.2). From these cross-sections, the area of the image corresponding to either plant tissue or air space was calculated using three particular gray-scale values of the image. These three gray-scale values were used in order to encompass the range of possible pixel values within the image corresponding to the material of interest and to produce error estimates of the photographic analysis. The resulting area of the plant tissue or air space was then multiplied by the height of the image slice in order to calculate the volume of each material. This process was repeated for each image slice in the CT scan for each of the three

seagrass species. The sum of the calculated volumes for each slice was combined to produce an overall material volume for each specimen. Finally, the plant tissue volume estimates were combined with the measurements of the mass of the tissue in order to render an estimate of the plant tissue density for each of the three seagrass species.

Acoustic Models

The acoustic models used here were based on an effective medium model originally proposed by Wood (1930) to describe low-frequency acoustic propagation in multiphase material including gaseous, liquid and solid components. The effective acoustic sound speed c_{eff} in the multi-component mixture, which is also c_{exp} , the sound speed measured here after correction for the elastic waveguide effect, is given by

$$\frac{1}{c_{\text{eff}}^2} = \frac{1}{c_{\text{exp}}^2} = \left[\sum_i \phi_i \kappa_i\right]\left[\sum_i \phi_i \rho_i\right] = \left[\sum_i \frac{\phi_i}{c_i^2 \rho_i}\right]\left[\sum_i \phi_i \rho_i\right], \tag{2}$$

and

$$\sum_i \phi_i = 1, \tag{3}$$

where κ_i, c_i , ρ_i , and ϕ_i represent the compressibility, the intrinsic sound speed, the density and the volume fraction of phase or component *i.* Compressibility is the inverse of the bulk modulus and is used here for mathematical convenience. The right-most equality in Eq. (2) arises because the acoustic sound speed is defined as $c = \sqrt{1/(\kappa\rho)}$ (Kinsler, 2000). Effective medium models are attractive because they do not require knowledge of the shapes or exact locations of the various material phases or components within the mixture. Only knowledge of the intrinsic acoustic material properties of each component and their volume fractions are required. For an effective medium model to be valid, the components must be distributed homogeneously

throughout the mixture and the effective acoustic wavelength must be large compared to the physical size of all mixture components. The name effective medium is used because the multi-component material behaves effectively the same as a hypothetical homogeneous material with the same acoustic properties. Alternatively, if the mixture sound speed is known, then one unknown input parameter can be determined from Eq. (2), given knowledge of all the remaining parameters. The latter was used here to determine the effective compressibility of the seagrass leaves (tissue + air). See Figure 1.3 for a flow chart that illustrates the three implementations of Eq. (2) that were used here. In this work, photosynthetic bubbles external to the plants were excluded. No visible air bubbles were attached to leaves or present in the water.

Results

Computed Tomography

The *Syringodium* leaves used in this experiment had the highest tissue volume (1.28 ±0.02 cm^3) and air volume (0.29 ±0.02 cm^3), followed by *Thalassia* (1.26 ±0.14 cm^3; 0.093 ±0.084 cm^3) and *Halodule* (0.31 ±0.01 cm^3; 0.036 ±0.002 cm^3) (Table1). *Thalassia* leaves had the highest wet mass when compared to *Syringodium* and *Halodule*. *Syringodium* leaves had the highest leaf porosity among the three species (~18.88%) while *Thalassia* had the lowest leaf porosity (~6.90%). Finally, *Thalassia* leaves had the highest tissue density (1032.34 ± 115.42 $kg \cdot m^{-3}$) compared to *Halodule* leaves (964.96 ± 21.72 $kg \cdot m^{-3}$) and *Syringodium* leaves (664.17 ± 10.38 $kg \cdot m^{-3}$).

Low Frequency Resonator Experiments

All three species of seagrass caused a decrease in sound speed from seawater with an increase in leaf number and total biomass within the resonator (Figure 1.4). *Thalassia* had the largest overall decrease in sound speed per number of leaves added to the resonator. However, *Halodule* showed the largest decrease in sound speed per unit wet mass added into the resonator. Since a single *Halodule* leaf is much smaller than a *Thalassia* or *Syringodium* leaf, the addition of *Halodule* leaves did not produce a decrease in resonator sound speeds comparable to the other two species on a per leaf basis. Despite the measurement containing the largest overall volume of tissue and air, *Syringodium* leaves still caused the smallest decrease in sound speed within the resonator when compared to the other two species. In both the *Thalassia* and *Syringodium* experiments, there was a sharp decline in sound speed within the resonator with the addition of the first leaf, which was followed by a more gradual decline in sound speed with each additional leaf. This was not the same for *Halodule*, as the rate of decrease in sound speed only increased in magnitude with the addition of plant material into the resonator.

Model Results

Wilson and Dunton (2009) used a two-component (air/water) version of Eq. (2) and their measurements to show that the acoustic properties of seagrass tissue and its air content both contributed to the effective sound speed of seagrass plants in water, but they could go no further because they lacked sufficient knowledge of the total plant tissue volume and the total enclosed air volume. In the present work, those volumes were measured, and hence Eq. (2) was used to determine the effective compressibility of seagrass leaves (tissue + enclosed air), under the assumption that the leaves themselves behave as an effective medium, as shown in Figure 1.3(a). The acoustic measurements and the CT scan analysis yielded all the required input parameters for Eq. (2), except for the seagrass leaf compressibility κ_{leaves}. The total mass density of the

leaves ρ_{leaves} was calculated using the CT-derived air and tissue volume, the measured mass of the tissue, and the known density of air. Equation (2) was then solved for κ_{leaves} and the corresponding sound speed c_{leaves}. These results are presented in Table 1.2.

Two other implementations of Eq. 2 were utilized, in attempts to extract the compressibility of the leaf tissue itself, which remained unknown even in light of the above results. These models were not successful, but they are described here for completeness and to guide future model development. If one assumes all three phases (water, tissue, air) are independent and homogenously distributed, then Eq. 2 can be solved directly for the tissue compressibility, as shown in Figure 1.3(b). This was done for all three species and in each case, a negative compressibility was found. This represents a non-physical result, and hence indicates that a three-phase effective medium model as implemented by Eq. (2) is not the correct model for sound propagation through seagrass leaves in water. In retrospect, this result is expected. Although the seagrass leaves were homogenously distributed throughout the length of the water-filled resonator in this work, the air phase is entirely contained within the seagrass tissue, and hence is not homogenously distributed throughout the medium. Further, compression of the leaf does not yield independent compression of both the tissue and the air within, violating two of the assumptions governing Eq. 2. (Povey, 1997).

The second attempt to extract the leaf tissue properties involved using a two-component version of Eq. (2), with air and tissue components to describe the acoustic behavior of the leaves. This was embedded within another two-component version of Eq. (2), describing the water and leaf mixture, as shown in Figure 1.3(c). Again, the only unknown in this model is the tissue compressibility, and the model was solved for the tissue compressibility. This time, in all three species, an imaginary number was found, which again is a non-physical result that indicates the

model is not appropriate. Further examination indicates that the measured sound speeds c_{exp} are too high to be described by the nested pair of two-component models for the volume fractions present and with air as one of the materials. This indicates that tissue structure, in addition to tissue elasticity and volume fraction is contributing to the observed sound speed. This means that an effective medium model based on fluid behavior, as has been used up to this point, will not be able to describe the acoustic properties of seagrass tissue. A more complex model that accounts for the geometry of the tissue will have to be included in the model. Further, the tissue material will likely have to be modeled as an elastic solid. The latter two requirements greatly increase the complexity of the model. Idealize shapes, such as a hollow cylinder for *Syringodium*, may potentially suffice, but to capture the true porous geometry of these tissues, a Finite Element (FE) numerical model will be required. One could use the presently-measured leaf compressibility, as inferred by the model in Figure 1.3(a), and an FE model that related tissue elasticity and geometry to effective leaf compressibility to determine the elastic properties of the tissue.

Discussion

Acoustic Modeling

Similar to previous experiments by Wilson and Dunton in 2009, this study showed that the addition of seagrass to seawater within an acoustic resonator causes a decrease in the effective sound speed of the mixture. Furthermore, this decrease in sound speed is dependent on overall biomass and is unique among the three species of seagrass used in this experiment. The use of imagery from the CT scans has helped to further the understanding of the relationship between leaf morphology and the acoustic properties of seagrasses as it was possible to obtain

precise measurements of the materials comprising a seagrass leaf. These material values provided the means to successfully calculate the effective compliance of a leaf structure κ_{leaves} from the model described in Figure 1.3(a) as a combination of the components of plant tissue and internal gas volume (Table 1.2). However, the candidate models described in Figure 1.3(b) and (c), which attempt to describe the compressibility of the plant tissue independent of the internal gas volume, yielded non-physical results and were unsuccessful in producing values for plant tissue compliance.

The shortcomings of the two failed acoustic models provide a valuable insight into the acoustic behavior of seagrasses. For instance, the failure of Wood's three-medium model, Figure 1.3(b), provides evidence that seagrasses do not acoustically behave as free gas bubbles nor as a dispersed medium throughout seawater. Seagrasses instead behave acoustically as a finite structure on the benthos. The results of the nested two-phase model, Figure 1.3(c), also provide evidence that the combination of the seagrass tissue and air within the aerenchyma are not acoustically independent from one another. Tissue structure must play a role.

It is interesting to note the contradiction between observed sound speeds and the outcome of the models in Figure 1.3(b) and (c), in light of the individual leaf morphologies, the volume of air contained within the seagrass leaves and the density of the plant tissue. For example, *Syringodium* leaves contained the highest overall volume of air within the aerenchyma and the plant tissue had the lowest density compared to the other two species. One might think that the acoustic models would therefore predict *Syringodium* leaves to have the highest acoustic contrast to that of seawater, yet this species had the lowest acoustic contrast to seawater. Similarly, *Thalassia* leaves had a much higher tissue density and contained a smaller volume of air within the aerenchyma when compared to *Syringodium*, but *Thalassia* had a higher degree of acoustic

contrast to seawater compared to *Syringodium*. Because each of the two acoustic models, Figure 1.3(b) and (c), stress the importance of both air volume and material density of dispersed mediums, the models were unable to accurately describe the sound speed of the plant tissue. The present results corroborate a similar finding reported by Wilson and Dunton (2009).

The failure of the models in Figures 1.3(b) and (c) is most likely due to the importance of the shape of individual seagrass leaves and the inherent stiffness of the tissue structure. When considering the cross-sectional shape of the individual seagrass leaves, the round *Syringodium* and *Halodule* leaves are more resistant to mechanical expansion due to inherent hoop stress when compared to the flat elongated cross-section of *Thalassia*. Also, tissue densities of *Syringodium* and *Halodule* leaves were lower than the density of the surrounding seawater while the tissue density of *Thalassia* leaves mirrors that of seawater. For the *Syringodium* and *Halodule* leaves to keep their shape in a denser medium, the tissue must be sufficiently stiff. This trait is not necessarily required of *Thalassia* leaves, which shares the density of the surrounding water. As a result, the tissue stiffness required to maintain static shape in *Syringodium* and *Halodule* is also more resistant to the mechanical expansion experienced during acoustic excitation as compared to *Thalassia* leaves, which explains the acoustic behavior observed here.

Computed Tomography Imagery

This paper is the first to present high-resolution three-dimensional imagery of seagrass tissue using computed tomography. Although the final analysis of CT scans is very similar to microscopic image analysis, the use of CT has a suite of advantages when compared to the mechanical cross sections used in microscopy. CT imagery offers the same opportunity to measure aspects of leaf morphology without the destruction of the plant material, which allows

for short-term preservation of the plant samples. CT imagery also allows the investigator to examine multiple plant specimens in their entirety as opposed to microscopy, which only allows for a representative number of mechanical slices. In this study, three *Syringodium* and *Thalassia* leaves and nine *Halodule* leaves were scanned and analyzed at one time. This significantly reduced the time required for precise measurements of leaf morphology. Finally, the use of CT imagery may reduce error in measurement through three-dimensional reconstruction of the plant tissue sample. Each image slice recorded during a CT scan is in the same three-dimensional plane and the distance between sequential slices is automated and predetermined by the investigator. The success of the CT scan is then easily validated by combining sequential image slices to form a three-dimensional rendering of the plant tissue (Figure 1.5). For the measurements in this study, the three dimensional validation of the coiled seagrass leaves served to eliminate any pixels selected incorrectly during the processing of the two-dimensional image slices. This was particularly useful in eliminating the pixels of any air spaces observed between coiled leaves. The ease of retrieving and validating these image slices is a drastic improvement over the use of mechanical tissue slicers and microscopic imagery.

Implications

Similar to results published by Wilson and Dunton in 2009, this study showed that *Thalassia*, *Syringodium*, and *Halodule* leaves are acoustically unique from one another and that the acoustic contrast of these plants to seawater is dependent on the amount of biomass present for each of the three species. New here is the determination of the effective acoustic compressibility (Table 1.2) of the leaf structure of each species, for waves propagating in the vertical direction (along the long axes of the leaves). Inversion of the models in Figures 1.3(b)

and (c) for the tissue compressibility failed, indicating that in addition to knowledge of tissue density and volume, knowledge of the tissue structure is required for the development of an accurate acoustic model of sound propagation in water and seagrasses. Further development of an accurate acoustic model will improve underwater mine detection and the capabilities for acoustically mapping seagrass beds. This work did not address the effect of primary productivity on acoustic measurements as experiments were conducted in sufficiently low light conditions to inhibit photosynthesis. However, future studies should investigate the role of photosynthesis and gas production rates on the propagation of sound through water containing seagrass. Finally, this study is the first to present estimates of the plant tissue densities of *T. testudinum*, *S. filiforme*, and *H. wrightii*.

Acknowledgments

The authors would like to thank Kim Jackson for her help in plant tissue collection and the High-Resolution X-ray Computed Tomography Facility of the University of Texas at Austin for their help in data acquisition. Partial support for this study was provided by the University of Texas Applied Research Laboratories.

References

Caffrey, J.M. and W. M. Kemp, 1991. Seasonal and spatial patterns of oxygen production, respiration and root rhizome release in *Potamogeton perfoliatus* L. and *Zostera marina* L. *Aquat. Bot*., Vol. 40, pp. 109–128.

Duarte, C.M., 2002. The future of seagrass meadows. Environ. Conserv., Vol. 29, pp. 192–206.

Ferwerda, J.G., J. de Leeuw, C. Atzberger, and Z. Vekerdy, 2007. Satellite-based monitoring of tropical seagrass vegetation: current techniques and future developments. *Hydrobiologia*, Vol. 591, pp. 59–71.

Fletcher, R.S., W. Pulich Jr., and B. Hardegree, 2009. A semiautomated approach for monitoring landscape changes in Texas seagrass beds from aerial photography. *J. Coast. Res*., Vol. 25, pp. 500–506.

Fonseca, M.S. and J. A. Cahalan, 1992. A preliminary evaluation of wave attenuation by 4 species of seagrass. *Est. Coastal Shelf Sci*., Vol. 35, pp. 565–576.

Heck, K.L. and T. A. Thoman, 1984. The nursery role of seagrass meadows in the upper and lower reaches of the Chesapeake Bay. *Estuaries*, Vol. 7, pp. 70–92.

Hermand, J.P., P. Nascetti, F. Cinelli, 1998. Inversion of acoustic waveguide propagation features to measure oxygen synthesis by *Posidonia oceanica*. *Proceedings of the Oceans '98 IEEE/OES Conference*. Vol. 2, pp. 919-926.

Hermand, J.P., 2004. Handbook of Scaling Methods in Aquatic Ecology: Measurement, Analysis, Simulation. CRC, Boca Raton, Fl, pp. 65–96.

Kemp, W.M. and L. Murray, 1986. Oxygen release from roots of the submersed macrophyte *Potamogeton perfoliatus* L.: Regulating factors and ecological implications. *Aquat. Bot*., Vol. 26, pp. 271–283.

Kinsler, L. E., Frey, A. R., Coppens, A. B. and Sanders, J. V., 2000. Fundamentals of Acoustics. : Wiley, New York.

Komatsu, T., C. Igarashi, K. Tatsukawa, S. Sultana, Y. Matsuoka, and S. Harada, 2003. Use of multi-beam sonar to map seagrass beds in Otsuchi Bay on the Sanriku Coast of Japan. *Aquat. Living Resour.*, Vol. 16, pp. 223–230.

Kutser, T., E. Vahtmae, C.M. Roelfsema, and L. Metsamaa, 2007. Photo-library method for mapping seagrass biomass. *Est. Coastal Shelf Sci*., Vol. 75, pp. 559–563.

Lafleur, L. D. and Shields, F. D., 1995. Low-frequency propagation modes in a liquid-filled elastic tube waveguide. *J. Acoust. Soc. Am.*, Vol. 97, pp. 1435–1445.

McCarthy, E.M. and B. Sabol, "Acoustic characterization of submerged aquatic vegetation: Military and environmental monitoring applications. *Proceedings of OCEANS 2000 MTS/IEEE Conference and Exhibition*, Vol. 3, pp. 1957–1961.

Mulhearn, P.J., 2001. Mapping seabed vegetation with sidescan sonar. *DSTO Report No.TN-0381, Defense Science and Technology Organization*, Australia.

Olesen, B., N. Marba, C. M. Duarte, 2004. Recolonization dynamics in a mixed seagrass meadow: The role of clonal versus sexual processes. *Estuaries*, Vol. 27, pp. 770–780.

Pasqualini, V., P. Clabaut, G. Pergent, L. Benyoussef, and C. Pergent-Martini, 2000. Contribution of side scan sonar to the management of Mediterranean littoral ecosystems. *Int. J. Remote Sens.*, Vol. 21, pp. 367–378.

Phillips, R.C. and E. G. Menez, 1988. Seagrasses . Smithsonian Institution Press, Washington, DC.

Povey, M. J. W., 1997. Ultrasonic Techniques for Fluids Characterization. Academic Press,London.

Short, F.T. and H.A. Neckles, 1999. The effects of global climate change on seagrasses. *Aquat. Bot*., Vol. 63, pp. 169–196.

Wilson, P.S. and K. Dunton, 2009. Laboratory investigation of the acoustic response of seagrass tissue in the frequency band of 0.5–2.5 kHz. *J. Acoust. Soc. Am*., Vol. 125, pp. 1951–1959.

Wood, A. B., 1930. A Textbook of Sound. Macmillan, New York, first edition.

Figure 1.1.

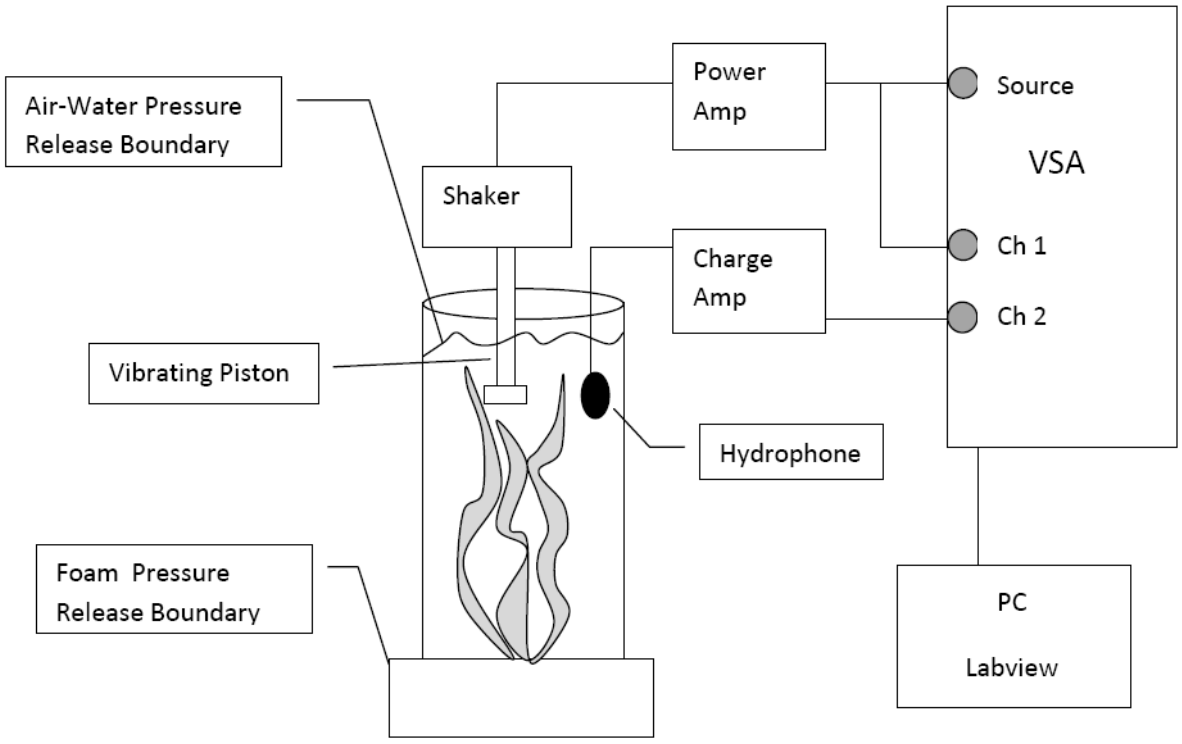

Figure 1.1. A schematic of the one-dimensional acoustic resonator apparatus is shown.

Figure 1.2a.

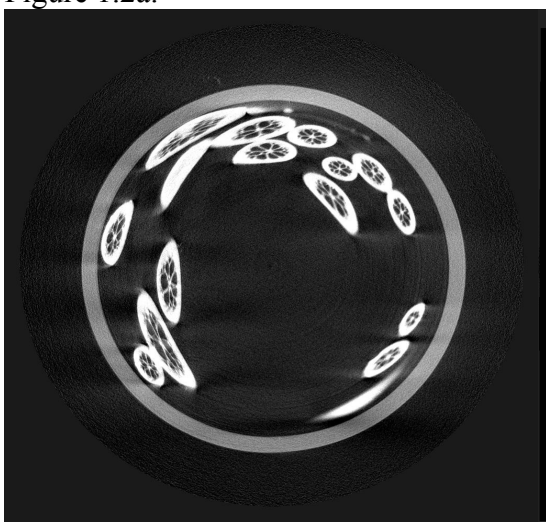

Figure 1.2b.

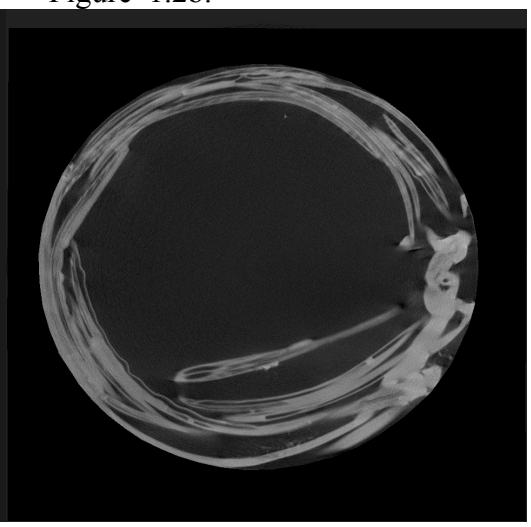

Figure 1.2c.

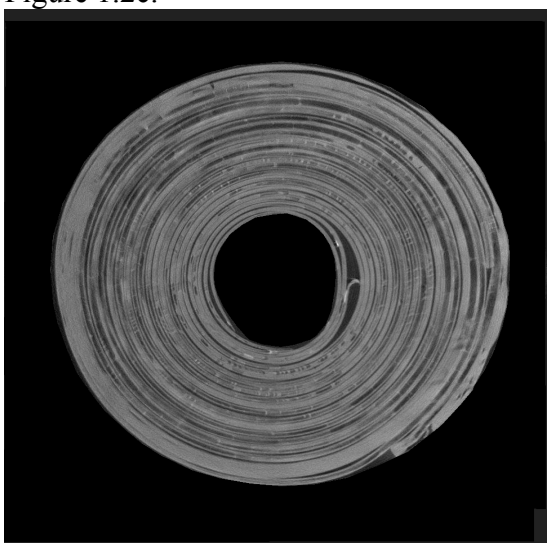

Figure 1.2. An image slice from a CT scan for a) *Syringodium filiforme* b) *Halodule wrightii* and c) *Thalassia testudinum*. The grey circle on the edge of 2a is the sample container. The light grey pixels in each image represent plant tissue and the dark grey pixels represent air spaces.

Figure 1.3.

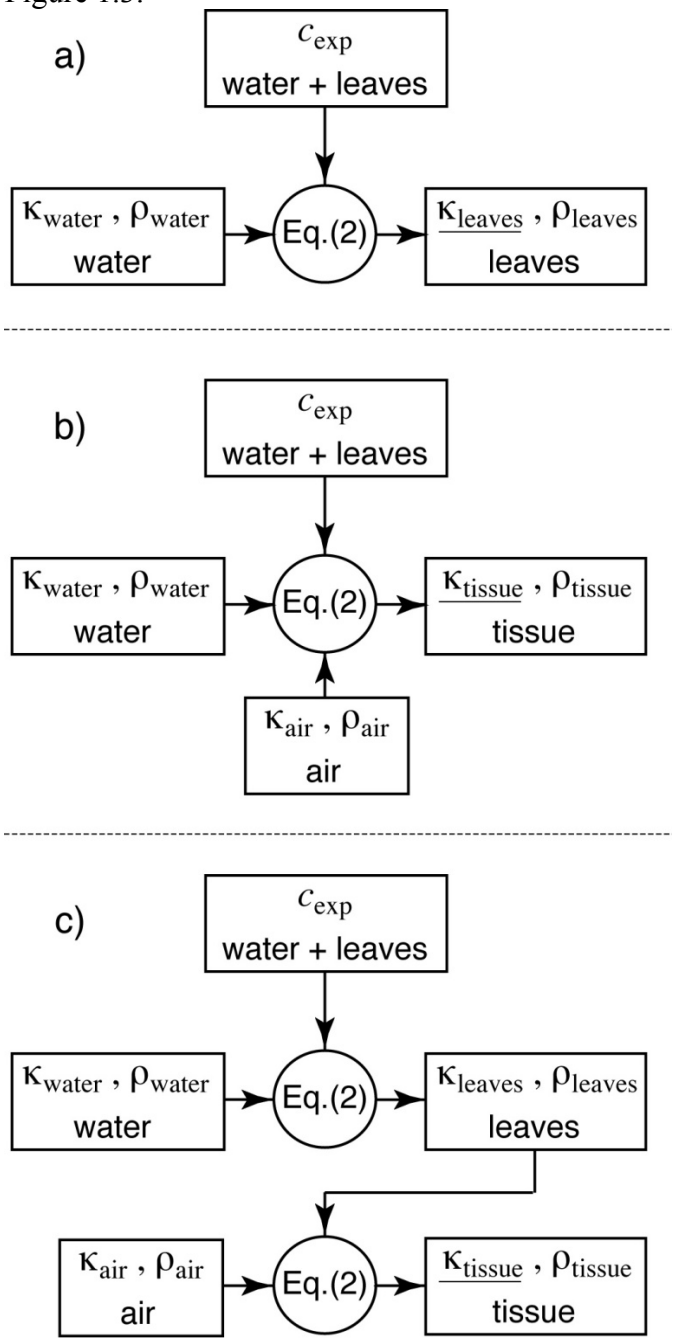

Figure 1.3. The flow charts illustrate the different implementations of Eq. (2) to describe the effective sound speed in water containing seagrass leaves. For each implementation, the model attempted to describe the only unknown term, which is underlined in each section. Scheme (a) was successfully inverted for the leaf compressibility κ_{leaves} of all three species. Schemes (b) and (c) could not describe the observed sound speeds of the plant tissue κ_{tissue} for any of the species.

Figure 1.4a.

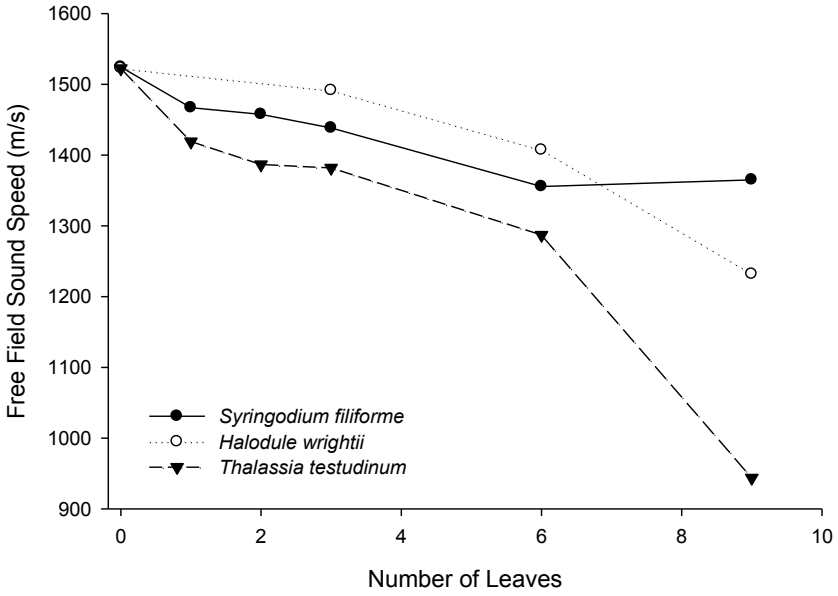

Figure 1.4b.

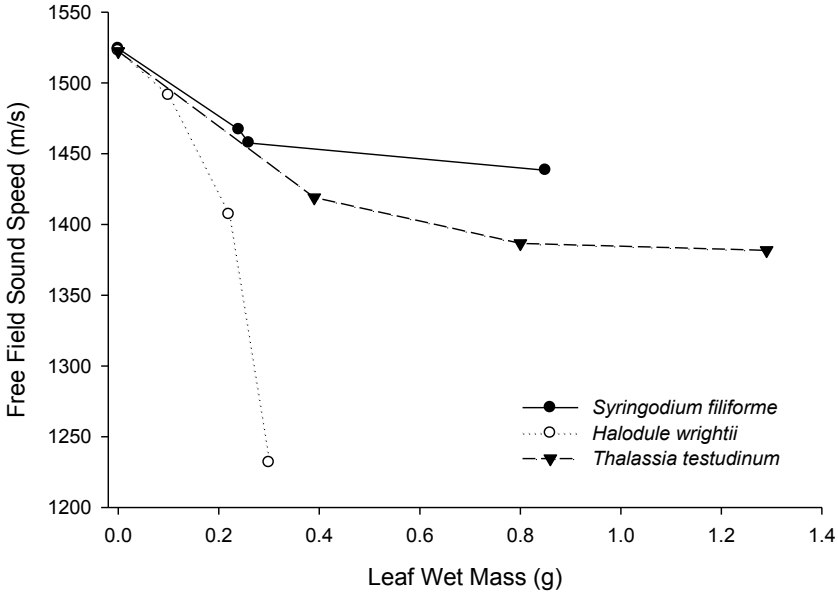

Figure 1.4. The decrease in sound speed within the resonator as a function of a) number of leaves and b) leaf wet mass (g) Filled circles: *Syringodium*; empty circles: *Halodule;* triangles: *Thalassia*.

Figure 1.5a.

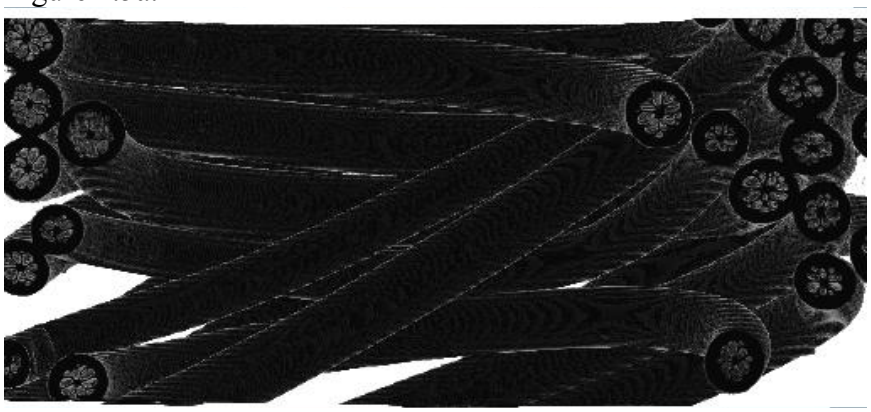

Figure 1.5b.

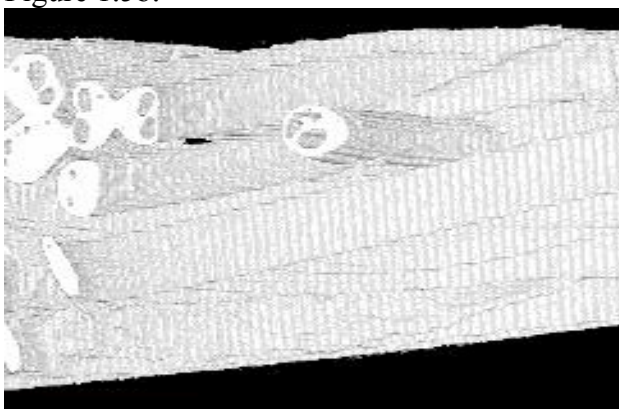

Figure 1.5c.

Figure 1.5. Three-dimensional representations of a) *Syringodium* b) *Halodule* and c) *Thalassia* leaves from CT imagery. Aerenchyma are evident as the contrasting pixel color in the middle of each leaf.

Table 1.1.Values obtained from CT image analysis for plant tissue density, plant tissue volume and the volume of air within the aerenchyma of the seagrass leaves.

Genus	Density (kg/m^3)	Tissue Volume (m^3)	Air Volume (m^3)
Syringodium	664.17 ± 10.38	$1.28 \pm 0.02 \times 10^{-6}$	$2.98 \pm 0.15 \times 10^{-7}$
Halodule	964.96 ± 21.72	$3.11 \pm 0.07 \times 10^{-7}$	$3.55 \pm 0.24 \times 10^{-8}$
Thalassia	1032.34 ± 115.42	$1.26 \pm 0.14 \times 10^{-6}$	$9.34 \pm 8.41 \times 10^{-8}$

Values are mean ± standard deviation for three gray scale values (n=3) used to calculate the areas of plant tissue and air in the CT images.

Table 1.2.Values obtained from CT and imagery and acoustic resonator experiments used to test three phase fluid models.

Genus	ρ_{tissue} (kg/m^3)	ρ_{air} (kg/m^3)	ρ_{water} (kg/m^3)
Syringodium	664.17	1.21	1023.7
Halodule	964.96	1.21	1024.0
Thalassia	1032.34	1.21	1024.0
	c_{water} (m/s)	c_{air} (m/s)	c_{exp} (m/s)
Syringodium	1524.2	315 (Wood 1930)	1438.3
Halodule	1522.7	315 (Wood 1930)	1231.7
Thalassia	1522.3	315 (Wood 1930)	1381.7
	ϕ_{tissue}	ϕ_{air}	ϕ_{water}
Syringodium	1.222×10^{-3}	2.845×10^{-4}	0.998494
Halodule	2.969×10^{-4}	3.389×10^{-5}	0.999669
Thalassia	1.203×10^{-3}	8.917×10^{-5}	0.998707
	κ_{leaves} (1/Pa)	c_{leaves} (m/s)	ρ_{leaves} (kg/m^3)
Syringodium	3.50×10^{-8}	230.3	539
Halodule	6.73×10^{-7}	41.41	866
Thalassia	7.02×10^{-8}	121.7	961

Values of c_{leaves} were determined from inversion of Wood's two-medium model (Wood 1930) as illustrated in Figure 1.3(a).

Chapter 2

Assessing the low frequency acoustic characteristics of *Macrocystis pyrifera*, *Egregia menziessi*, and *Laminaria solidungula*.

Abstract

The acoustic properties of kelp forests are not well known, but are of interest for potential environmental remote sensing applications. To begin to address this deficiency, the present study examined the low-frequency acoustic properties of three species of kelp (*Macrocystis pyrifera*, *Egregia menziessi*, and *Laminaria solidungula*) using a one-dimensional acoustic resonator. Acoustic observations and measurements of kelp morphology were then used to test the validity of Wood's multi-phase medium model in describing the acoustic behavior of the kelp. The relative acoustic contribution of air-filled pneumatocyst structures was also investigated. All three kelp species proportionally decreased the effective sound speed of seawater with increased biomass within the resonator. For *Macrocystis* and *Egregia*, the two species of kelp possessing pneumatocysts, the change in sound speed was highly dependent on the volume of free air contained in the kelp. The volume of air alone, however, was unable to predict the effective sound speed of the multi-phase medium using a simple two-phase (air + water) form of Wood's model. A separate implementation of this model (frond + water) successfully yielded the acoustic compressibility of the frond structure for each species (*Macrocystis* = $1.39 \pm 0.82 \cdot 10^{-8}$ Pa^{-1}; *Egregia* = $2.59 \pm 5.75 \cdot 10^{-9}$ Pa^{-1}; *Laminaria* = $8.65 \pm 8.22 \cdot 10^{-9}$ Pa^{-1}). As with another air-filled aquatic plant (seagrass), both tissue properties and air content govern the low frequency acoustic properties of the water/plant collection. This investigation demonstrates that the acoustic characteristics of kelp are species-specific, biomass-dependent, and differ between

species with and without pneumatocyst structures, which is important in the future development of predictive acoustic models for kelp forest communities.

Introduction

As marine ecosystems change in response to natural and anthropogenic stressors, the ability to effectively monitor these submerged habitats becomes increasingly important[1]. Kelp forests are found in cold and temperate regions in all of the world's oceans and foster an incredibly diverse ecosystem[2]. Currently, aerial and satellite imagery are the primary methods used in remotely assessing the health and condition of these habitats[3], but each of these methods has major limitations. Aerial biomass surveys of kelp forests are highly dependent on tidal stage and current velocity and will only provide a two-dimensional geographic extent of the habitat[4,5]. Although the interpretation of satellite imagery has improved, it is still difficult to make reliable measurements at small spatial scales and over heterogeneous landscapes[6]. It is therefore imperative to continue to research novel methods that could reliably assess the condition of kelp forests at a variety of spatial scales through time.

Acoustic methods are emerging as a useful tool for delineating macroalgal communities. Riegl et al.[7] demonstrated the use of acoustic echo sounding to describe the presence and abundance of drift macroalgae within a seagrass bed. Similarly, Quintino et al.[8] conducted an acoustic survey of a bed of *Caulerpa prolifera* in Florida. Each of these studies clearly exhibited the capabilities of acoustic mapping techniques at very small spatial scales. However, acoustic echo sounding is also useful for examining the extent of macroalgae at much larger spatial scales. Meleder et al.[9] recently described the use of low frequency acoustics to map the height and extent of kelp forest communities. Although echo sounding provided valuable information,

Meleder et al.[9] concluded that future investigations should focus on the species-specific acoustic spectra of the kelp plants in order to improve mapping techniques.

In order to advance the development of predictive acoustic models used in remote sensing, the current study examined three genera of kelp plants and focused on the role of pneumatocyst structures in the acoustic characteristics of the tissue. Pneumatocysts are air-filled bladders, which aid in the flotation of a kelp plant. In *Egregia menziessi*, pneumatocysts are found scattered along a strap-like frond. For *Macrosystis pyrifera*, the pneumatocysts are located at the base of each blade at the intersection of the blade and the frond. The pneumatocysts in each species of kelp vary in size along the length of the frond and correspond with age, as older pneumatocysts are larger than newly-formed pneumatocysts. We used the endemic arctic kelp *Laminaria solidungula,* whose thick frond does not contain pneumatocysts, as a reference species for comparison purposes.

Low frequency (0.2- 4.5 kHz) acoustic measurements were conducted in a one-dimensional acoustic resonator as described by Wilson and Dunton[11] with fresh specimens of *Macrocystis pyrifera*, *Egregia menziessi*, and *Laminaria solidungula.* Morphological measurements of the kelp tissue and information gathered in resonator experiments were then used to test predictions based on Wood's equation for a multi-phase medium. Since no previous modeling of kelp forest acoustics is known to the authors, Wood's[10] multi-phase effective medium model was considered the simplest model that might explain the acoustic behavior of a kelp forest and a logical starting place. The two species of kelp that contained air bladders decreased the speed of sound within the resonator, and this characteristic was highly dependent on the volume of air within the tissue. *Laminaria*, which did not contain air bladders, also

decreased the speed of sound within the resonator, but to a lesser degree than the two species of kelp that contained pneumatocysts.

Acoustic Response of Kelp Tissue

This study tested the hypothesis that kelp tissue is acoustically similar to seawater and that the acoustic response of kelp is fully described by the volume of air contained within pneumatocysts. Based on this hypothesis, it was predicted that *Laminaria* was acoustically similar to seawater and that the addition of *Macrocystis* or *Egregia* tissue would decrease the effective sound speed of the multi-phase medium. This experiment tested three different forms of an effective medium model originally proposed by Wood[8]. For this model, the effective sound speed c_{eff} in the multi-phase mixture is given by

$$\frac{1}{c_{\text{eff}}^2} = \frac{1}{c_{\text{exp}}^2} = \left[\sum_i \phi_i \kappa_i\right]\left[\sum_i \phi_i \rho_i\right] = \left[\sum_i \frac{\phi_i}{c_i^2 \rho_i}\right]\left[\sum_i \phi_i \rho_i\right] \tag{1}$$

and

$$\sum_i \phi_i = 1 \tag{2}$$

where κ, c, ρ, φ represent the compressibility, intrinsic sound speed, density, and volume fraction of phase or component i, respectively.

There were several different implementations of the model used in this work. The first implementation modeled the kelp and seawater mixture as a bubbly fluid. For this implementation, it was assumed that the kelp tissue was acoustically similar to seawater and that sound propagation within the seawater was only affected by the volume of air within the pneumatocysts. In order to evaluate the hypothesis that kelp tissue is acoustically the same as seawater, effective sound speeds observed in the resonator experiments were statistically

compared to model predictions of a bubbly fluid using a Student's paired t-test ($p < 0.05$). A significant difference between observed and predicted sound speeds would serve as a basis to reject the hypothesis that kelp tissue is acoustically similar to seawater.

Two additional variations of the multi-phase medium model were then used in an attempt to describe the sound speed and acoustic compressibility of the kelp tissue. Since all of the other model parameters were previously known or measured in the experiments, it was theoretically possible to solve for the compressibility of the kelp tissue as the only remaining variable. This was first attempted using a three-phase model (tissue + air + water) with the kelp tissue and air within the pneumatocysts as individual phases affecting the propagation of sound energy through seawater. The final implementation used a two phase form of the model (frond + water) and assumed the kelp to be a single composite phase with both tissue and air components. Since each of these model variations were used to solve for an unknown parameter, the lack of a real number solution to the model represented both a non-physical result and a failure of the model variation.

Description of the Experiment

The acoustic experiments were conducted in a one dimensional acoustic resonator following the methodology described by Wilson and Dunton[11]. The resonance chamber consisted of a steel tube of length 62.5± 0.2 cm, cross-section 11.43± 0.01 cm, and wall thickness 0.79± 0.01 cm. A block of closed cell foam at the bottom of the chamber and the air-water interface at the top of the chamber served as pressure-release boundaries. Gaussian white noise was generated by a vector signal analyzer (VSA) and directed through a power amplifier to an electromechanical shaker. An aluminum piston fitted to the electromechanical shaker was

used to generate a standing acoustic wave within the liquid- and plant-filled steel resonator in the frequency range of 0.2 kHz to 4.5 kHz. A miniature hydrophone sensed the acoustic pressure within the resonator. The signal obtained from the hydrophone was conditioned with a charge amplifier and digitized by the VSA. Transfer functions between the drive voltage and the conditioned hydrophone signal were calculated on the VSA and yielded the acoustic response of the sample-loaded resonator. The system's resonance frequencies coincide with the peaks of the pressure spectra, and these were used to calculate the sound speed c within the resonator using Eq. (3), where L is the water column length and f_n is the n-th resonance peak of the spectra. The term in brackets is the slope of a linear function relating the measured resonance frequencies f_n to the mode number n. A least-squares linear fit of the measured resonance frequencies yields the slope, from which the sound speed c was calculated. The uncertainty of the resonator length (± 0.2 cm) would subsequently provide an error of ± 4 m s^{-1} in the sound speed calculation.

$$f_n = \left[\frac{c}{2L}\right] n. \quad (3)$$

Seawater used in the acoustic experiments was obtained from the Gulf of Mexico. The seawater was filtered, degassed, and chilled prior to the experiment. The water was chilled in order to limit stress on the kelp plants, which produce mucus during unfavorable conditions. The water temperature emulated natural conditions for each species used, and therefore differed in acoustic experiments between species. Seawater temperature differed less than 1˚C for all experiments on the same kelp species and did not affect species-specific implementations of acoustic models.

Macrocystis and *Egregia* specimens were collected in February 2010 from the southern coast of California and were shipped on ice to the University of Texas Marine Science Institute

(UTMSI). Upon arrival, the kelp plants were rinsed and placed in an indoor refrigerated aquarium. The kelp plants were stored in the aquarium under natural temperatures for no longer than 48 h prior to the acoustic experiments. The *Laminaria* specimens were collected from the northern coast of Alaska in August 2010 and shipped to UTMSI on ice. These specimens were also rinsed and placed in a refrigerated aquarium under natural conditions prior to the acoustic experiments.

Macrocystis and *Egregia* specimens consisted of several long fronds > 2 m in length. Because the length of the resonator was shorter than the length of an entire frond, smaller kelp sections were cut from the larger fronds and these smaller sections were treated as individual replications within the resonator. The use of these smaller sections ensured that the kelp was distributed homogenously throughout the entire length of the acoustic chamber. Since individual *Laminaria* specimens are smaller than the other two species examined, whole intact fronds were placed in the resonator during each acoustic experiment. Following the acoustic experiments for all species, frond length and volume were measured. Frond volume was measured by water displacement. The volume of air contained within the pneumatocysts of *Egregia* and *Macrocystis* was measured by recording the amount of water it took to fill each pneumatocyst using a 5-ml syringe. Finally, the water in the pneumatocysts was drained and the wet mass of the specimen was measured with a digital laboratory balance. A linear regression analysis was used to examine the relationship between air volume and wet mass as well as air volume and effective sound speed for both *Egregia* and *Macrocystis* experiments. Regression slopes for each species were compared using a z test ($p < 0.05$) described by Paternoster et al.[12]

Additional experiments were conducted on *Egregia* and *Macrocystis* to investigate the acoustic significance of the air-filled pneumatocysts. These experiments first proceeded with a

section of a frond placed within the resonator as previously described. The pneumatocysts of the individual frond sections were filled with seawater and placed back into the resonator where additional acoustic spectra were obtained. These experiments recorded the relative acoustic difference of the kelp specimens that was attributable to the presence of gas within the pneumatocysts. A linear regression analysis was used to test the relationship between removed air volume and change in effective sound speed. The trials for both *Egregia* and *Macrocystis* were combined in this statistical analysis.

Results

Each of the three kelp species observed possessed distinctive morphological characteristics. *Macrocystis* had the highest average tissue density (1217 ± 190 $kg \cdot m^{-3}$) compared to *Egregia* (1031 ± 144 $kg \cdot m^{-3}$) and *Laminaria* (970 ± 133 $kg \cdot m^{-3}$). *Laminaria* was the only species to have a tissue density less than seawater, which enables this species to float without pneumatocysts. The volume of air within the pneumatocysts of *Macrocystis* and *Egregia* frond sections increased proportionally with the mass of the tissue (Figure 2.1). This result is expected, as the primary function of the pneumatocysts is to provide buoyancy to the kelp. However, there was more variation around this relationship for *Egregia* ($r^2 = 0.56$) compared to *Macrocystis* ($r^2 = 0.85$). This is largely due to variation in the number and size of pneumatocysts present along a particular frond section. For instance, the average percent volume of air (compared to total frond volume including the air volume) was higher for *Egregia* fronds (9.9%) compared to *Macrocystis* fronds (5.1%), but this percentage was far more variable for *Egregia* (coefficient of variation = 0.5) than *Macrocystis* (coefficient of variation = 0.1).

There was a decrease in the effective sound speed of the resonator with the addition of both *Egregia* and *Macrocystis* fronds. The decrease in effective sound speed was correlated with total air volume contained within pneumatocysts, and a significant difference ($p < 0.01$) in the slopes of these regressions indicates a species-specific acoustic response to increasing air volume (Figure 2.2). *Laminaria*, which lacks pneumatocysts, exhibited a small change in the effective sound speed of seawater with an increase in biomass (Figure 2.3). The slope of this regression was statistically significant ($p < 0.05$), which indicates that the kelp tissue of *Laminaria solidungula* is not acoustically similar to seawater.

Removal of air from the pneumatocysts of *Macrocystis* reduced the acoustic contrast of the frond segment compared to seawater (Figure 2.4a). However, the difference in sound speeds for specimens with and without air is not directly correlated to the volume of air that was removed from the frond segment. For instance, the first trial of this experiment used a specimen with the fewest number of individual pneumatocysts (6) and the smallest volume of air (4.9 ml), but this segment exhibited the greatest acoustic change upon air removal. The third trial contained a frond segment with the highest number of pneumatocysts (12) and greatest volume of air 5.7 ml, yet this frond segment exhibited the least acoustic change upon air removal. The results of these trials suggest that the tissue component of individual frond sections may be more important than simply the number and size of air-filled pneumatocysts. The pneumatocysts present in the third trial were smaller and are indicative of new growth. These newly formed pneumatocysts have thick walls and small air volumes and appear far more rigid than the older, larger pneumatocysts present in the first replication. Therefore, the differences observed in these trials are possibly attributed to the combined interactions of air volume, pneumatocyst size, and age-mediated tissue rigidity.

Similar to *Macrocystis*, removal of air from the pneumatocysts of *Egregia* reduced the acoustic contrast of the tissue to seawater (Figure 2.4b). However, unlike the *Macrocystis* experiments, the change in effective sound speeds observed in *Egregia* trials did appear related to both the volume of air removed from the tissue and the number of pneumatocysts present on the frond. The first trial specimen had the most pneumatocysts (6) and the second largest volume of air (3.6 ml). This trial showed the largest acoustic difference upon air removal. Similarly, the third trial exhibited the smallest acoustic difference with air removal, contained the lowest volume of air (1.5 ml) and the fewest number of pneumatocysts (3). These preliminary results suggest that differences in the variability of tissue stiffness may be less important in *Egregia* fronds compared to *Macrocystis* fronds.

The volume of air within the pneumatocysts did not sufficiently predict the effective sound speed of the medium for either *Macrocystis* or *Egregia* when using the two-phase (air + water) version of Wood's equation. In each case, the model predicted an effective sound speed significantly lower ($p < 0.01$) than what was observed (Figure 2.5). Furthermore, the volume of air removed from the pneumatocysts was not statistically correlated to the observed change in effective sound speed (Figure 2.6). These findings serve as a basis to reject the hypothesis that the kelp tissue of *Macrocystis* and *Egregia* fronds is acoustically the same as seawater. Each implementation of the three-phase version of Wood's equation (tissue + air + water) was also unsuccessful as the model was unable to produce a real number solution for the sound speed of the kelp tissue. The failure of each of these two models highlights the importance of the kelp tissue in modeling the acoustic behavior of the vegetation. The failure of Wood's two-phase model, for air and water components, illustrates the importance of the kelp tissue in restricting the acoustic compressibility provided by the free gas within the pnuematocysts. The lack of a

real number solution to the three-phase implementation of Wood's equation indicates that the effective fluid model is inappropriate for this system and also suggests that the kelp behaves acoustically as a solid structure on the benthos and not as a heterogeneous fluid mixture of solid, liquid, and gas components. In retrospect this might have been anticipated, as the same outcome has been reported for seagrass[12] but the potential attractiveness of the simplicity of the effective medium approach made it worth trying.

The final implementation of the Wood's equation used two phases (frond + water) consisting of the seawater and the kelp frond as a composite of both air and tissue components. This model successfully produced values for the sound speed and acoustic compressibility of the composite of all three kelp species examined in this study (Table 2.1). The success of this model suggests that the sound energy is not acting separately on the gas and solid phases of a kelp plant, but rather, on the entire kelp structure simultaneously. Again, the same result was found for seagrass[12].

Conclusions

The low-frequency acoustic properties of kelp plants were examined in relation to kelp morphology using a one dimensional acoustic resonator technique. Three implementations of Wood's equation were used to investigate the relative importance of the kelp tissue and gas volume components on the acoustic characteristics of the plant. Gas content alone through Wood's model did not accurately predict the effective sound speed of kelp, which highlights the importance of investigating the material properties of kelp tissue in the development of future acoustic models. This study described the acoustic compressibility of the composite of kelp tissue and air components for *Macrocystis* and *Egregia* using a two-phase form of Wood's

equation. This form of the model also successfully produced the acoustic compressibility of *Laminaria* tissue, which does not contain pneumatocysts.

References

[1] Harley, C.D.G., A.R. Hughes, K.M. Hultgren, B.G. Miner, C.J.B. Thornber, L.F. Rodriguez, L. Tomanek, S.L. Williams. 2006. The impacts of climate change in coastal marine systems. *Ecology Letters*. Vol. 9, pp. 228-241.

[2] Dayton, P.K. 1985. Ecology of kelp communities. Ann. Rev. Ecol. Syst. Vol. 16, pp. 215-245.

[3] Daysher, L.E. 1993. Evaluation of remote sensing techniques for monitoring giant kelp populations. *Hydobiologia*. Vol. 260/261, pp. 307-312.

[4] Britton-Simmons, K., J.E. Eckman, D.O. Duggins. 2008. Effects of tidal currents and tidal stage on estimates of bed size in the kelp *Nereocystis luetkeana*. *Mar Eco Prog Ser*. Vol. 355, pp. 95-105.

[5] Stekoll, M.S., L.E. Deysher, M. Hess, 2006. A remote sensing approach to estimating harvestable kelp biomass. *Journal of Applied Phycology*. Vol. 18, pp. 323-334.

[6] Cavanaugh, K.C., D.A. Siegel, B.P. Kinlan, D.C. Reed. 2010. Scaling giant kelp field measurements to regional scales using satellite observations. *Mar Eco Prog Ser.* Vol. 403, pp. 13-27.

[7] Riegl, B.M., R. P. Moyer, L. J. Morris, R. W. Virnstein, S. J. Purkis, 2005. Distribution and seasonal biomass of drift macroalgae in the Indian River Lagoon (Florida, USA) estimated with acoustic seafloor classification (QTCview, Echoplus). *J. Exp. Mar. Biol. Ecol*. Vol 326, pp. 89-104.

[8] Quintino, V., R. Freitas, R. Mamede, F. Ricardo, A. M. Rodrigues, J. Mota, A. Perez-Ruzafa, C. Marcos, 2009. Remote sensing of underwater vegetation using single-beam acoustics. *ICES Journal of Marine Science*. Vol. 67, pp. 594-605.

[9] Meleder, V., J. Populus, B. Guillamont, T. Perrot, P. Mouquet, 2010. Predictive modeling of 21 seabed habitats: case study of subtidal kelp forests on the coast of Brittany, France. *Mar Biol*. Vol. 157, pp. 1525-1541.

[10] Wood, A. B., 1930. A Textbook of Sound. Macmillan, New York, first edition.

[11] Wilson, P.S. and K.H. Dunton, 2009. Laboratory investigation of the acoustic response of seagrass tissue in the frequency band of 0.5–2.5 kHz. *J. Acoust. Soc. Am*., Vol. 125, pp. 1951– 1959.

[12] Paternoster, R. R. Brame, P. Mazerolle, A. Piquero. 1998. Using the correct statistical test for the equality of regression coefficients. *Criminology*. Vol. 36, pp. 859-866.

[13] Wilson, C.J., P.S. Wilson and K.H. Dunton. 2010. Seagrass leaves in 3-D: Using computed tomography and low-frequency acoustics to investigate the material properties of seagrass tissue. *Journal of Experimental Marine Biology and Ecology*. Vol 35 pp.128-134.

Figure 2.1.

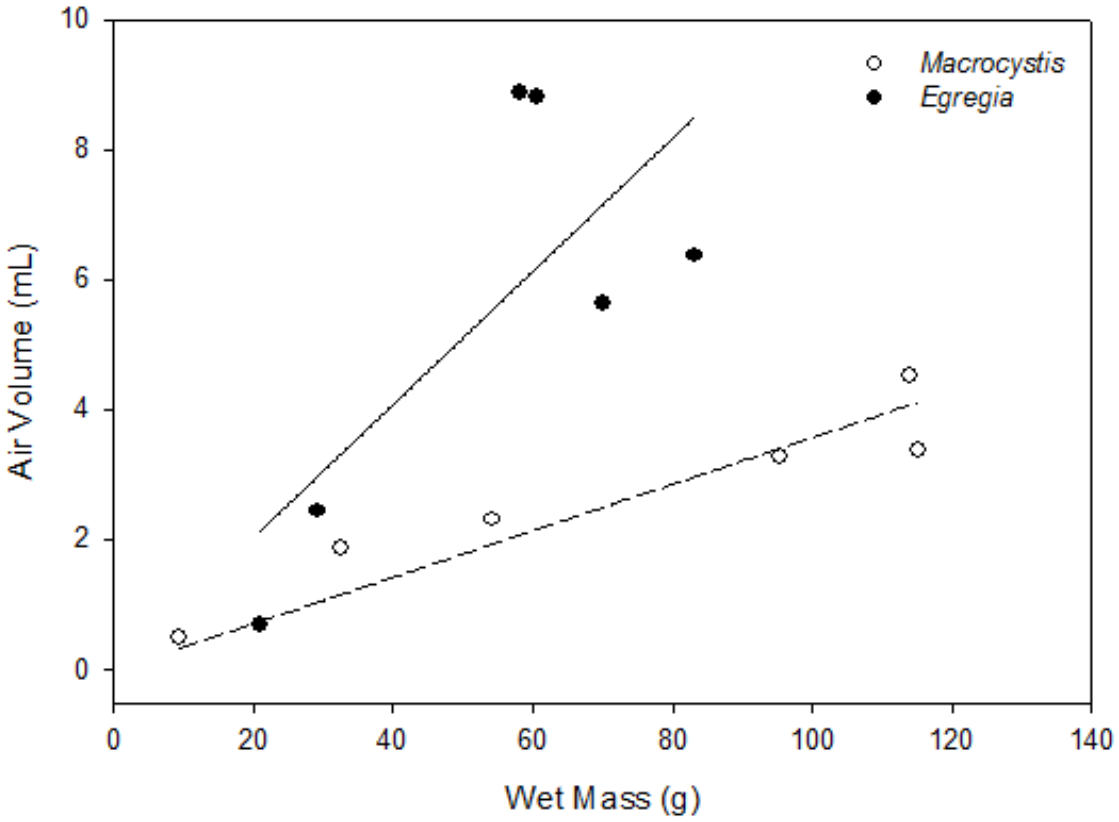

Figure 2.1. Empirical relationship between air volume within the pneumatocysts and kelp wet mass for individual *Macrocystis pyrifera* ($r^2 = 0.85$; slope = 0.04; $p < 0.01$) and *Egregia menziessi* ($r^2 = 0.56$; slope = 0.10; $p < 0.01$) frond sections. The slope of the regression was significantly higher for *Egregia* compared to *Macrocystis* ($z = 4.2$; $p < 0.01$). Measurement uncertainty is ± 0.15 ml and ± 0.005 g for air volume and wet mass, respectively.

Figure 2.2.

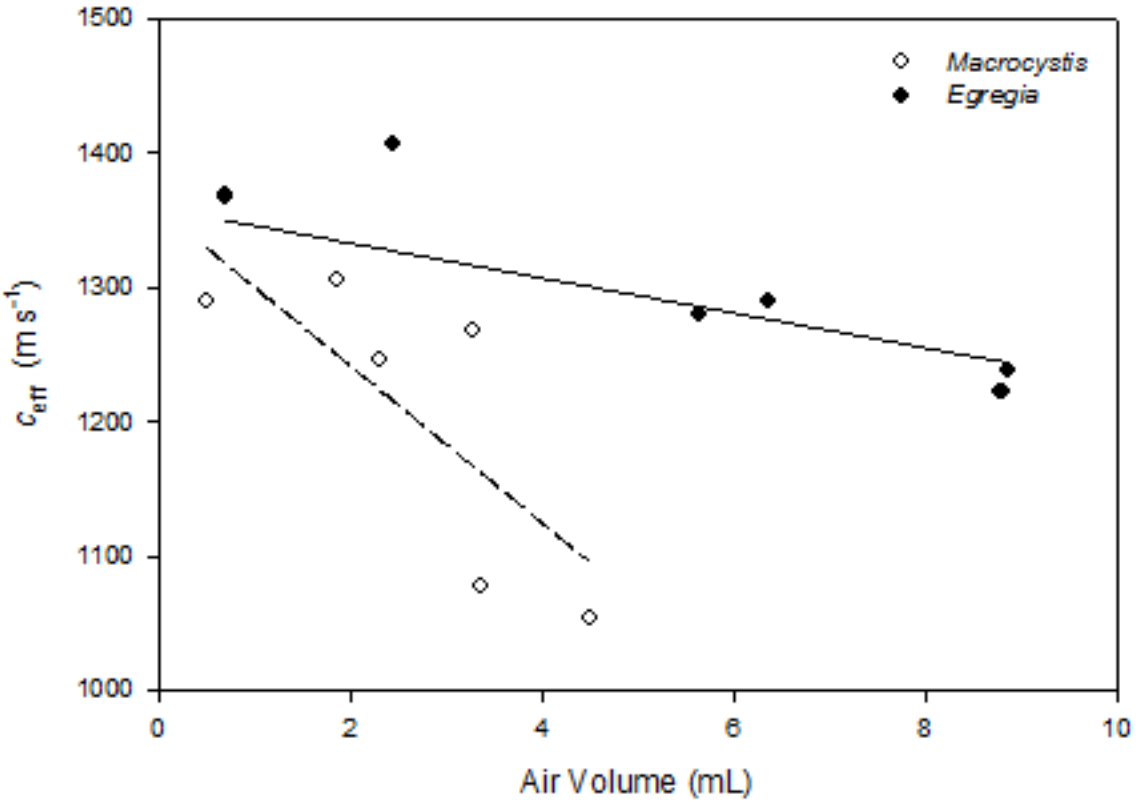

Figure 2.2. Decrease in effective sound speed in relation to free gas volume within pneumatocysts for *Macrocystis pyrifera* ($r^2 = 0.61$; slope = -58.51; $p < 0.01$) and *Egregia menziessi* frond sections ($r^2 = 0.72$; slope = -13.00; $p < 0.01$). The slope of the regression was significantly greater for *Macrocystis* compared to *Egregia* ($z = 4.53$; $p < 0.01$). Measurement uncertainty is ± 0.15 ml and ± 4 m s^{-1} for air volume and effective sound speed, respectively.

Figure 2.3.

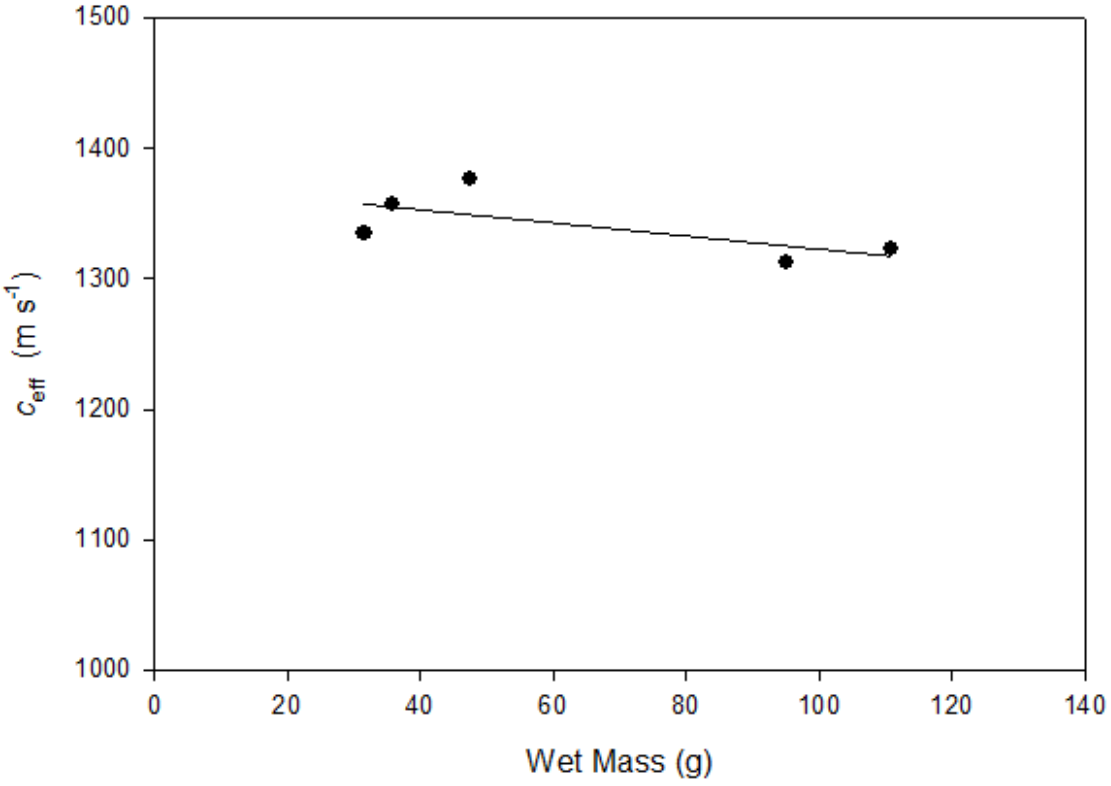

Figure 2.3. Decrease in effective sound speed in relation to total biomass for *Laminaria solidungula* ($r^2 = 0.46$; slope = -0.50; $p < 0.05$). Measurement uncertainty is ± 0.005 g and ± 4 m s^{-1} for air wet mass and effective sound speed, respectively.

Figure 2.4a.

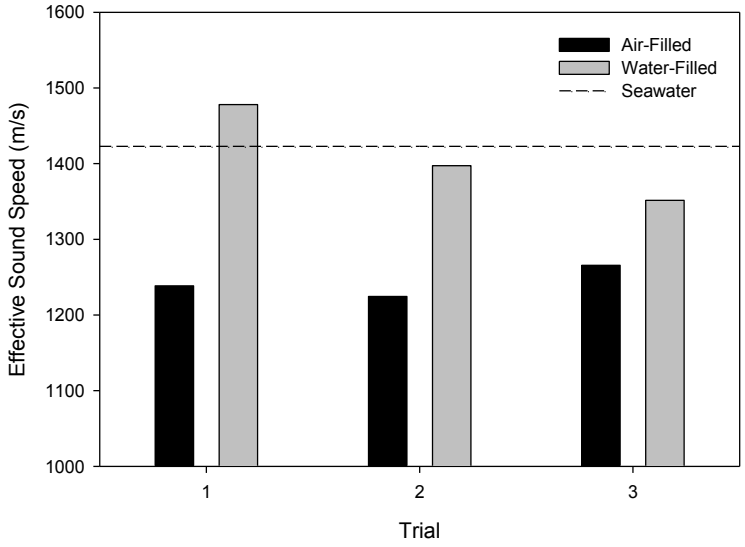

Figure 2.4b.

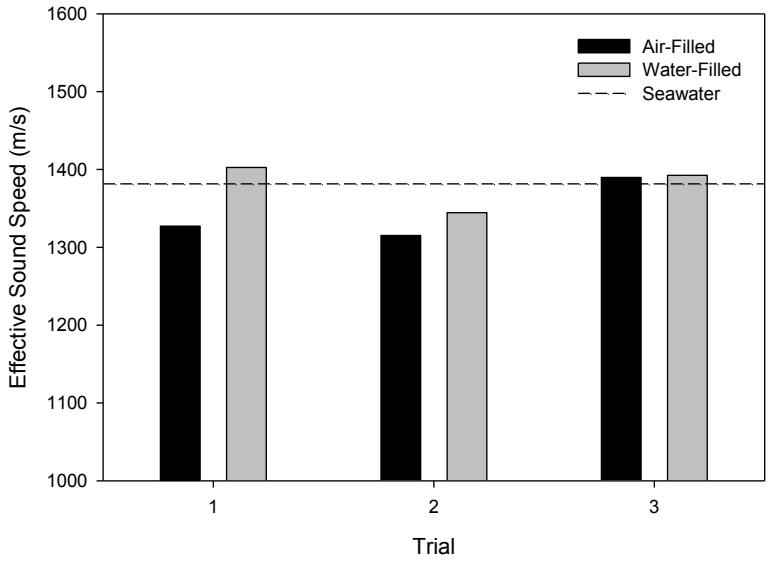

Figure 2.4. Effective sound speed of air-filled pneumatocysts compared to water-filled pneumatocysts of the same frond segments for a) *Macrocystis pyrifera* and b) *Egregia menziessi.* Measurement uncertainty is ± 4 m s^{-1} for effective sound speed.

Figure 2.5a.

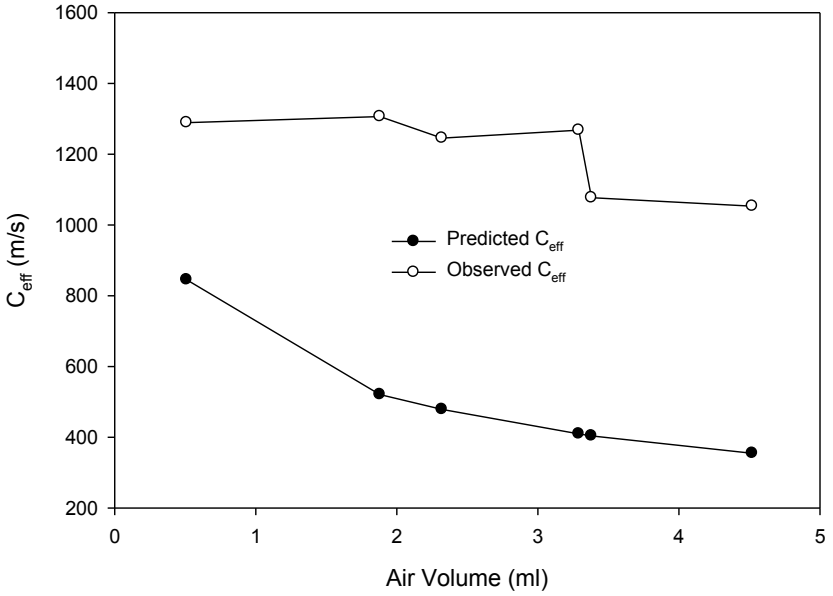

Figure 2.5b.

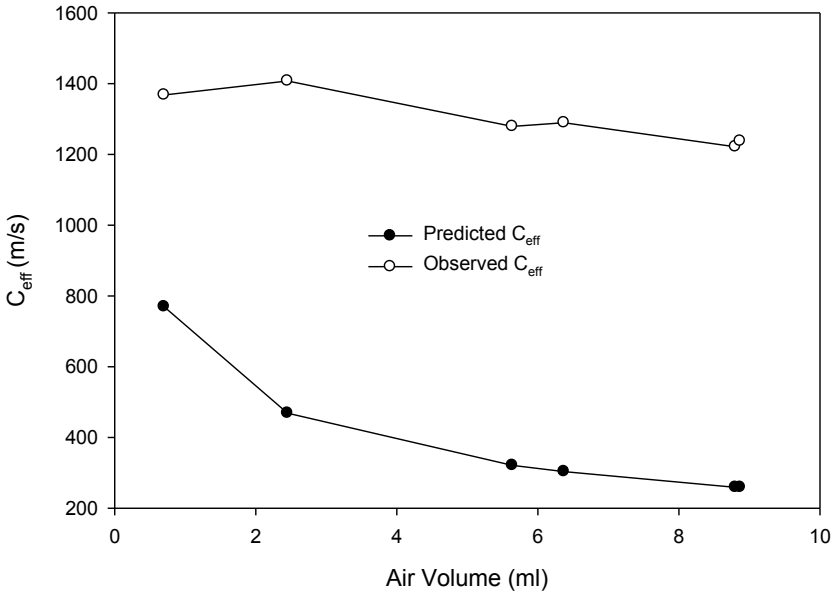

Figure 2.5. Effective sound speeds predicted by Wood's two-phase medium model for air and water components compared to observed effective sound speeds for frond segments of a) *Macrocystis pyrifera* and b) *Egregia menziessi.* A Student's paired t-test revealed a significant difference between predicted and observed effective sound speeds for both *Macrocystis* and *Egregia* experiments ($p < 0.01$).

Figure 2.6.

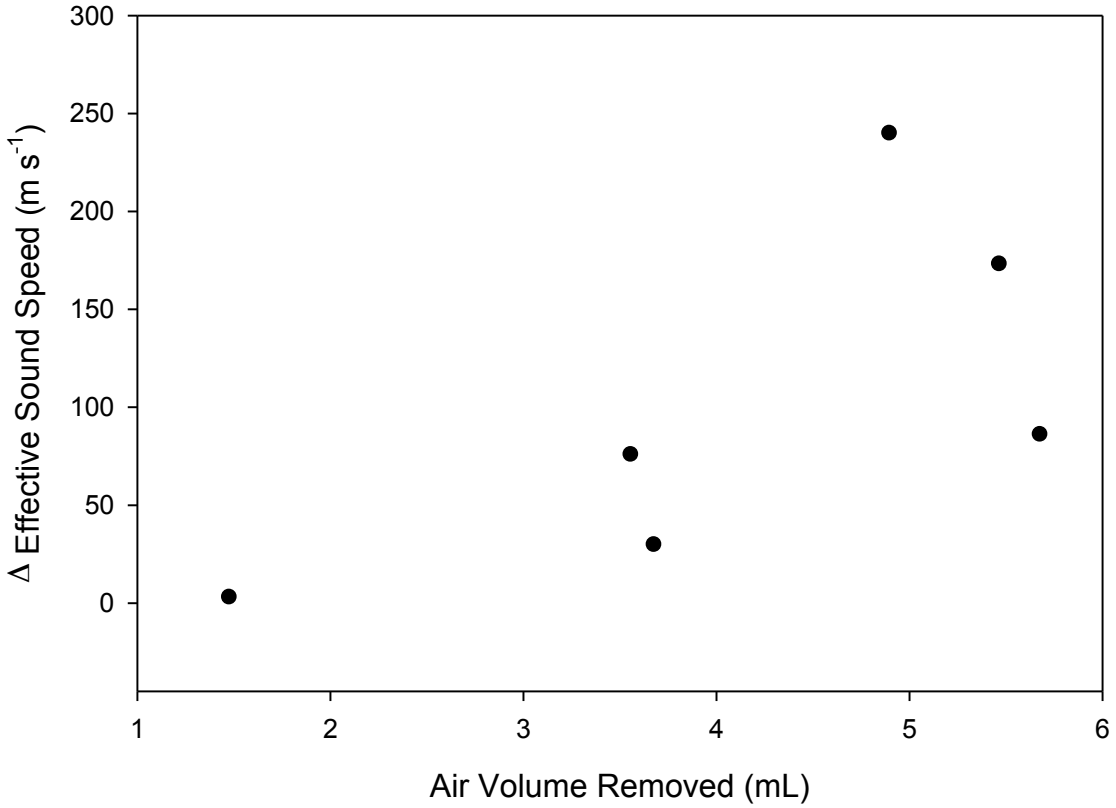

Figure 2.6. Change in effective sound speed upon air removal within pneumatocysts for *Macrocystis pyrifera* and *Egregia menziessi* frond segments. Trials for both species were plotted together (regression was not significant). Measurement uncertainty is ± 0.15 ml and ± 4 m s^{-1} for air volume and effective sound speed, respectively.

Table 2.1.
Model parameters obtained from morphological measurements and acoustic resonator experiments used to test multi-phase medium models. $C_{composite}$ and $\kappa_{composite}$ values are based on results from the derivation of Wood's two-phase medium model (Wood 1930). Values represent mean ± standard deviation for *Macrocystis* (n = 6), *Egregia* (n = 6), and *Laminaria* (n = 5).

Genus	ρ_{tissue} **(kg ·m^{-3})**	ρ_{air} **(kg ·m^{-3})**	ρ_{water} **(kg ·m^{-3})**
Macrocystis	1217.06 ± 190.31	1.31	1025
Egregia	1031.37 ± 144.23	1.31	1025
Laminaria	970.28 ± 133.86	1.31	1014
	C_{water} **(m/s)**	C_{air} **(m/s)**	C_{eff} **(m/s)**
Macrocystis	1358.66	316	1206.38 ± 111.61
Egregia	1359.41	316	1300.48 ± 73.16
Laminaria	1372.82	316	1340.38 ± 25.91
	χ_{tissue}	χ_{air}	χ_{water}
Macrocystis	$1.14 \pm 0.64 \cdot 10^{-2}$	$5.59 \pm 2.91 \cdot 10^{-4}$	$9.88 \pm 0.07 \cdot 10^{-1}$
Egregia	$1.12 \pm 0.55 \cdot 10^{-2}$	$1.14 \pm 0.69 \cdot 10^{-3}$	$9.88 \pm 0.06 \cdot 10^{-1}$
Laminaria	$3.66 \pm 2.28 \cdot 10^{-3}$		$9.96 \pm 0.02 \cdot 10^{-1}$
	$C_{composite}$ **(m/s)**	$\kappa_{composite}$ **(1/Pa)**	
Macrocystis	279.19 ± 96.76	$1.39 \pm 0.82 \cdot 10^{-8}$	
Egregia	114.44 ± 515.20	$2.59 \pm 5.75 \cdot 10^{-9}$	
Laminaria	92.16 ± 538.25	$8.65 \pm 8.22 \cdot 10^{-9}$	

Chapter 3

Using high-frequency acoustics to monitor oxygen evolution in whole seagrass plants

Abstract

The use of high-frequency acoustics has recently emerged as a viable method for mapping the areal coverage of seagrasses. Free gas contained within the aerenchyma of seagrass leaves and bubbles produced during photosynthesis scatter and absorb acoustic energy. Since the bubbles produced by seagrasses are partly responsible for the signal observed during acoustic mapping, we hypothesized that changes in the rate of primary production would alter sound propagation throughout a seagrass canopy. Specfically, we hypothesized that as rates of primary production increase, bubble formation would increase and sound propagation would decline. To test this hypothesis, we examined the propagation of high-frequency (100 kHz) sound energy through the seagrass canopies of *Syringodium filiforme*, *Halodule wrightii* and *Thalassia testudinum* in a shallow outdoor mesocosm. Relative changes in the received acoustic energy were recorded every hour during a 24-h period and compared to independently-measured rates of oxygen production. The mean acoustic intensity of energy transmitted throughout the seagrass canopy varied by 3.5 dB for *Syringodium,* 4.4 dB for *Thalassia* and 4.7 dB for *Halodule* over a 24-h period. The 24-h trends in sound propagation were quite different between *Syringodium* and *Halodule* over the experimental period, which suggests different interactions between leaf morphology and acoustic energy for each species. Finally, changes in sound propagation occurring during morning hours of photosynthesis were used to generate both chemical and acoustic *Photosynthesis vs. Irradiance* relationships. Acoustic measurements consistently

underestimated the maximum rate of photosynthesis (P_{max}), saturation irradiance (I_k) and compensation irradiance (I_c) while overestimating the light limited slope of photosynthesis (α) relative to chemically derived parameters.

Introduction

Acoustic systems are now widely used by scientists to map and characterize submerged macrophytes. Seagrasses, in particular, have a unique acoustic signal compared to other substrates (Pasqualini et al. 2001; Mulhearn 2001). This unique acoustic signal has been attributed to the free gas contained within the aerenchyma of the seagrass tissue and the bubbles present on the surface of the plant tissue as products of photosynthesis (Hermand et al. 1998). The abundance of free gas creates an acoustically compressible substrate, which reflects and attenuates sound energy due to scattering and absorption. Multiple studies have demonstrated the use of acoustic systems to efficiently map both the lateral extent of seagrass meadows and the height of the canopy (Komatsu et al. 1998; Warren and Peterson 2007). Recent acoustic surveys have even started to distinguish between multiple seagrass species from unique backscatter characteristics (Paul et al. 2011). These studies clearly demonstrate the potential for developing novel acoustic measures to assess seagrass health and production.

Since seagrass plants produce oxygen bubbles in the presence of sunlight, it is possible that the acoustic signature used to map the vegetation also changes as a result of photosynthesis. Two published studies have already employed acoustic methods to observe photosynthesis in seagrass meadows (Hermand et al. 1998, Hermand 2004). Both of these studies used a low-frequency broadband source and a receiving hydrophone array to measure sound propagation over *Posidonia oceanica* meadows through time. In these experiments, the sound speed and

received acoustic energy followed a circadian cycle that matched photosynthesis. Specifically, the sound speed of the seagrass layer and the received acoustic energy decreased during the highest rates of oxygen production. The authors hypothesized that free gas bubbles generated during photosynthesis caused the temporal variations in sound propagation (Hermand et al. 1998, Hermand 2004).

Although many studies have measured seagrass photosynthesis from observations of dissolved oxygen, relatively few studies have examined free gas evolution and mass flow in these plants (Silva et al., 2009). Roberts and Caperon (1986) demonstrated the utility of free gas release as a measure of primary production. These authors recorded the volume of free gas produced by three different seagrasses and related the free gas volume to rates of total oxygen production. The rate of free gas release was positively correlated with the rate of total oxygen production, which demonstrated that measurements of free gas release are a reasonable proxy for calculating primary production. The utility of free gas evolution as a measure of production is important because oxygen in a dissolved state minimally impacts sound transmission relative to the presence of free gas bubbles.

Transport and release of free gas bubbles by seagrasses is facilitated by channels in the leaf and rhizome tissue called arenchyma (Caffrey and Kemp 1991). These air-filled channels differ in size and shape between species, which influences the acoustic compressibility of the leaf structure (Wilson et al. 2010). Several studies have noted internal pressurization of the arenchyma in aquatic macrophytes (Dacey 1981; Schuette and Klug 1995). In these studies, pressurization occurs with the onset of photosynthesis in the early morning hours and reaches maximum levels by the early afternoon. Internal pressurization then decreases in late afternoon as light levels decline. Internal pressurization is species-specific and varies in magnitude. Since

the air volume contained within the aerenchyma contributes to the observed attenuation of sound energy within seagrass meadows, changes in the mechanical properties of these channels may become important for acoustic measurements of photosynthesis. Specifically, a change in the internal pressure of the leaf structure could also change the acoustic compressibility of the seagrass canopy.

The current study tested the hypothesis that high-frequency acoustic propagation within a seagrass meadow varies on a daily cycle and is modified by plant photosynthesis and respiration. We hypothesized that bubbles produced during photosynthesis decrease sound propagation, and that the magnitude of this decrease can serve as a proxy for oxygen production. Results from this study suggest that both bubble production and leaf pressurization are possible modifiers on acoustic transmission. It also appears that these mechanisms operate differently in *Syringodium*, *Halodule* and *Thalassia* plants at a sound frequency of 100 kHz.

Methods

Plant Collection

Whole plants were collected from seagrass meadows near the University of Texas Marine Science Institute in Port Aransas, Texas. Upon arrival, the plants were stored in filtered and aerated seawater from the Gulf of Mexico. All of the experiments were conducted within 72 h of plant collection. Prior to beginning the experiments, seagrasses were transferred to an outdoor experimental tank (depth = 0.5 m, radius = 0.5 m) where they were planted in an acrylic container (0.40 m x 0.40 m x 0.12 m) containing a mixture of beach sand and aquarium gravel. This mixture was used in order to limit sediment respiration and ensure the seagrass plants were not carbon limited throughout the experiment. The seagrasses were acclimated in the tank for at least 4 h prior to experimentation.

24-Hour Experiments

Separate 24-h experiments were conducted for *Syringodium filiforme*, *Halodule wrightii* and *Thalassia testudinum*. High-frequency acoustic measurements were obtained every hour during the 24-h period. These measurements used two stationary hydrophones (Reson Model TC4033), one placed on each side of the acrylic container that held the plants. One hydrophone served as the sound source generating a 100 kHz sound pulse, of 5 ms in duration, at a 200 Hz repetition rate and the other hydrophone served as the receiver (Figure 3.1). The receiving hydrophone was connected to an oscilloscope, which recorded continuous averages of 64 individual pulses. The peak-to-peak voltage of the first cycle coinciding with the direct path of transmission was obtained from this averaged signal. The acoustic data were then expressed as the change in received acoustic energy relative to the mean for the entire 24-h period; such that negative changes in energy reflected a decrease in sound propagation and positive changes reflected an increase in sound propagation relative to the 24-h average. Following each acoustic measurement, temperature, salinity and dissolved oxygen concentration were measured using a YSI 600 XLSM datasonde. Underwater irradiance was also measured for each hour of daylight using a LI-Cor LI-190 quantum sensor connected to a LI-COR LI-1000 datalogger.

Measurements of seagrass morphology were made following each acoustic experiment. Every shoot in the experiment was counted and used to calculate overall shoot density. A total of 30 leaves were haphazardly chosen for measurements of total leaf length. The epiphytic load on the leaf surface was measured by scraping a leaf section of epiphytes using a razor blade. The material on the blade was then transferred to a pre-weighed filter. Both the filter and the leaf section were then dried in a 60°C oven to a constant weight and the epiphytic load was expressed as a ratio by dividing the total dry weight of epiphytes by the dry weight of the leaf tissue.

Finally, above and below ground seagrass biomass used in the experiment was separated and dried in a 60°C oven to a constant weight.

Morning Photosynthesis Experiments

In order to relate photosynthesis, irradiance and acoustic transmission, additional outdoor experiments were conducted for *Syringodium* and *Halodule*. New seagrass plants were obtained for these experiments, which began before sunrise and ended the hour following maximum irradiance. This time period was chosen because it corresponds to the highest rates of photosynthetic production and contained the most dramatic changes in sound transmission observed in each species during the 24-h experiments. In order to achieve a range of light levels, *Halodule* experiments were conducted over three separate mornings. Only one morning was required to achieve the desired range of light levels for *Syringodium*. Measurements of acoustic transmission and light intensity were obtained every 15 min, and acoustic data were expressed as the relative change in received acoustic energy over the total time period of the experiment. Dissolved oxygen was measured continuously throughout these experiments with a fiber-optic flow-through sensor placed within the seagrass canopy. Following the outdoor experiment, the above and below ground biomass was separated and dried to a constant weight in a 60°C oven.

Various photosynthetic parameters were calculated from the morning photosynthesis experiments following the methods described by Fourqurean and Ziemen (1991) and Dunton and Tomasko (1994). Respiration rates were calculated from the difference in dissolved oxygen concentrations in the outdoor tank during a dark predawn time period preceding each morning experiment. Net photosynthetic rates for the outdoor tank were calculated as the difference in

dissolved oxygen concentrations observed at each light level. Gross production (P_g) was calculated as:

$$P_g = [\ P_m - R_m\ ] / B_{leaf} \quad (1)$$

where P_m is net photosynthetic rate, R_m is tank respiration rate and B_{leaf} is total dry weight biomass of all photosynthetic tissues. Gross production was expressed as μmol O_2 g^{-1} dry weight leaf tissue h^{-1}.

Photosynthesis versus irradiance (*P vs. I*) curves were generated from the light data and gross production calculations. These data were fitted to the hyperbolic tangent function (Eq. 2) first described by Jassby and Platt (1976):

$$P = P_{max}\ \tanh\ (\alpha\ I / P_{max}\ ) \quad (2)$$

where P_{max} is the light-saturated rate of photosynthesis, *I* is irradiance and α is the light-limited slope of the *P vs I* curve.

The statistical program Sigmaplot was used to fit the hyperbolic tangent function to the data using a least-squares nonlinear regression technique. Saturation irradiance, I_k, was calculated using Eq. (3) and the derived model parameters P_{max} and α.

$$I_k = P_{max}\ /\alpha \quad (3)$$

Whole plant compensation irradiance (I_{cp}) was calculated using the tank respiration rates in a relationship described by Dunton and Tomasko (1994):

$$I_{cp} = (P / P_{max}\ )\ \coth\ (\alpha / P_{max}\ ) \quad (4)$$

where R_m is set equal to the rate of photosynthetic oxygen evolution (P) (Eq. 4).

Photosynthetic parameters P_{max}, α and I_k were also derived from acoustic observations. In order to calculate P_g from the acoustic data, chemical and acoustic observations corresponding to the same light level were plotted together. The chemical equivalent of P_g was then derived graphically from the acoustic data assuming a 1:1 relationship between chemical and acoustic measurements. *P vs. I* curves were then fit to the equivalent P_g data using the same procedures described for the chemical observations. A pairwise statistical analysis described by Paternoster et al. (1998) was used to evaluate significant differences ($p < 0.05$) in the *P vs. I* curves calculated chemically and acoustically as well *P vs. I* curves between species. This analysis specifically compared the coefficients Pmax and α, which were calculated in the nonlinear regression.

Leaf Pressurization

Since pressurization of the arenchyma within leaf tissue has been observed in other aquatic macrophytes, we investigated this mechanism in *Halodule* and *Syringodium*. An increase in the internal pressure of a seagrass leaf would decrease the acoustic compressibility of the leaf structure. Furthermore, a decrease in the acoustic compressibility of a medium increases the effective sound speed of that medium (Kinsler 2000). We therefore investigated the pressurization of seagrass leaves by documenting changes in the effective sound speed of a seawater and seagrass medium with exposure of the seagrass tissue to sunlight.

These experiments employed a one-dimensional acoustic resonator technique first described by Wilson and Dunton (2009). The resonator consisted of glass tubing (circular cross section 64.0± 0.1 mm outer diameter, 4.9± 0.1 mm wall thickness, length 454± 2 mm) filled with filtered and degassed seawater from the Gulf of Mexico. Gaussian white noise was generated in

the frequency range of 1.0 kHz to 4.8 kHz by a vector signal analyzer (VSA). This signal was directed through a power amplifier before reaching an electromechanical shaker fitted with an aluminum piston, which was used to generate a standing acoustic wave within the resonator. Acoustic energy was sensed with a miniature hydrophone placed in the resonator and this signal was conditioned with a charge amplifier and digitized by the VSA. Transfer functions between the drive voltage and the conditioned hydrophone signal were calculated on the VSA and yielded the acoustic response of the sample-loaded resonator. Resonant frequencies were obtained from the VSA and identified as the peak pressure levels in the spectra. These resonant frequencies were then used to calculate the effective sound speed of the medium within the resonator as:

(5)

$$f_n = \left[\frac{c}{2L}\right] n$$

where L is the water column length and f_n is the n-th resonance peak of the spectra.

The bracketed term is a linear function relating the system's resonance frequencies to the mode number. A least-squares linear fit of the measured resonance frequencies yields the slope, which was used to calculate the effective sound speed of the seagrass and seawater medium. The change in compressibility was then calculated from Eq. 6, where κ is compressibility, c is the effective sound speed and ρ is the density of the medium (Kinsler et al. 2000).

(6)

$$c = \sqrt{1 / (\kappa\rho)}$$

Resonator experiments utilized one seagrass shoot connected to a rhizome section. Each seagrass shoot consisted of 2 leaves for *Syringodium* shoots and 5-9 leaves for *Halodule* shoots. Only shoots with intact connections to the rhizome were used. Initial resonator experiments measured five replicate seagrass shoots that were held in complete darkness overnight. Following the first resonator experiment, the shoots were then brought outdoors for 1 h in afternoon sunlight. After 1 h, the seagrass shoots were returned to the laboratory and resonator measurements were repeated immediately. Finally, the total leaf length and the dry weight biomass were measured for each trial. A Student's paired t-test was used to evaluate significant differences ($p < 0.05$) in the mean response of effective sound speeds measured after dark and light treatments.

Seagrass Bubbles

Separate laboratory measurements examined the characteristics of free gas bubbles emanating from both *Halodule* and *Syringodium* leaves. For these measurements, whole seagrass plants were placed in a glass container with filtered and aerated seawater from the Gulf of Mexico. Rhizome sections of the plant were anchored with a weight and artificial light was placed above the glass container. Once bubble streams were identified, a ruler was suspended within the container directly behind a bubble stream as a measurement scale. The bubble stream was recorded using a high-definition digital camera. Images from the clearest portions of the video recording were enhanced and bubble radii were measured using ImageJ software (Abramoff et al. 2004). Most of the bubbles were not spherical, but rather elongate in shape so a vertical, horizontal, and bisecting diameter was obtained for each of 10 bubbles for each seagrass species. The largest of the three diameters – usually the vertical measurement – was used to calculate a bubble radius and radii from the 10 bubbles were averaged for each species. Finally,

the mean rate of leaf bubble formation (bubbles min^{-1} $leaf^{-1}$) was calculated from video observations of three individual leaves from whole *Syringodium* and *Halodule* plants. A Student's t-test was used to test for significant differences ($p < 0.05$) in the mean bubble radii and bubble formation rates between species.

Results

24-Hour Experiments

Sound transmission varied over time for all three species during a 24-h period (Figure 3.2). In the *Syringodium* experiment, received acoustic energy increased overnight and then declined rapidly from 0800 to 0900, which corresponds to an increase in measured irradiance from 374 µmol photons m^{-2} s^{-1} to 479 µmol photons m^{-2} s^{-1}. Although *Halodule* plants also altered sound transmission, the observed pattern was different from *Syringodium*. In the *Halodule* experiment, sound transmission progressively decreased overnight and then increased rapidly from 0800 to 0900, which corresponds to a large increase in measured irradiance from 289 µmol photons m^{-2} s^{-1} to 1313 µmol photons m^{-2} s^{-1}. These higher transmission levels were generally sustained throughout the daylight hours. Transmission levels varied throughout the entire *Thalassia* experiment and differed from both *Syringodium* and *Halodule* experiments. However, this study did not document any consistent trends in acoustic transmission occurring with time of measurement or levels of surface irradiance for this species. There was a greater range in the mean acoustic intensity of received energy observed during the *Halodule* trials (4.7 dB) than in the *Thalassia* (4.4 dB) or *Syringodium* (3.5 dB) trials. Maximum irradiance levels were similar for all species, but intermittent cloud cover produced more variation in irradiance values during the *Halodule* trial (Figure 3.3).

Morning Photosynthesis Experiments

Differences in the photosynthetic capacity of *Halodule* and *Syringodium* plants emerged during the morning photosynthesis experiments (Figure 3.4a). P_{max} was significantly higher ($p < 0.01$) for *Syringodium* plants compared to *Halodule* plants (Table 3.1). This difference was evident in both chemical (*Syringodium* = 275.5 µmol O_2 g^{-1} dw leaf h^{-1}, *Haldoule* = 177.0 µmol O_2 g^{-1} dw leaf h^{-1}) and acoustic (*Syringodium* = 209.3 µmol O_2 g^{-1} dw leaf h^{-1}, *Halodule* = 126.5 µmol O_2 g^{-1} dw leaf h^{-1}) measurements of oxygen production. Saturation irradiance (I_k) was higher for *Halodule* plants and compensation irradiance (I_{cp}) was higher for *Syringodium* plants (Table 3.2). Both of these trends were also evident in the chemical and acoustic measurements. The light-limited slope of the *P vs I* curve (α) was significantly higher ($p < 0.01$) in *Syringodium* compared to *Halodule* in chemical measurements, but no significant difference was observed in acoustic measurements. Tank respiration rates were much lower in the *Halodule* trials (45.7 µmol O_2 g^{-1} dw leaf h^{-1}) compared to the *Syringodium* trial (136.2 µmol O_2 g^{-1} dw leaf h^{-1}).

During the morning photosynthesis experiments, both species exhibited an increase in sound propagation with increasing irradiance (Figure 3.4b). These trends are significant ($p < 0.05$) for both species, but there is far more variation around this trend for *Halodule* (r^2=0.16) compared to *Syringodium* (r^2=0.69). Acoustic *P vs. I* curves calculated significantly ($p < 0.05$) lower values for P_{max} for both seagrass species (Table 3.3). No significant differences were detected for acoustic and chemical determinations of α for either species. In an overall comparison of chemical and acoustic models for both species, acoustic models consistently underestimated P_{max}, I_k and I_c while overestimating α.

Resonator Experiments

Resonator measurements revealed that the acoustic compressibility of the leaf tissue changed with the onset of irradiance (Figure 3.6). However, no significant difference ($p > 0.05$) in the means of the effective sound speeds was observed between light and dark treatments for either species. Changes in tissue compressibility were not consistent across replications of *Syringodium* or *Halodule*. The compressibility of the plant tissue generally decreased for both species, but increased compressibility was also observed in one replication of the *Syringodium* and two replications of the *Halodule* trials. During the period of illumination, bubble streams were seen flowing from the plant material for both species. This suggests that the plants remained in light for a sufficient period of time to allow for leaf pressurization and subsequent changes in compressibility.

Seagrass Bubble Measurements

Measurements of bubble size revealed that the bubble radii were significantly larger emanating ($p < 0.05$) from *Syringodium* leaves than *Halodule* leaves (Table 3.4). The rate of bubble production was higher on average for *Halodule* leaves (*Halodule* = 52.3 ± 31.4 bubbles min^{-1} $leaf^{-1}$; *Syringodium* = 44.1 ± 27.5 bubbles min^{-1} $leaf^{-1}$), but was highly variable for both species (*Halodule* = 29-88 bubbles min^{-1} $leaf^{-1}$; *Syringodium* = 14-68 bubbles min^{-1} $leaf^{-1}$) and not statistically significant ($p = 0.75$). When the mean bubble size and formation rate are combined, *Syringodium* leaves released slightly more free gas than *Halodule* leaves during this analysis (*Syringodium* = 1.45 mL $leaf^{-1}$ h^{-1}; *Halodule* = 2.16 mL $leaf^{-1}$ h^{-1}).

Discussion

24-Hour Experiments

This work corroborates earlier studies that illustrate the importance of oxygen evolution in altering acoustic propagation within seagrass meadows. In the 24-h experiments, the received acoustic energy in the *Syringodium* trial decreased markedly during the morning hours, which is a very similar result to each of the previously published *Posidonia* experiments (Hermand et al., 1998; Hermand 2004). Bubble streams are clearly evident during this time period and are likely responsible for the attenuation of acoustic energy. In contrast*, Halodule* plants altered sound propagation quite differently from both *Syringodium* and *Posidonia*. Specifically for a *Halodule* canopy, there were two distinct acoustic states corresponding to illumination. During dark periods, the received acoustic energy steadily declined. With the onset of light, there was a rapid transition to a state of increased acoustic transmission. Finally, although no consistent trend in sound propagation was observed during the 24-h *Thalassia* experiment, the mean intensity of received acoustic energy was not consistent throughout the time period. These results clearly illustrate unique differences in acoustic transmission between the seagrass species.

It is not surprising that *Syringodium* and *Halodule* plants differ as a medium for sound propagation. Earlier work has shown that total biomass and leaf morphology influence the acoustic compressibility of a seagrass and seawater medium (Wilson and Dunton 2009). Both the shoot density and the total biomass of *Halodule* plants far exceeded *Syringodium* plants in this study (Table 3.5). Bubble measurements also revealed that the size of bubbles is significantly different between each of the two species, and it is well known that the interaction of acoustic energy and free gas bubbles is highly dependent on the bubble radii and the frequency of energy (Medwin 1977). Finally, Wilson et al. (2010) demonstrated that the leaf structure of *Halodule* plants is far more compressible than *Syringodium* plants (*Halodule* = 6.73 x 10^{-7} Pa^{-1}; *Syringodium* = 3.50 x 10^{-8} Pa^{-1}). It is therefore possible that the mechanical properties

of the leaf structure are more susceptible to change in *Halodule* plants as a result of internal pressurization or temperature differences occurring on daily cycles. At this point, the relative contributions of bubble production and changes in leaf mechanical properties to sound propagation are not fully resolved. However, we hypothesize that bubble formation is the principle mechanism involved in producing the 24-h trend observed in the *Syringodium* experiment, while changes in the mechanical properties of the leaf tissue are responsible for the observed trends in the *Halodule* 24-h experiment. Given the striking differences observed in the *Halodule* and *Syringodium* experiments, it is difficult at this time to extrapolate these results to additional seagrass species and leaf morphologies.

Resonator Experiments

Resonator measurements illustrated that the acoustic compressibility of seagrass tissue changes upon illumination. Compressibility generally decreased with exposure to light and provided evidence for leaf pressurization during photosynthesis. It is important to note, however, that the change in compressibility varied in magnitude and that an increase in compressibility was also observed. This variation is likely attributed to the structural integrity of individual leaves. Older leaves or leaves with tissue damage may allow for gas to escape and provide a pressure-release mechanism. Bubble streams flowing from the leaf tissue provide evidence for such a mechanism. Furthermore, heating of the leaf tissue without a paired increase in internal pressure of the leaf may serve to increase the compressibility of a leaf structure. Conversely, intact shoots that do not vent bubble streams allow for the transport of photosynthetically produced oxygen, and it is possible in this scenario that both the leaf and rhizome tissues become pressurized during transport. This pressurization would serve to decrease the compressibility of the tissue. In conclusion, the structural integrity of the leaf

would play a large role in mediating leaf pressurization and subsequent changes acoustic compressibility.

Morning Photosynthesis Experiments

Chemical measurements of morning oxygen evolution and the photosynthetic capacity of *Syringodium* and *Halodule* plants differed somewhat from other published studies. The photosynthetic parameters of P_{max} and I_c derived from chemical measurements for *Halodule* are within the ranges previously published by Dunton and Tomasko (1994) for this same species. However, values of α (0.33 μmol O_2 g^{-1} dw leaf h^{-1}(μmol photons m^{-2} s^{-1})$^{-1}$; 0.5-1.6 μmol O_2 g^{-1} dw leaf h^{-1} (μmol photons m^{-2} s^{-1})$^{-1}$ Dunton and Tomasko 1994) and I_k (536 μmol photons m^{-2} s^{-1}; 37-177 μmol photons m^{-2} s^{-1} Dunton and Tomasko 1994) are not within previously described ranges for *Halodule*. For the *Syringodium* experiment, derived values of P_{max} and α are within ranges previously published by Major and Dunton (2000), but I_c (162.1 μmol photons m^{-2} s^{-1}) and I_k (328.3 μmol photons m^{-2} s^{-1}; 370 μmol photons m^{-2} s^{-1} Major and Dunton 2000) are somewhat different. The described differences in the photosynthetic parameters are attributed to dissimilarities in the experimental design. In both the Dunton and Tomasko (1994) and Major and Dunton (2000) experiments, plants were incubated within closed chambers. In order to limit the formation of gas bubbles, these experiments also artificially reduced the saturation state of the water column. Neither of these conditions was possible in the present study. Bubbles are the most obvious mechanism altering acoustic propagation within a vegetated substrate. As a result, although a closed system and an artificial reduction of the oxygen saturation state would improve measurements of dissolved oxygen concentrations, this design would produce an unnatural condition for bubble formation, rise and release. The experimental design implemented in this

study presented a trade-off, which ensured natural bubble dynamics while underestimating total oxygen production.

Considering the individual mechanisms involved, there is remarkable agreement between the chemically and acoustically derived photosynthetic parameters. This agreement is more evident for *Syringodium* than *Halodule* and varies based on individual parameters (Table 3.2). For both species, the acoustically derived parameters underestimated the chemical determinations of P_{max}, I_k and I_c while overestimating α. The shared characteristics of the acoustically derived parameters in both species are encouraging and suggest a few general qualities of acoustic photosynthetic measurements. First, acoustic changes occurring during photosynthesis are smaller in magnitude than chemical changes in dissolved oxygen, which results in an underestimation of P_{max} and subsequently of I_k and I_c. Second, differences in sound propagation occur more rapidly during photosynthesis compared to changes in dissolved oxygen concentrations. The rapid changes in sound propagation result in a larger value of α than is determined chemically. The general similarity between chemical and acoustic parameters is remarkable considering sound propagation is not affected by changes in dissolved oxygen concentrations. This suggests that some other mechanism must be occurring concurrently and with comparable magnitude as the changes in dissolved oxygen concentrations. Both free gas production and leaf pressurization are known to increase with irradiance in submerged macrophytes (Roberts and Caperon 1986; Dacey 1981). An increase in free gas production would decrease acoustic propagation. Conversely, leaf pressurization would increase sound propagation. Since sound propagation generally increased for both species during morning photosynthesis experiments, it is logical to conclude that leaf pressurization is more important acoustically during this period of time.

Implications for Acoustic Remote Sensing

The dynamic acoustic signature of individual seagrass species is a characteristic that warrants consideration in future acoustic mapping efforts of submerged vegetation. In acoustic surveys of the benthos, the acoustic designation of a particular feature is determined from a series of acoustic signatures paired with direct visual observations of the same locations (Pasqualini et al. 2001; Mulhearn 2001). The acoustic signature of seagrass meadows is determined largely from the backscatter strength of the meadow, which is significantly higher than in bare sediments (Warren and Peterson 2007). This study has demonstrated that high-frequency acoustic transmission within a seagrass canopy changes as much as 3.5 – 4.7 dB during a single daily cycle. As a result, the acoustic signature of a seagrass meadow is not a consistent feature when surveyed at different times throughout the day. Future acoustic surveys of submerged vegetation should therefore ground-truth acoustic signatures of seagrass species during multiple time periods throughout the day in order to improve the accuracy of areal cover and biomass estimates.

The pairing of chemical and acoustic methods provides a complementary analysis of seagrass primary production. Dissolved oxygen measurements are the most widely-used and longest-tenured method for measuring oxygen production in seagrass plants (Silva et al. 2009). However, these measurements are not capable of assessing free gas evolution and are restricted to water conditions below oxygen saturation. Since saturation is quickly achieved in a seagrass environment, *in situ* chemical measurements of oxygen production are only applicable in the early morning hours or if the saturation state of the water column is artificially reduced. Conversely, sound propagation is largely unaffected over short distances by dissolved gasses, but is significantly attenuated in the presence of free gas bubbles. As a result, the coupling of

chemical and acoustic methods affords an investigator with the capability to assess the production of oxygen in both the gaseous and dissolved states and delivers a thorough evaluation of the health and condition of seagrass meadows.

Seagrass Bubble Production

The production of free gas bubbles by leaf and rhizome tissues of seagrass plants is a physiological mechanism that warrants further investigation. In this study, the rate of leaf bubble production varied markedly between leaves, with some leaves producing no bubbles at all (Table 3.4). It appears, qualitatively, that the bubble production rate is comparable to the bubble size. Larger bubbles form and are released at a slower rate compared to small bubble streams. Although bubble streams clearly form along newly damaged sections of a leaf, natural explanations for bubble streams, other than herbivory, are not immediately apparent. It is possible that high rates of herbivory or anthropogenic sources of tissue damage could result in increased bubble formation. This would serve to further decrease acoustic transmission and alter some of the general trends reported here. Specifically, in locations with prominent tissue damage, bubble production may be more important that leaf pressurization in acoustic measurements of seagrass photosynthesis.

Seagrass bubble production is also important ecologically. It is widely accepted that seagrasses possess a lacunae system that transports photosynthetically derived oxygen into an anoxic rhizosphere (Kemp and Murray 1986). Every bubble produced along a leaf edge reduces the ability of the seagrass plant to oxidize the rhizosphere. Using the mean bubble radius (*Halodule* = 0.48 mm, *Syringodium* = 0.58 mm) and bubble production rate (*Halodule* = 52.3 bubbles $leaf^{-1}$ min^{-1}, *Syringodium* = 44.1 bubbles $leaf^{-1}$ min^{-1}) measured in this study, it was

possible to estimate the amount of oxygen lost from the seagrass leaf to the overlying water column (*Halodule* = 65 µmol O2 $leaf^{-1}$ h^{-1}, *Syringodium* = 96 µmol O2 $leaf^{-1}$ h^{-1}). These values represent a significant sink of oxygen to the water column and illustrate how extensive leaf damage may inhibit the growth of seagrasses in reducing sediments. Since there are no obvious benefits associated with releasing gas bubbles to the water column, it is advantageous for seagrass plants to repair damaged tissues quickly in order to ensure transport of oxygen to the rhizosphere. Furthermore, in locations with reduced soils and increased herbivory, it is logical to hypothesize that seagrass plants that repair tissues quickly have a competitive advantage over other species.

Conclusion

The seagrass acoustic experiments described here are the first to use high-frequency (100 kHz) sound energy to monitor oxygen evolution. In previously published *Posidonia oceanica* experiments, a lower frequency range (0.1 - 16.0 kHz) and a much longer propagation distance (53-1541 m) were used (Hermand et al. 1998; Hermand 2004). By increasing the frequency of energy, we were able to conduct these experiments in shallow water (0.50 m) and over a very short propagation distance (0.45 m), which is suitable to any seagrass environment. Although it is now clear that sound transmission at both high and low frequencies is altered by photosynthesis, the interaction of species and sound frequency is less obvious. The mechanical properties of the plant leaves and the radii of bubbles released from the tissue vary markedly between different seagrass species. These differences likely affect the propagation of some sound frequencies more than others. Future studies should therefore investigate a wider range of sound frequencies in order to calibrate acoustic measurements to species-specific physiological mechanisms of interest. Further calibrations of acoustic measurements may then help to

distinguish the relative importance of bubble production and tissue compressibility on acoustic transmission.

References

Abramoff, M.D., Magalhaes, P.J., Ram, S.J. "Image Processing with ImageJ". Biophotonics International, volume 11, issue 7, pp. 36-42, 2004.

Caffrey, J.M. and W. M. Kemp, 1991. Seasonal and spatial patterns of oxygen production, respiration and root rhizome release in *Potamogeton perfoliatus* L. and *Zostera marina* L. *Aquat. Bot*., Vol. 40, pp. 109-128.

Dacey, J. W. H. 1981. Pressurized ventilation in the yellow waterlily. *Ecology*. Vol. 62, pp. 1137-1147.

Dunton, K.H., Tomasko, D.A., 1994. In situ photosynthesis in the seagrass *Halodule wrightii* in a hypersaline subtropical lagoon. *Mar. Ecol. Prog. Ser*. 107, 281–293.

Fourqurean, J.W. and J.C. Zieman. (1991). Photosynthesis, respiration and whole plant carbon budget of the seagrass *Thalassia testudinum*. *Mar. Ecol. Prog. Ser*. 69: 161-170.

Hermand, J.P., Nascetti, P., Cinelli, F., 1998. Inversion of acoustic waveguide propagation features to measure oxygen synthesis by Posidonia oceanica: Proceedings of the Oceans ’98 IEEE/OES Conference, Vol. 2, pp. 919–926.

Hermand, J.P. 2006. Continuous acoustic monitoring of physiological and environmental processes in seagrass prairies with focus on photosynthesis. In: Caiti A, Chapman NR, Hermand JP, Jesus S (eds) Acoustic sensing techniques for the shallow water environment: inversion methods and experiments. Springer, Dordrecht, p 183–196.

Jassby, A.D. and T. Platt. (1976). Mathematical formulation of the relationship between photosynthesis and light for phytoplankton. *Limnol. Oceanogr*. 21: 540-547.

Kinsler, L.E., Frey, A.R., Coppens, A.B., Sanders, J.V., 2000. Fundamentals of acoustics.Wiley, New York

Komatsu, T., C. Igarashi, K. Tatsukawa, S. Sultana, Y. Matsuoka, and S. Harada, 2003. Use of multi-beam sonar to map seagrass beds in Otsuchi Bay on the Sanriku Coast of Japan,” *Aquat. Living resource*, Vol. 16, pp. 223-230.

Major, K. M., K. H. Dunton. 2000. Photosynthetic performance in *Syringodium filiforme*: seasonal variation in light-harvesting characteristics. *Aquat. Bot*. Vol. 68, pp. 249-264.

Medwin, H. 1977. Acoustical determinations of bubble-size spectra. *J. Acoust. Soc. Am*. Vol. 62, pp. 1041-1044.

Mulhearn, P.J., 2001. Mapping seabed vegetation with sidescan sonar,” DSTO Report No. TN-0381, Defense Science and Technology Organization, Australia.

Pasqualini, V., P. Clabaut, G. Pergent, L. Benyoussef, and C. Pergent-Martini, 2000. Contribution of side scan sonar to the management of Mediterranean littoral ecosystems. *Int. J. Remote Sens*., Vol. 21, pp. 367-378.

Paul, M., A. Lefebvre, E. Manca, C.L. Amos. 2011. An Acoustic method for the remote measurement of seagrass metrics. *Estuarine, Coastal and Shelf Science*. Vol. 93, pp. 68-79.

Roberts, D. G., J. Caperon. 1986. Lacunar gas discharge as a measure of photosynthesis in seagrasses. *Mar. Ecol. Prog. Ser*. Vol. 29, pp. 23-27.

Schuette, J. L., M. J. Klug. 1995. Evidence for mass flow in flowering individuals of the submersed vascular plant *Myriphyllum heterophyllum*. *Plant Physiol*. Vol. 108, pp. 1251-1258.

Silva, J., Y. Sharon, R. Santos, S. Beer, 2009. Measuring seagrass photosynthesis: methods and applications. *Aquat Biol*. Vol. 7, pp. 127-141.

Warren, J. D., B. J. Peterson. 2007. Use of a 600-kHz Acoustic Doppler Current Profiler to measure estuarine bottom type, relative abundance of submerged aquatic vegetation, and eelgrass canopy height. *Estuarine, Coastal and Shelf Science*. Vol. 72, pp. 53-62.

Wilson, P.S. and K. Dunton, 2009. Laboratory investigation of the acoustic response of seagrass tissue in the frequency band of 0.5-2.5 kHz. *J. Acoust. Soc. Am*., Vol. 125, pp. 1951-1959.

Wilson, C.J., P.S. Wilson, C.A. Greene, and K.H. Dunton. 2010. Seagrass leaves in 3-D: Using computed tomography and low-frequency acoustics to investigate the material properties of seagrass tissue. *Journal of Experimental Marine Biology and Ecology*. Vol 35 pp. 128-134.

Figure 3.1.

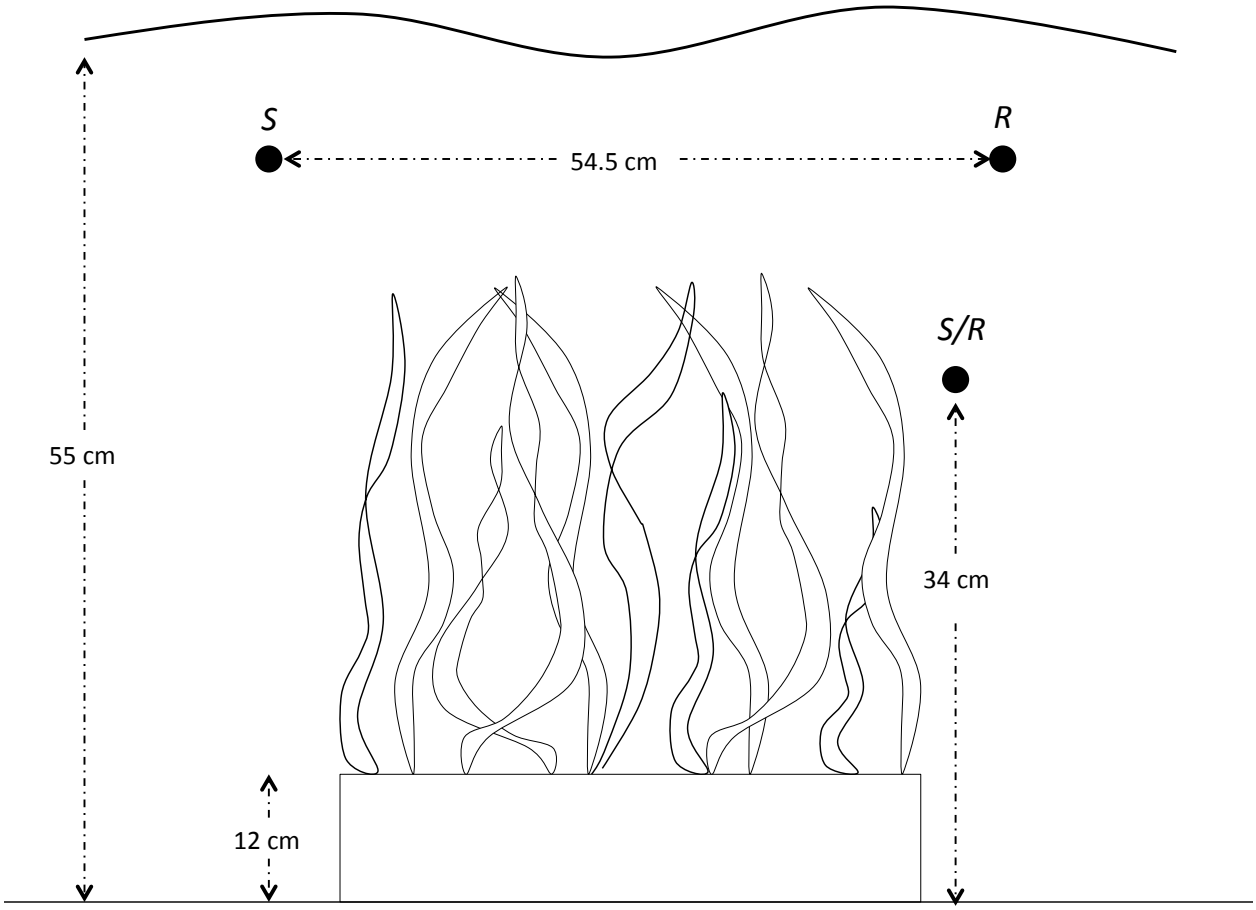

Figure 3.1. Orientation of the sound source (S) and receiver (R) in relation to the seagrass canopy in the outdoor experimental tank. The mean canopy height for *Syringodium* (33.4 ± 9.0 cm) *Halodule* (32.8 ± 6.5 cm) and *Thalassia* (37.0 ± 9.4 cm) was calculated from the sum of mean leaf length (n = 30) and sediment height (12 cm).

Figure 3.2a.

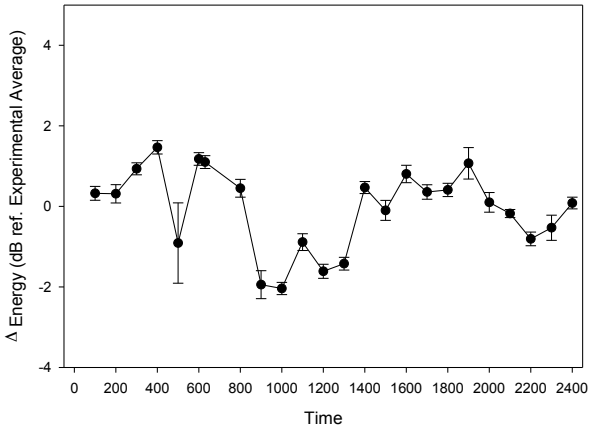

Figure 3.2b.

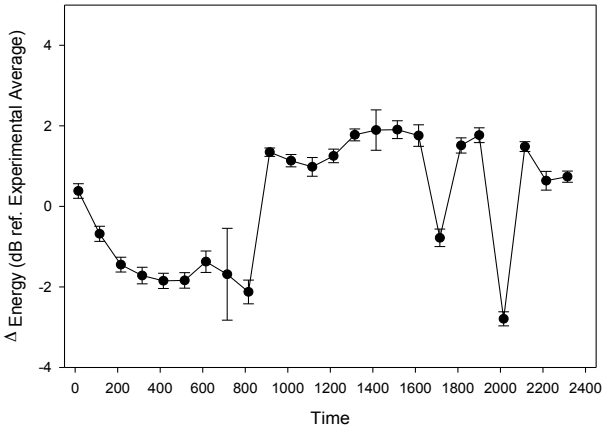

Figure 3.2c.

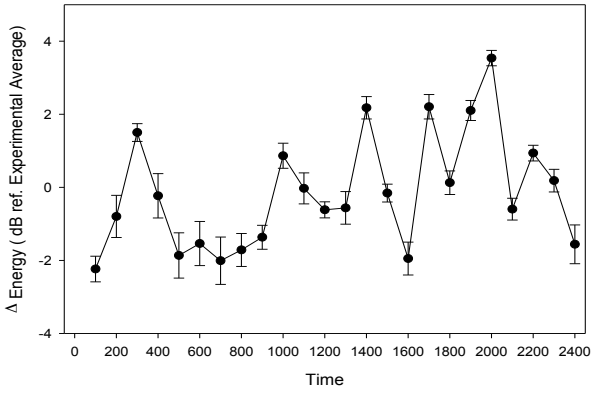

Figure 3.2. Change in received acoustic energy over the 24-h experiment for a) *Syringodium filiforme*, b) *Halodule wrightii* and c) *Thalassia testudinum*. Data points represent the mean acoustic intensity relative to the 24-h experimental average and the error bars represent standard deviation (n=10).

Figure 3.3.

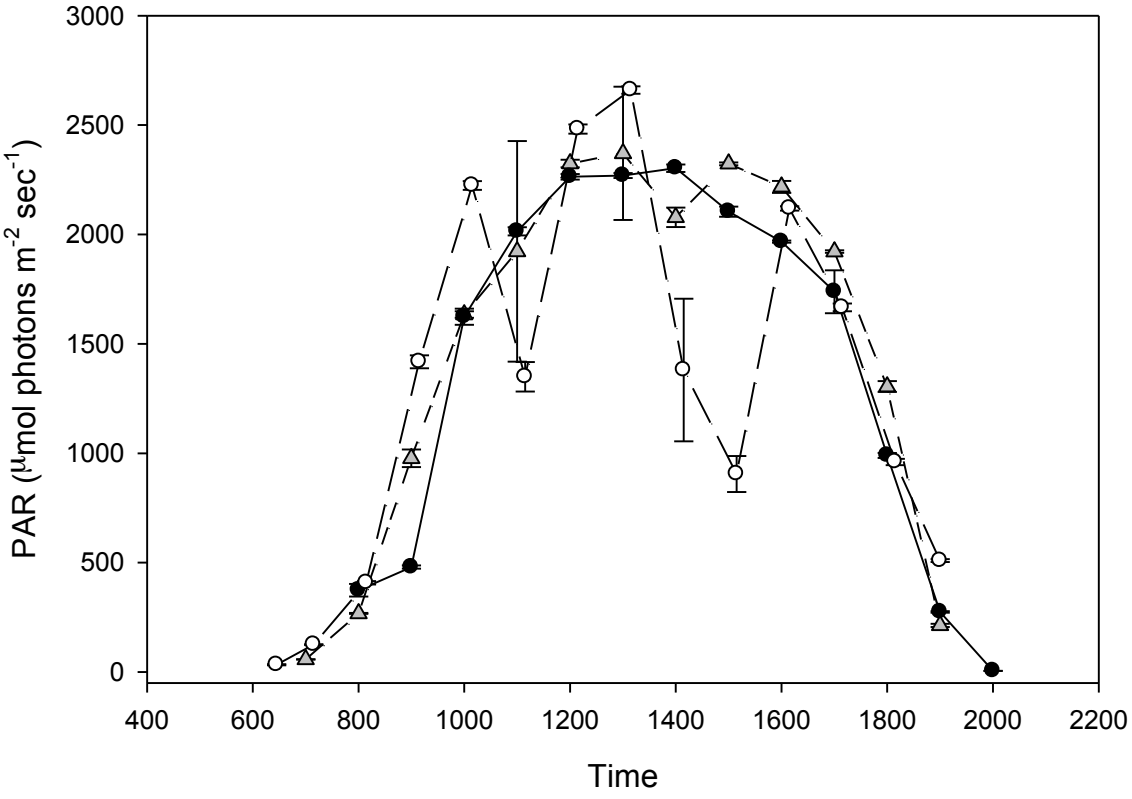

Figure 3.3. Photosynthetically active radiation (PAR) measured each hour during the 24-h experiments. Filled circles represent the mean value for the *Syringodium,* empty circles represent the mean value of the *Halodule*, and triangles the mean value of the *Thalassia* experiment (n = 5 replicate light measurements obtained each hour). Error bars represent standard deviation.

Figure 3.4a.

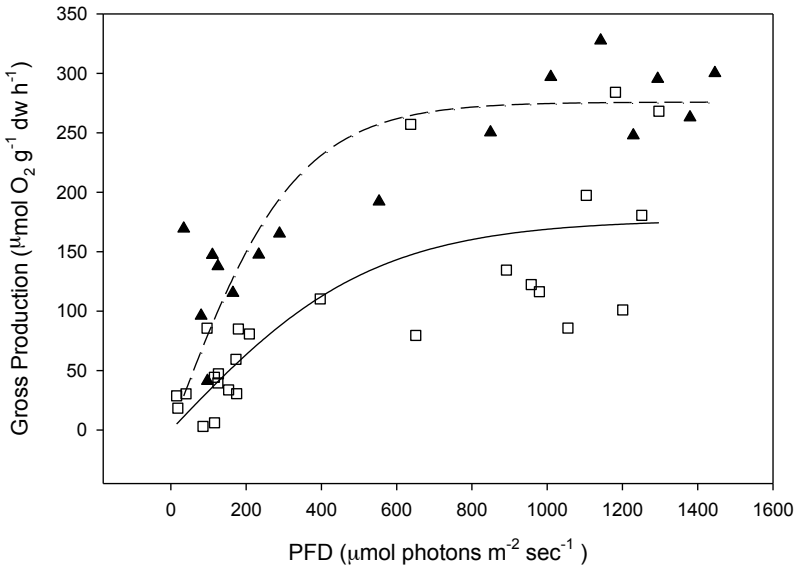

Figure 3.4b.

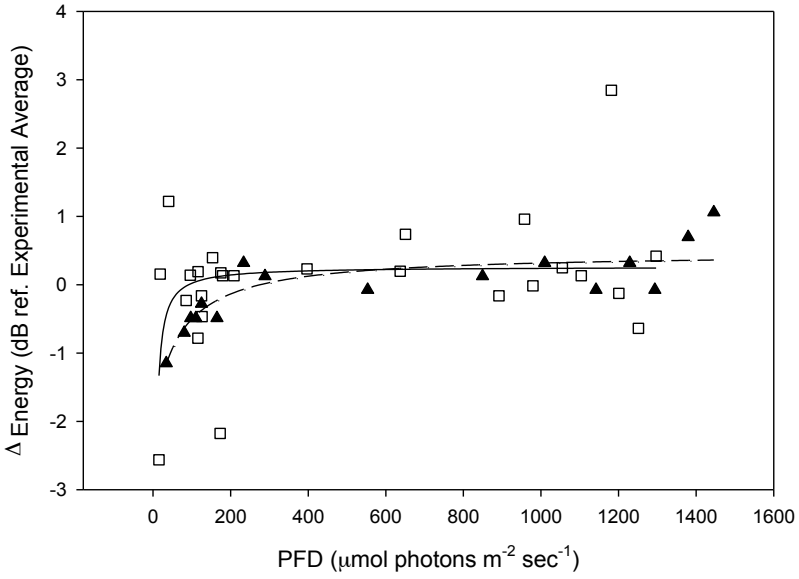

Figure 3.4. Relationship between surface photon flux density (PFD) and a) gross production measured chemically from dissolved oxygen and b) acoustic intensity relative to the morning experimental average. Triangles represent *Syringodium* observations and squares represent *Halodule* observations.

Figure 3.5a.

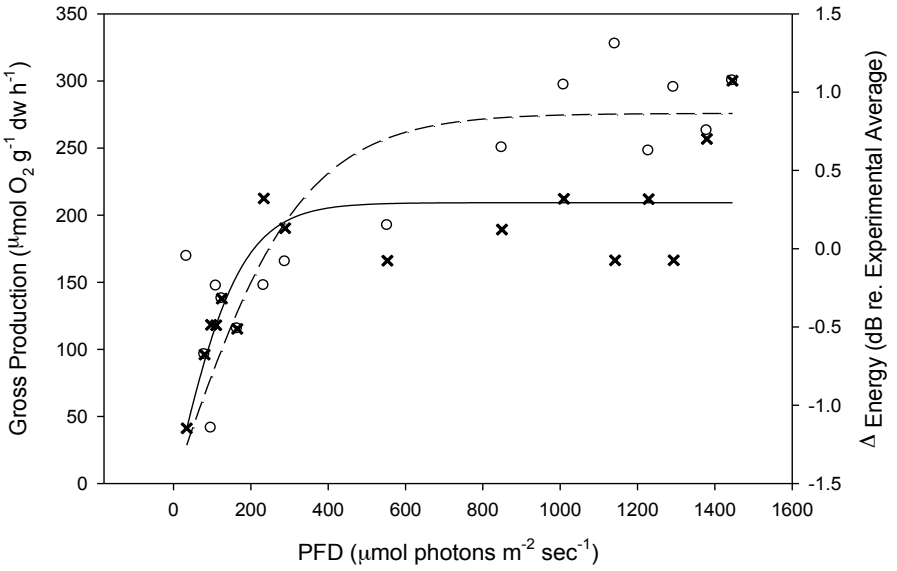

Figure 3.5b.

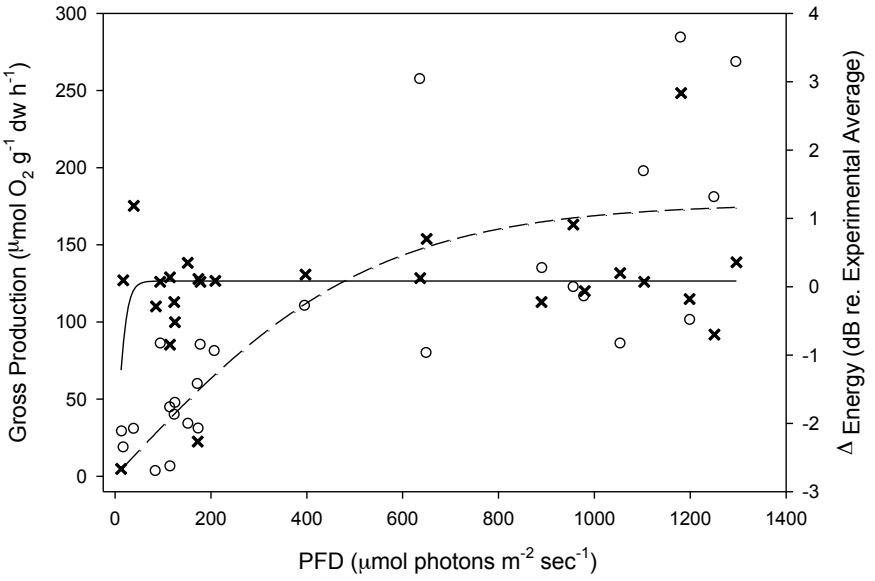

Figure 3.5. Photosynthesis vs. irradiance curves generated chemically (empty circles) and acoustically (x) for a) *Syringodium* and b) *Halodule*.

Figure 3.6.

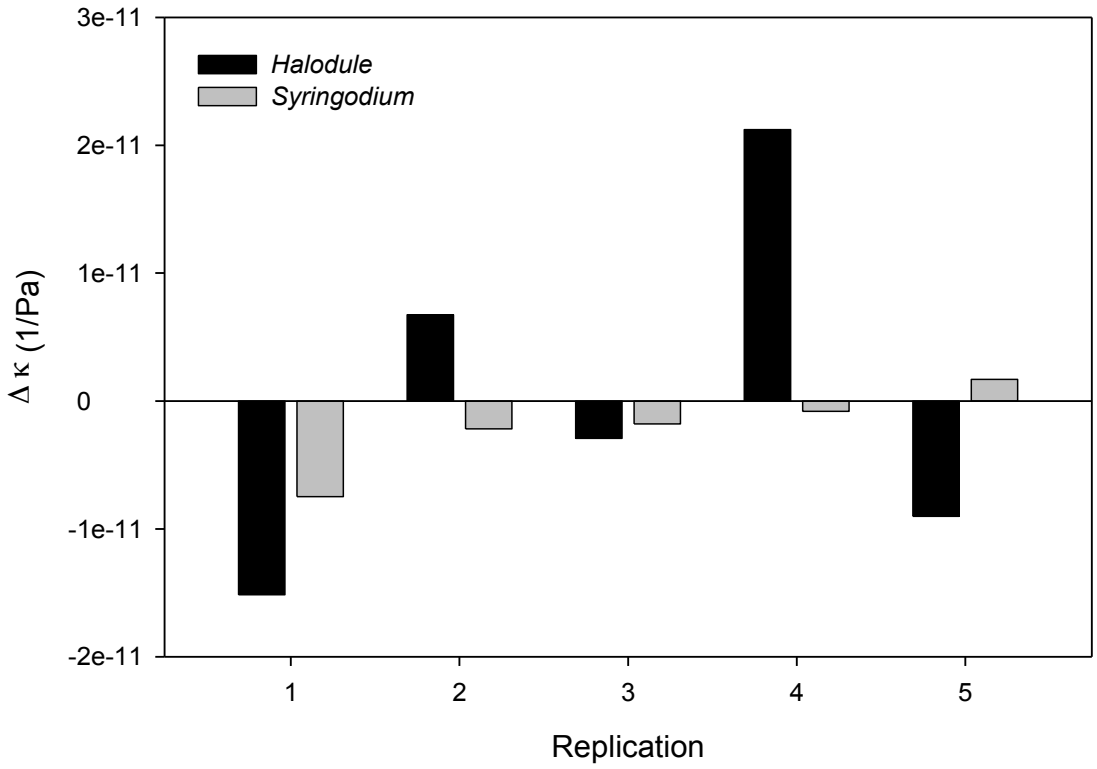

Figure 3.6. Change in compressibility (κ) of the seagrass + seawater medium after 1 h of afternoon sunlight for the acoustic resonator measurements. Each replication represents an independent shoot connected to a section of rhizome.

Table 3.1. Statistical species comparison of nonlinear regression coefficients calculated in the P vs. I curves generated chemically and acoustically during morning photosynthesis experiments.

	Chemical			
	Halodule wrightii	*Syringodium filiforme*	z-value	*p*-value
P_{max}	177	275.8		
P_{max} (SE)	22.85	19.67	3.28	< 0.01
α	0.33	0.84		
α (SE)	0.10	0.17	5.26	< 0.01
	Acoustic			
	Halodule wrightii	*Syringodium filiforme*	z-value	p-value
P_{max}	126.5	209.3		
P_{max} (SE)	8.57	12.68	5.41	< 0.01
α	6.12	1.22		
α (SE)	3.15	0.21	1.55	0.12

Table 3.2. Seagrass physiological parameters calculated from morning photosynthesis experiments. Acoustically derived parameters were calculated using equivalent values of gross production and assuming a 1:1 relationship between the chemical and acoustic measurements. The *Halodule* experiment was conducted over three separate mornings in order to achieve a wide range of light levels. For this species, $R_{chamber}$ was calculated for each of the three individual mornings. Therefore, $R_{chamber}$ and the subsequent calculation for I_{cp} represent the mean value for this experiment (n=3).

	Halodule wrightii		*Syringodium filiforme*	
	Chemical	Acoustic	Chemical	Acoustic
P_{max} (µmol O2 g-1 dw h-1)	177	126.5	275.8	209.3
$R_{chamber}$ (µmol O2 g-1 dw h-1)	45.71		136.19	
α	0.33	6.12	0.84	1.22
I_k (µmol photons m-2 s-1)	536.4	20.6	328.3	171.6
I_{cp} (µmol photons m-2 s-1)	138.5	7.5	162.1	111.6

Table 3.3. Statistical comparison of nonlinear regression coefficients calculated in chemical and acoustic *P vs. I* curves for *Syringodium* and *Halodule*.

	Halodule wrightii			
	Chemical	Acoustic	z-value	*p*-value
P_{max}	177	126.5		
P_{max} (SE)	22.85	8.57	2.07	0.039
α	0.33	6.12		
α (SE)	0.0955	3.145	1.84	0.066
r^2	0.6	0.16		
	Syringodium filiforme			
	Chemical	Acoustic	z-value	*p*-value
P_{max}	275.8	209.3		
P_{max} (SE)	19.67	12.68	2.84	0.0045
α	0.84	1.22		
α (SE)	0.167	0.21	1.42	0.1556
r^2	0.65	0.69		

Table 3.4. Species comparison of mean bubble radius (n = 10) and bubble formation rate (n = 3).

	Syringodium	***Halodule***	
Seagrass Bubble Radius (mm)	0.58 ± 0.03	0.48 ± 0.13	$p < 0.05$
Bubble Formation Rate (Bubbles min^{-1})	44.1 ± 27.5	52.3 ± 31.4	n.s.

Table 3.5. Measurements of seagrass morphology acquired after the 24-h acoustic experiments. Leaf length (n=30) and epiphytic biomass (n=3) values represent the mean ± standard deviation.

	Syringodium	***Halodule***	***Thalassia***
Leaf Length (cm)	21.4 ± 9.0	20.8 ± 6.5	25.0 ± 9.4
Above-Ground Biomass (g DW)	17.61	37.24	27.6
Below-Ground Biomass (g DW)	19.86	93.61	43
Epiphytic Biomass (DW Epiphytes: DW Leaf Tissue)	0.13 ± 0.01	0.11 ± 0.04	0.23 ± 0.02
Shoot Density (shoots m^{-2})	2238	9725	550

Chapter 4

Seagrass meadows as an acoustic refuge for fish

Abstract

It has been widely accepted that fish reside within seagrass meadows because of the visual protection and structure provided by the standing biomass. However, for many larger species of estuarine fish, marine mammals that use echolocation to forage represent a significant threat. We hypothesized that seagrasses may serve as an acoustic refuge to fish from marine mammal predators by sufficiently attenuating the high-frequency sounds used in echolocation. In order to test this hypothesis, we measured the attenuation of a 100 kHz acoustic signal with increasing distance into a seagrass meadow. The transmission loss of low-frequency sound energy relevant to fish calls (300 Hz to 500 Hz) was also investigated in order to address the hypothesis that marine mammals may use passive acoustic detection to locate fish in vegetated substrates. Our results show that seagrasses attenuate high-frequency sounds during summer months and reduce prey detection thresholds by 58% to 88% relative to bare substrates. Also, based on the low-frequency hearing threshold of bottlenose dolphins, we calculated that passive acoustic detection of low-frequency fish calls are audible to dolphins in vegetation at a distance of roughly 2.50 m to 4.25 m, which is within the detection threshold of 2.82 m to 9.81 m for dolphins using echolocation. This study demonstrates that acoustically complex features, such as seagrass meadows, can significantly alter bioacoustic signal transmission, possibly providing an important seasonal refuge to fish from marine mammal predators.

Introduction

Estuaries possess highly productive soundscapes where marine mammals use high- and low-frequency sounds to communicate and find prey, while many fish species generate low-frequency calls used in communication (Au and Hastings 2008; Ramcharitar et al. 2006; Roundtree et al. 2006). Although sound propagation is important in a variety of ecological relationships, very few studies to date have examined the biological significance of acoustic transmission loss within estuaries containing vegetated substrates. One such study, published by Quintana-Rizzo et al. (2000), examined the propagation distance of low-frequency whistles used by dolphins and porpoises over multiple substrate types. Quintana-Rizzo et al. (2000) showed that seagrass meadows caused increased attenuation of low-frequency (5 kHz to 19 kHz) whistles, which significantly decreased effective communication distances. Consequently, it is logical to hypothesize that seagrass meadows attenuate the high-frequency clicks used by marine mammals for echolocation, serving to provide fish an acoustic refuge from marine mammal predators.

Bottlenose dolphins (*Tursiops truncatus*) feed predominantly on fish that can be found within seagrass meadows, but the use of these meadows as foraging habitat is still under debate. Barros and Wells (1998) related the stomach contents of stranded bottlenose dolphins to shipboard feeding observations of the same individuals and noted that pinfish (*Lagodon rhomboides*) dominated their diet. Barros and Wells (1998) reported that foraging often occurred in the vicinity of seagrass beds, and hypothesized that dolphins may use passive acoustic detection to locate fish, since most of the documented prey species were soniferous. Later, Allen et al. (2001) documented the behaviors of foraging bottlenose dolphin groups with the use of shipboard surveys, comparing foraging locations with measured abundances of pinfish within

bare and vegetated substrates. They reported that dolphins foraged extensively on the edge of seagrass beds, but rarely foraged in the middle of the vegetation despite higher concentrations of prey and hypothesized that submerged vegetation was limiting the success of prey capture (Allen et al. 2001).

Nowacek (2005) performed the first acoustic survey of bottlenose dolphin foraging near seagrass meadows, combining video observations with underwater acoustic recordings to document the types of calls used by dolphins in a variety of habitats. The lowest rates of echolocation were observed within vegetated substrates, and a low-frequency call, named a "pop," was observed in this dolphin population for the first time. Nowacek (2005) suggested that the cluttered seagrass environment might inhibit echolocation, and the pops, which are much lower in frequency than the echolocation clicks, may scare the fish out from the vegetation.

The free gas contained within the lacunae system of seagrass plants and the bubbles produced during photosynthesis attenuate sound energy within seagrass meadows (Hermand et al., 1998). Field investigations continue to document the unique acoustic signature of seagrass beds relative to bare substrates (Komatsu et al., 1998; Pasqualini et al., 2001; Mulhearn 2001). Acoustic modeling efforts in the laboratory have demonstrated that the interaction of sound energy and seagrass tissue is both species-specific and biomass-dependent (Wilson and Dunton 2009; Wilson et al., 2010).

This study tested the hypotheses that 1) seagrasses attenuate sound energy in the frequency range that is used by dolphins for echolocation and 2) that low-frequency sounds propagate far enough within vegetation to enable passive acoustic detection of fish calls. These hypotheses were tested by measuring transmission loss of high- and low-frequency sound energy

within bare and vegetated substrates in a shallow subtropical estuary. Our results suggest that seagrasses may provide an important seasonal refuge to fish from the high-frequency echolocation clicks emitted by potential dolphin predators. Furthermore, passive acoustic detection thresholds of low-frequency energy were within the range of detection thresholds measured for high-frequency echolocation, suggesting that passive acoustic detection of fish targets is not a viable alternative to echolocation for marine mammals foraging within seagrass meadows.

Methods

Study Site

Field experiments were conducted within the seagrass meadows of East Flats in Port Aransas, Texas (27° 49'N, 97° 07'W). This location contains pristine populations of both turtle grass (*Thalassia testudinum*) and shoal grass (*Halodule wrightii*), which were the focal species of vegetation examined in this work. Field experiments were conducted in February and June 2011. The water depth for all transmission loss measurements varied between 0.5 m to 1.0 m (February = 0.85 m to 1.0 m; June = 0.52 m to 0.63 m). Salinity and temperature ranged from 32.7‰ to 37.3 ‰ and 20.1°C to 29.8°C, respectively, throughout the entire study period, with little variation over each sampling date.

Transmission Loss

High-frequency transmission loss experiments utilized two hydrophones (Reson Model TC4033) and a pulser/receiver system (Olympus 5073PR). Both hydrophones were secured to weighted polyvinyl chloride (PVC) stands at a height of 0.34 m above the sediment. These stands allowed for rapid relocation of the hydrophones while ensuring a constant vertical

position above the sediment. Acoustic signals were transmitted at a direction parallel to the bottom and consisted of a 100 kHz transient sound pulse, of 5 ms in length, generated at a 200 Hz repetition rate by the pulser/receiver. The resulting signal has a broad spectrum centered around 100 kHz that resembles a dolphin echolocation signal. The receiving hydrophone was connected to the receive side of the pulser/receiver, which filtered (1 kHz to 20 MHz) and amplified the signal before reaching a digital storage oscilloscope. The acoustic pressure was obtained from the peak-to-peak amplitude of the average of 64 individual pulses that coincided with the direct path of acoustic transmission. A spherical spreading model provides a reasonable estimation of transmission loss for marine mammal clicks (DeRuiter et al. 2010). We therefore modeled acoustic transmission loss (TL) using Eq. 1, where R is the propagation distance and α is a coefficient representing the combined losses attributed to scattering and absorption. The α-value was obtained by using a nonlinear least-squares approach to fit a spherical spreading model (Eq. 2) to the observed data, where p is the observed acoustic pressure and p_o represents the initial pressure amplitude.

$$TL = 20 \log R + \alpha R \text{ , where} \quad (1)$$

$$p = (p_o / R) * e^{-\alpha R} \quad (2)$$

Low-frequency transmission loss experiments used a frequency generator and an underwater speaker (Electrovoice UW-30) connected to a power amplifier. The speaker was mounted on a weighted frame at a height of 0.20 m above the sediment and the receiving hydrophone was secured to a weighted PVC stand at a height of 0.34 m above the bottom. Low-frequency signals consisted of continuous 300 Hz, 400 Hz and 500 Hz pure sine tones, which are relevant to the frequencies used by soniferous fish residents of seagrass habitats (Ramcharitar et

al., 2006; Connaughton et al. 1997; Fine et al. 2004). Acoustic signals were transmitted in a direction parallel to the ocean bottom. The receiving hydrophone was connected to a charge amplifier, which both band pass filtered (10 Hz to 10 kHz) and amplified the signal before reaching the oscilloscope. The acoustic pressure was obtained from the root-mean-square voltage of the average of 64 individual waveforms.

Field surveys were conducted within both bare and vegetated substrates. High-frequency experiments investigated turtle and shoal grass meadows separately, while low-frequency experiments were conducted in meadows comprised of a mixture of both turtle and shoal grasses. For both winter (February) and summer (June) sampling events, high-frequency transmission loss was measured over a total distance of 0.25 m through 1.75 m in 0.25-m increments within each of the three substrate types. Three replicate transmission paths for each distance and substrate combination were investigated at each sampling event. The low-frequency transmission loss experiments were conducted as part of the June sampling event in both bare and vegetated substrates. Low-frequency transmission loss was measured for each of the three frequencies over a total distance of 1.0 m through 6.0 m in 1.0-m increments. Due to a loss in battery power, we were unable to measure the 5-m distance for the vegetated bottom treatment.

Seagrass Biomass

For both sampling events, a variety of morphological measurements were obtained for both turtle and shoal grass. At the conclusion of the acoustic experiments, seagrass biomass was collected from three replicate cores of diameter 0.10 m (*Halodule*) or 0.15 m (*Thalassia*). The core locations were randomly chosen within the path of acoustic transmission. The seagrass

material was then rinsed with filtered seawater at the laboratory and stored for no more than 72 h prior to analysis. For each seagrass core, the total number of shoots and the lengths of 30 randomly chosen leaves were recorded. The above-ground and below-ground biomass was then separated and dried to a constant weight in a 60°C oven. Finally, for each sampling date, three replicate shoots from each of the two species were used to measure epiphytic abundance. To quantify epiphyte cover, a known leaf area was scraped with a razor blade. The epiphytes were transferred from the blade to a pre-weighed filter and dried to a constant weight in a 60°C oven. The epiphyte abundance was then expressed as the dry weight of epiphytic material scaled to the leaf area.

Canopy Height and Sound Transmission

A separate laboratory experiment was used to investigate the importance of the vertical position of sound transmission relative to the seagrass canopy. For this experiment, freshly collected turtle grass was placed in an outdoor tank filled with seawater from the Gulf of Mexico. Two hydrophones were placed on either side of the seagrass plot, and the same transmission characteristics used in the high-frequency field experiments were implemented here (Figure 4.1). The peak-to-peak amplitude from the direct path of sound transmission was obtained for a total of five vertical positions (0.30, 0.35, 0.40, 0.45 and 0.50 m above the bottom). Shoot length from a random selection of 30 plants was measured following the acoustic experiment.

Statistical Analyses

Differences in the means of the seagrass morphological measurements, derived attenuation coefficients (α) and prey detection threshold calculations for the high-frequency

transmission loss experiments were examined using a 2-way analysis of variance (ANOVA). For each of the parameters, the 2-way ANOVA was used to test for significant differences ($p < 0.05$) in the means of the observations for the main effects of substrate type, season and the interaction of substrate and season. For the low-frequency transmission loss experiments, a linear regression model was fit to the acoustic data. A source level of 150 dB re 1 μPa was used for all low-frequency experiments and the linear regression model applied this source level as the y-intercept. Regression slopes for the bare and vegetated substrate treatments for each frequency were compared using a *z* test ($p < 0.05$) described by Paternoster et al. (1998).

Results

High-Frequency Transmission Loss

High-frequency transmission loss varied between both season and substrate type (Figure 1.2). Significant differences in derived attenuation coefficients (α) were observed for the main effects of substrate type, season and their interaction ($p < 0.01$). Transmission loss varied more in summer (α = 1.24 – 16.5 dB re 1 μPa m^{-1}) than in winter (α = 0.159 – 0.468 dB re 1 μPa m^{-1}), and increased transmission loss was observed in the summer for all substrate types. *Thalassia* consistently attenuated more high-frequency sound energy than *Halodule* regardless of season. Differences in the derived α -values are clearly evident in calculations of the target detection thresholds for a potential prey item, as thresholds significantly ($p < 0.01$) decreased from winter to summer (Table 4.1). Sound transmission was also influenced by the vertical position within the seagrass canopy as laboratory measurements demonstrated that sound transmission increased linearly with increasing distance above the substrate (Figure 4.3).

Low-Frequency Transmission Loss

Low-frequency transmission loss varied for both frequency and substrate type. For all frequencies, there was a significant difference in the rate of attenuation over bare and vegetated substrates ($p < 0.05$). However, the rate of attenuation, as evident in the slope of the regression, was not the same for all frequencies and substrate types (Table 4.2). For 300 Hz and 400 Hz tones, sound was propagated farther in the presence of vegetation. Conversely, the vegetation reduced the propagation distance of the 500 Hz tone. The difference in attenuation rates between bare and vegetated substrate types is most evident in the 300 Hz tone (bare = 6.14 dB re 1 μPa m^{-1}, vegetated = 2.92 dB re 1 μPa m^{-1}) and least evident in the 400 Hz tone (bare = 5.41 dB re 1 μPa m^{-1}, vegetated = 4.42 dB re 1 μPa m^{-1}).

Seagrass Biomass

Morphological characteristics of the seagrass meadows differed markedly between sample dates (Table 4.3). Leaf length, shoot density, and below-ground biomass all increased significantly from February to June in both *Halodule* and *Thalassia* meadows ($p < 0.05$). The increase in leaf length was greater in *Thalassia*, while *Halodule* exhibited a greater increase in shoot density. Overall, shoot density was an order of magnitude greater in *Halodule* beds ($p < 0.01$), but this species contained half as much above- ($p < 0.05$) and below- ($p < 0.05$) ground biomass when compared to *Thalassia*. Epiphyte cover increased significantly ($p < 0.05$) from summer to winter, but did not differ significantly between species.

Discussion

High-Frequency Transmission Loss and Echolocation

Seasonal differences in high-frequency sound propagation were clearly evident during this study. This is not surprising given the significant changes in morphology of the seagrass

meadows between sampling dates. In the *Thalassia* meadow, seagrass leaves doubled in length from February to June. Since the vertical position of the source and receiver remained constant between sampling dates, we believe that leaf length alone describes the seasonal differences observed in sound transmission in the *Thalassia* meadow. During the February sampling, the leaf canopy height, as determined from leaf length measurements, was below the path of acoustic transmission. However in the June sampling event, the leaf canopy height was taller than the height of the hydrophones, which placed leaf tissue directly in the transmission path. The laboratory experiment corroborated the importance of transmission height relative to the height of the seagrass canopy, as sound propagation readily declined with increasing depth into the seagrass canopy.

Although leaf length increased in *Halodule* meadows from winter to summer, the height of the canopy was below the path of acoustic transmission during both sampling events. The lack of leaf tissue between the source and receiver is a likely explanation for why *Thalassia* attenuated more sound energy than *Halodule* during the summer sampling event. Since the leaf canopy was always contained below the path of acoustic transmission, seagrass morphological measurements provide no obvious explanation for the observed seasonal differences in acoustic propagation in the *Halodule* meadow. Since transmission loss in the *Halodule* meadow was significantly greater than the bare substrate, there must be a feature of the meadow, other than leaf morphology, that is serving to attenuate sound energy. Bubbles produced by seagrass meadows during photosynthesis have been shown to scatter and absorb acoustic energy (Hermand et al. 1998; Hermand 2006). It is therefore logical to hypothesize that photosynthetically derived bubbles produced during the summer sampling event served to attenuate more sound energy in the *Halodule* meadow compared to the bare substrate.

Transmission loss measurements clearly demonstrate the functional capacity for seagrass meadows to serve as an acoustic refuge from echolocation (Table 4.1). In this study, the quality of the refuge was highly seasonal with seagrass beds providing very little protection (via acoustic transmission loss) during the winter. However, these seasonal and species-specific differences in refuge quality are likely to differ by location. In tropical regions, seasonal differences are likely reduced due to the continuous growth and replacement of the seagrass canopy. Similarly, it is possible that species-specific differences observed here could change depending on regional characteristics of the health and condition of individual meadows (May-Ku et al. 2010; Creed 1997).

Acoustic modeling studies have consistently demonstrated that the sound propagation characteristics of a seagrass and seawater medium are highly dependent on total biomass (Wilson and Dunton 2008; Wilson et al. 2010). Biomass-dependent sound propagation is also evident in the high-frequency surveys conducted here, as an increase in biomass consistently decreased acoustic propagation across comparisons of both species and season. Numerous studies have demonstrated that climax species of seagrass, such as *Thalassia*, generally contain more standing biomass than pioneer species like *Halodule wrightii* or *Syringodium filiforme* (Iverson and Bittaker 1986; Zieman et al. 1989; Onuf 1996). Therefore, it appears that seagrass meadows consisting of climax plant populations provide a better acoustic refuge than meadows of pioneer seagrass species. As a result, natural or anthropogenic disturbances that replace climax species with colonizing species could also serve to decrease the functional quality of an acoustic refuge.

Acoustic detection of fish targets by marine mammals is influenced by the morphology of the individual fish. As one would expect, larger fish display a greater acoustic target strength than smaller fish (Boswell et al. 2008). The structure and size of a fish's swim bladder also

dictates the acoustic target strength for different fish species (Au et al. 2009). These differing acoustic signatures would therefore promote differential exploitation of an acoustic refuge. For instance, smaller fish and species with an inconspicuous swim bladder could remain hidden within smaller expanses of vegetation. It is also likely that some fish would reach a size threshold when they are no longer acoustically obscured by the seagrass canopy. As a result, the benefits of acoustic protection are more evident for small individuals. This describes a possibly novel characteristic of the nursery function of seagrass meadows.

It is highly unlikely that fish actively choose to live within seagrass meadows because of the acoustic protection provided by the vegetation. Seagrass meadows provide both a food source and visual protection (Kirsch et al. 2002; Heck and Thoman 1981). Since these traits are perceivable by fish, they are undoubtedly the primary qualities influencing habitat choice. It is not yet known if fish prefer to live in a habitat that reduces ambient noise. It is widely accepted, however, that most fish are unable to hear the high-frequencies of sound used in echolocation (Astrup 1999; Ramcharitar et al. 2006). It is therefore entirely possible that fish are completely unaware of the acoustic protection provided by the vegetation. Thus, although the size distributions of fish in seagrass patches may be influenced by the acoustic protection provided by the structure, this is strictly a top-down control mechanism. Nevertheless, acoustic detection and subsequent predation of large fish in small seagrass patches may provide an important ecological control on the distribution of estuarine species.

Low-Frequency Transmission Loss and Passive Acoustic Detection

The unique propagation characteristics of low-frequency energy have important ecological implications. In this study, 300 Hz and 400 Hz tones propagated further in the

presence of vegetation than over a bare substrate. It appears as if the seagrass tissue acted as a resonant structure transmitting these frequencies of energy. In contrast, the 500 Hz tone was inhibited by the presence of the vegetation. For this frequency of energy, it is likely that air contained within the seagrass tissue scattered and absorbed sound energy similar to the observed attenuation of higher frequencies. For fish with lower frequency calls (300 Hz to 400 Hz), such as red drum (*Sciaenops ocellatus*) and Atlantic croaker (*Micropogonias undulatus*), the presence of seagrass enables the transmission of vocalizations. Conversely, for fish such as spotted seatrout (*Cynoscion nebulosus*), higher frequency components of vocalizations (400 Hz to 500 Hz) are possibly inhibited by submerged vegetation. Recent acoustic surveys have documented the abundance of fish vocalizations in nearshore environments (Holt 2008; Luczkovitch et al. 2008). However, fine-scale acoustic investigations have yet to reveal whether these fish are actively choosing specific habitats based on their ability to convey acoustic information.

Since the low-frequency sounds generated by soniferous fish are clearly audible to marine mammals, one might conclude that passive acoustic detection is a viable hunting strategy for marine mammals without the use of echolocation. However, a closer look into the sound pressure level of vocalizations and the low-frequency hearing threshold of marine mammals provides little evidence that passive acoustic detection is an advantageous strategy. For instance, a call generated by Atlantic croaker has a sound pressure level of 114 dB re 1µPa (Barimo and Fine 1998). This sound pressure level is below the detection threshold for low-frequencies of roughly 120 dB re 1µPa exhibited by bottlenose dolphins (Finneran et al. 2001). Spotted seatrout has a vocalization sound pressure level of 139.6 dB re 1µPa and spans a frequency range of 400 Hz to 500 Hz (Ramcharitar et al. 2006; Baltz 2002). Based on our transmission loss measurements, this call should be audible to dolphins hunting in vegetation at a distance of 2.50

m to 4.25 m. This range is well within the detection threshold of 2.82 m to 9.81 m for dolphins using echolocation in vegetated substrates, and therefore demonstrates no measureable advantage associated with the use of passive acoustic detection (Table 4.1).

Seagrass Condition and Refuge Quality

It is important to note that in this study, seagrass meadows did not attenuate more sound energy than bare substrates during the winter sampling event. Specifically for the *Halodule* meadow, the height of the canopy was below the transmission path during both sampling events, but there was a large seasonal difference in sound attenuation. Leaf length and shoot density were both lower in the winter sampling event, but a conspicuous seagrass canopy was still present. This suggests that the condition of the seagrass tissue, and not simply the presence of standing biomass, is an important determinant in acoustic refuge quality. Sound is attenuated in seagrass meadows by the air contained within the lacunae system of the tissue and the bubbles produced during photosynthesis. During winter months, photosynthesis, growth and subsequently bubble formation, decrease (Roberts and Caperon 1986; Kaldy and Dunton 2000; Kowalski et al. 2009). As a result, lack of bubble formation and the inability to repair damaged leaf tissue, likely serve to decrease acoustic scattering and absorption characteristics of seagrass meadows.

The functional quality of an acoustic refuge is likely more sensitive to environmental stressors than a structural refuge. Coastal eutrophication has been implicated in macroalgal growth and phytoplankton blooms, which decrease light availability for seagrasses (Duarte 1995). If light conditions are limited such that seagrasses can persist at a lower growth rate, then the functional quality of a visual refuge is largely unaffected. Conversely, reduced light

availability decreases the rate of primary production, which results in reduced bubble production and tissue regeneration (Roberts and Caperon 1986; Lee and Dunton 1997; Neely 2000). The ultimate consequence of eutrophication and subsequent light reduction is a decline in the functional quality of the acoustic refuge. This example reiterates the idea that the presence of a seagrass canopy does not ensure the function of an acoustic refuge, even during the growing season.

The relative importance of a visual refuge vs. an acoustic refuge warrants further investigation. Field studies using artificial seagrass units (ASU's) report lower species richness and abundance of resident fauna in artificial meadows than in natural meadows under the same environmental conditions (Bell et al. 1997; Lee et al. 2001). ASU's mimic natural seagrasses in leaf shape, shoot density and color, and therefore, provide the same visual refuge as natural meadows. However, ASU's are made from buoyant plastic or nylon strips and do not produce bubbles (Bell et al. 1997; Lee et al. 2001). These artificial substrates are likely acoustically similar to the water column and may not provide acoustic protection to seagrass residents. It is possible that the reported differences in resident fauna between natural and artificial meadows are attributable to the lack of noise reduction in ASU's and subsequent protection from echolocation. As a result, future investigations should examine levels of noise reduction within ASU's to determine the relative importance of an acoustic refuge to a visual refuge.

Conclusion

Marine organisms are known to utilize acoustic information for reproduction, settlement and feeding (Roundtree et al. 2006; Simpson et al. 2000). Estuaries have inherently high rates of primary and secondary production, but these shallow waters are also considered acoustically

complex systems. This study demonstrated how the presence of vegetation alters the transmission of biologically-relevant segments of the acoustic spectrum. Our results suggest that both echolocation and fish communication are influenced by the presence of vegetation, which has important ecological implications. Future research should continue to investigate how complex acoustic environments alter the dissemination of bioacoustic information and how these features impact ecosystem function.

References

Allen, M. C., A. J. Read, J. Gaudet, L. S. Sayigh, 2001. Fine-scale habitat selection of foraging bottlenose dolphins *Tursiops truncates* near Clearwater, Florida. *Mar Ecol Prog Ser*. Vol 222, pp. 253-264.

Astrup, J. 1999. Ultrasound detection in fish – a parallel to the sonar-mediated detection of bats by ultrasound-sensitive insects? *Comparative Biochemistry and Physiology Part A*. Vol. 124, pp. 19-27.

Au, W.W.L., and K.J. Snyder. 1980. Long-range target detection in open waters by an echolocating Atlantic bottlenose dolphin (*Tursiops truncatus*). *J. Acoust. Soc. Am*. Vol. 68, pp. 1077-1084.

Au, W.W.L., D.W. Lemonds, S. Vlachos, P.E. Nachtigall, H.C. Roitblat. 2002. Atlantic bottlenose dolphin hearing threshold for brief broadband signals. *J. Comp. Psychol*. Vol. 116, pp. 151-157.

Au, W.W.L., K.J. Beniot-Bird, R.A. Kastelein. 2007. Modeling the detection range of fish by echolocating bottlenose dolphins and harbor porpoises. *J. Acoust. Soc. Am*. Vol. 121, pp. 3954-3962.

Au, W.W.L. and M.C. Hastings. 2008. Princicples of Marine Bioacoustics. DOI: 10.1007/978-0-387-78365-9_1, Springer Science + Business Media, LLC. New York, NY.

Au, W.W.l., B.K. Brainstetter, K.J. Beniot-Bird, R.A. Kastelein. 2009. Acoustic basis for fish prey discrimination by echolocation dolphins and porpoises. *J. Acoust. Soc. Am.* Vol. 126, pp. 460-467.

Baltz, D. 2002. Spotted seatrout spawning requirements and essential fish habitat: a microhabitat approach using hydrophones. In Listening to Fish: Passive Acoustic Applications in Marine Fisheries (ed. R. Rountree, C. Goudey and T. Hawkins), Cambridge, MA: Massachusetts Institute of Technology. pp. 90-93.

Barimo, J. F. and Fine, M. L. 1998. Relationship of swim-bladder shape to the directionality pattern of underwater sound in the oyster toadfish. *Can. J. Zool.* Vol. 76, pp. 134-143.

Barros, N.B. and R.S. Wells. 1998. Prey and feeding patterns of resident bottlenose dolphins (*Tursiops truncatus*) in Sarasota Bay, Florida. *Journal of Mammalogy*. Vol. 79, pp. 1045-1059.

Bell, J. D., M. Westoby, A.S. Steffe. 1987. Fish larvae settling in seagrass: do they discriminate between beds of different leaf density? J. Exp. Mar. Biol. Ecol. (111) pp. 133-144.

Boswell, K.M., M.D. Keller, J.H. Cowan Jr., C.A. Wilson. 2008. Evaluation of target strength-

fish length equation choices for estimating estuarine fish biomass. *Hydrobiologia*. Vol. 610, pp. 113-123.

Connaughton, M.A., M.L. Fine, M.H. Taylor. 1997. The effects of seasonal hypertrophy and atrophy on fiber morphology, metabolic substrate concentration and sound characteristics of the weakfish sonic muscle. *J. Exp. Biol*. Vol. 200, pp. 2449-2457.

Creed, J.C. 1997. Morphological variation in the seagrass Halodule wrightii near its southern distributional limit. *Aquatic Botanty*. Vol. 59, pp. 163-172.

Duarte, C. M. 1995. Submerged aquatic vegetation in relation to different nutrient regimes. *Ophélia*. Vol. 41, pp. 87-112.

Fine, M.L., J. Shrinil, T.M. Cameron. 2004. The effect of loading on disturbance sounds of the Atlantic croaker *Micropogonias undulatus*: air versus water. *J. Acoust. Soc. Am.* Vol. 116, pp. 1271-1275.

Finneran, J.J., D.A. Carder, S.H. Ridgeway. 2001. Low-frequency acoustic pressure, velocity, and intensity thresholds in a bottlenose dolphin (*Tursiops truncatus*) and white whale (*Delphinapterus leucas*). *J. Acoust. Soc. Am*. Vol. 111, pp. 447-456.

Heck, K.L. and T.A. Thoman. 1981. Experiments on predator-prey interactions in vegetated aquatic habitats. *J. Exp. Mar. Biol. Ecol*. Vol. 53, pp. 125-134.

Hermand, J.P., Nascetti, P., Cinelli, F., 1998. Inversion of acoustic waveguide propagation features to measure oxygen synthesis by Posidonia oceanica: Proceedings of the Oceans ’98 IEEE/OES Conference, Vol. 2, pp. 919–926.

Hermand, J.P. 2006. Continuous acoustic monitoring of physiological and environmental processes in seagrass prairies with focus on photosynthesis. In: Caiti A, Chapman NR, Hermand JP, Jesus S (eds) Acoustic sensing techniques for the shallow water environment: inversion methods and experiments. Springer, Dordrecht, p 183–196.

Holt, S.A. 2008. Distribution of red drum spawning sites identified by a towed hyrdrophone array. *Transactions of the American Fisheries Society*. Vol. 137, pp. 551-561.

Iverson, R. L., and H. F. Bittaker. 1986. Seagrass distribution and abundance in eastern Gulf of Mexico coastal waters. *Estuarine, Coastal and Shelf Science*. Vol. 22, pp. 577-602.

Kaldy, J. E. and K. H. Dunton. 2000. Above- and below-ground production, biomass and reproductive ecology of Thalassia testudinum (turtle grass) in a shallow subtropical coastal lagoon. *Mar. Ecol. Prog. Ser*. Vol. 193, pp. 271-283.

Kirsch, K.D., J.F. Valentine, K.L. Heck. 2002. Parrotfish grazing on turtlegrass *Thalassia testudinum*: evidence for the importance of seagrass consumption in food web dynamics of the Florida Keys National Marine Sanctuary. *Mar. Ecol. Prog. Ser*. Vol. 227, pp. 71-

85.

Komatsu, T., C. Igarashi, K. Tatsukawa, S. Sultana, Y. Matsuoka, and S. Harada, 2003. Use of multi-beam sonar to map seagrass beds in Otsuchi Bay on the Sanriku Coast of Japan," *Aquat. Living resource*, Vol. 16, pp. 223-230.

Kowalski, J. L., H. R. DeYoe, T. C. Allison. 2009. Seasonal production and biomass of the seagrass, *Halodule wrightii* Aschers. (Shoal grass), in a shallow subtropical Texas lagoon. Estuaries and Coasts. Vol. 32, pp. 467-482.

Lee, K. S. and K. H. Dunton. 1997. Effect of *in situ* light reduction on the maintenance, growth and partitioning of carbon sources in *Thalassia testudinum* bank ex König. J. Exp. Mar. Biol. Ecol. Vol. 210, pp. 53-73.

Lee, S.Y., C. W. Fong, R. S. S. Wu. 2001. The effects of seagrass (Zostera japonica) canopy structure on associated fauna: a study using artificial seagrass units and sampling of natural beds. *J. Exp. Mar. Biol. Ecol*. (259) pp. 23-50.

Luczkovitch, J.J., R.C. Pullinger, S.E. Johnson, M.V. Sprague. 2008. Identifying sciaenid critical spawning habitats by the use of passive acoustics. *Transactions of the American Fisheries Society*. Vol. 137, pp. 576-605.

May-Kua, M.A., P.L. Ardisson, U. Ordonez-Lopez. 2010. Morphological variation in Thalassia testudinum in two shallow coastal environments from the southeastern Gulf of Mexico. *Botanica Marina*. Vol. 53, pp. 449-455.

Mulhearn, P.J., 2001. Mapping seabed vegetation with sidescan sonar," DSTO Report No. TN-0381, Defense Science and Technology Organization, Australia.

Neely, M. B. 2000. Somatic, respiratory, and photosynthetic responses of the seagrass *Halodule wrightii* to light reduction in Tampa Bay, Florida including a whole plant carbon budget. Seagrasses: Monitoring, ecology, physiology, and management. pp. 33-48.

Nowacek, D.P. 2005. Acoustic ecology of foraging bottlenose dolphins (*Tursiops truncatus*), habitat-specific use of three sound types. *Marine Mammal Science*. Vol. 24, pp. 587-602.

Onuf, C. P. 1996. Biomass patterns of seagrass meadows of the Laguna Madre, Texas. *Bulletin of Marine Science*. Vol. 58, pp. 404-420.

Paternoster, R. R. Brame, P. Mazerolle, A. Piquero. 1998. Using the correct statistical test for the equality of regression coefficients. *Criminology*. Vol. 36, pp. 859-866.

Pasqualini, V., P. Clabaut, G. Pergent, L. Benyoussef, and C. Pergent-Martini, 2000. Contribution of side scan sonar to the management of Mediterranean littoral ecosystems. *Int. J. Remote Sens*., Vol. 21, pp. 367-378.

Roberts, D. G., J. Caperon. 1986. Lacunar gas discharge as a measure of photosynthesis in seagrasses. *Mar. Ecol. Prog. Ser*. Vol. 29, pp. 23-27.

Quintana-Rizzo, E., D. Mann, R. Wells, 2006. Estimated communication range of social sounds used by bottlenose dolphins (*Tursiops truncatus*). *J. Acoust. Soc. Am*., Vol. 120, pp. 1671 1673.

Ramcharitar, J., D.P. Gannon, A.N. Popper. 2006. Bioacoustics of the fishes of the Family Scianidae (croakers and drums). *Transactions of the American Fisheries Society*. Vol. 135, pp. 1409-1431.

Roundtree, R.A., R.G. Gilmore, C.A. Goudey, A.D. Hawkins, J.J. Luczkovitch, D.A. Mann. 2006. Listening to fish: applications of passive acoustics to fisheries science. *Fisheries*. Vol. 31, pp. 433-446.

Wilson, P.S. and K. Dunton, 2008. Laboratory investigation of the acoustic response of seagrass tissue in the frequency band of 0.5-2.5 kHz. *J. Acoust. Soc. Am*., Vol. 125, pp. 1951-1959.

Wilson, C.J., P.S. Wilson, C.A. Greene, and K.H. Dunton. 2010. Seagrass leaves in 3-D: Using computed tomography and low-frequency acoustics to investigate the material properties of seagrass tissue. *Journal of Experimental Marine Biology and Ecology*. Vol 35 pp. 128-134.

Zieman, J. C., J. W. Fourqurean, R. L. Iverson. 1989. Distribution, abundance and productivity of seagrasses and macroalgae in Florida Bay. *Bulletin of Marine Science*. Vol. 44(1), pp. 292-311.

Figure 4.1.

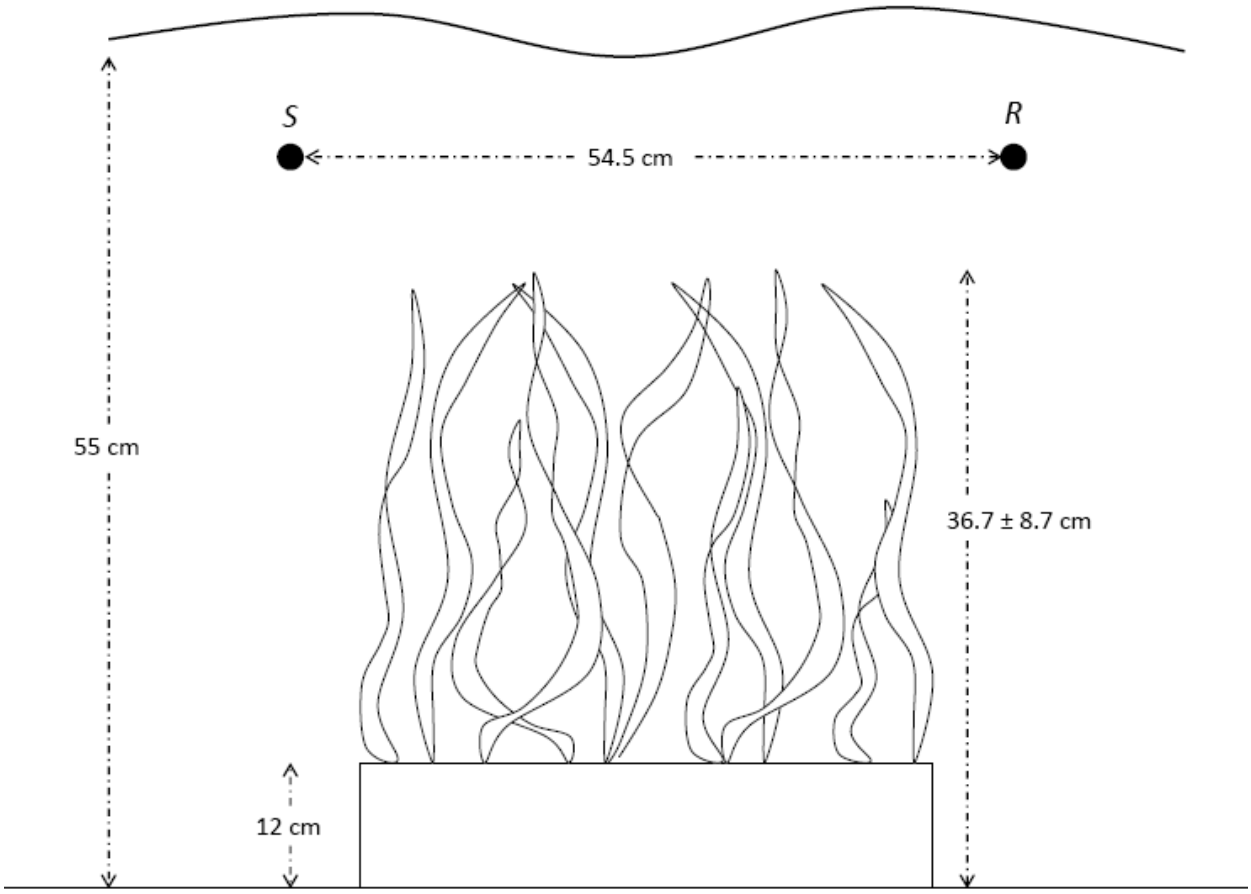

Figure 4.1. Configuration of the laboratory experiment measuring the importance of vertical positioning and sound transmission. The separation distance of the sound source (S) and receiver (R) remained constant for each of the five vertical positions (30, 35, 40 ,45 and 50 cm above the bottom). Vegetation height above the bottom represents the average ± standard deviation obtained from the leaf length (n = 30) and sediment box height.

Figure 4.2a.

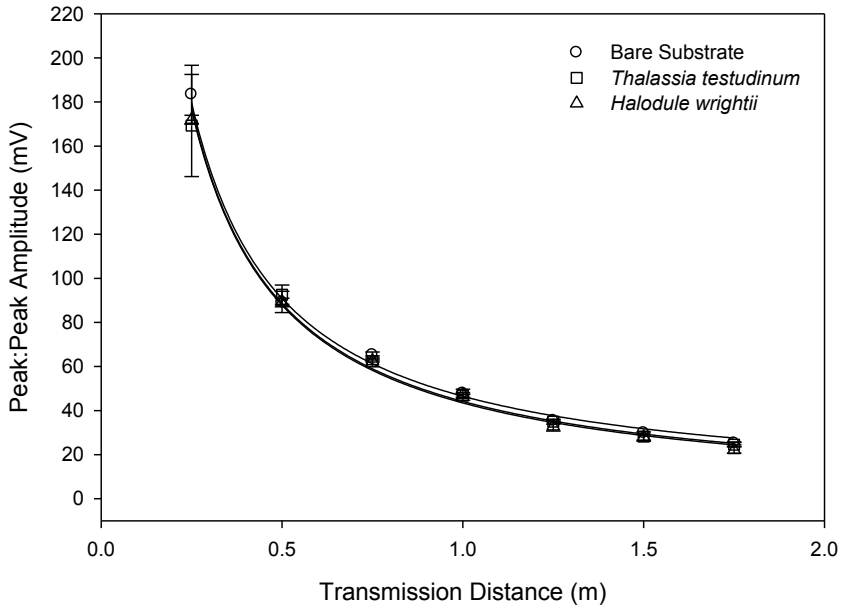

Figure 4.2b.

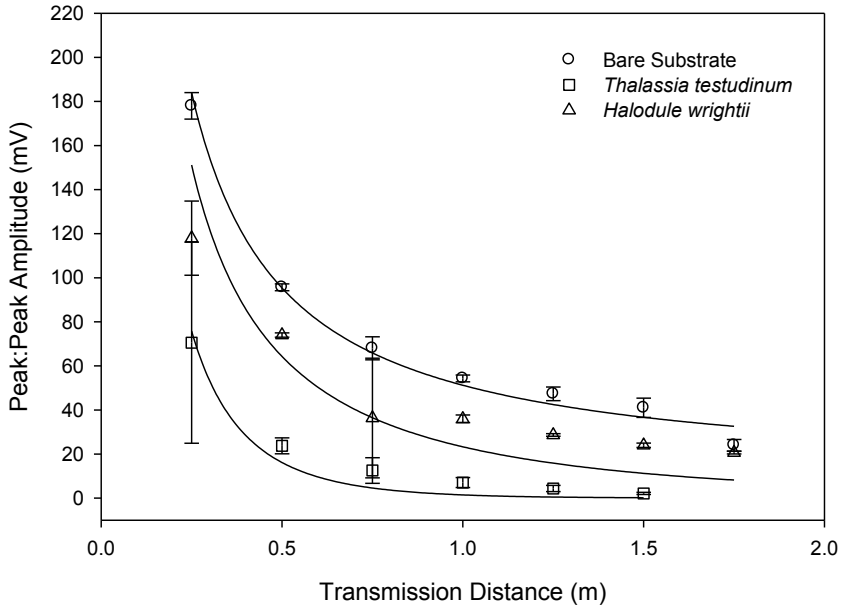

Figure 4.2. Observed peak-to-peak acoustic pressure as a function of transmission distance for the a) February and b) June high-frequency transmission loss experiments. Values of acoustic pressure represent the mean ± standard deviation of three replicate transmission paths. The data for each treatment were fitted with a spherical attenuation model (Eq. 2).

Figure 4.3.

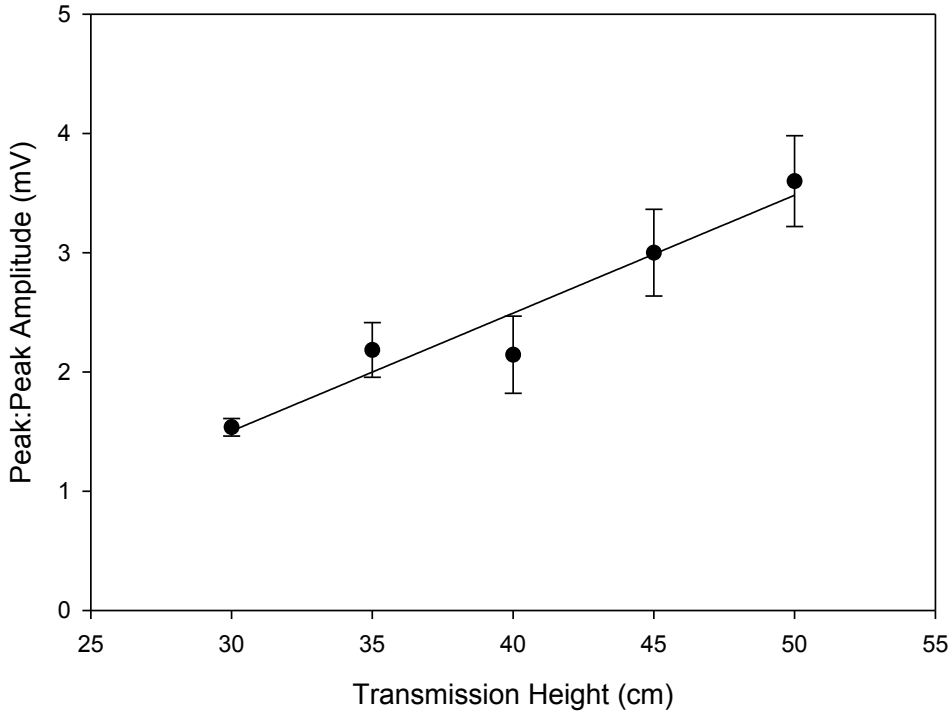

Figure 4.3. Measured peak-to-peak acoustic pressure as a function of transmission height above the tank bottom for the high-frequency laboratory experiment. Points represent the mean and standard deviation of 10 replicate acoustic measurements taken at each height ($r^2 = 0.93$; slope = 0.10; $p < 0.01$).

Figure 4.4a.

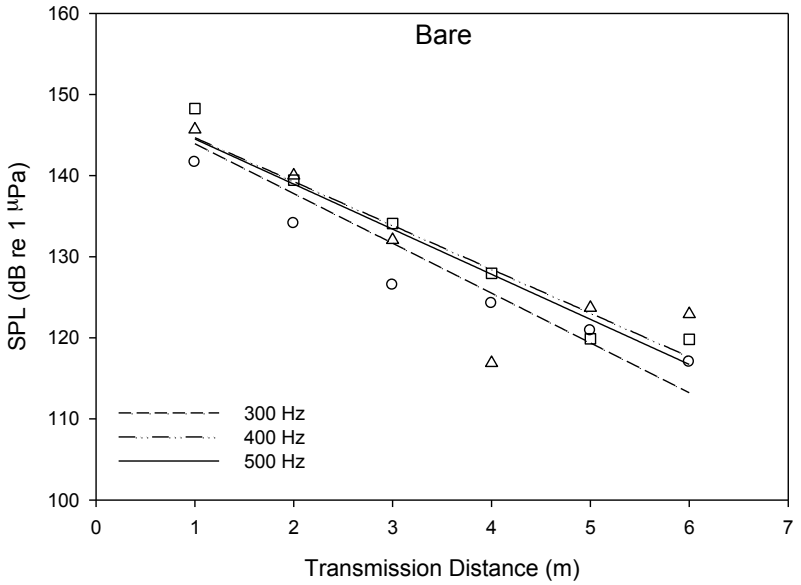

Figure 4.4b.

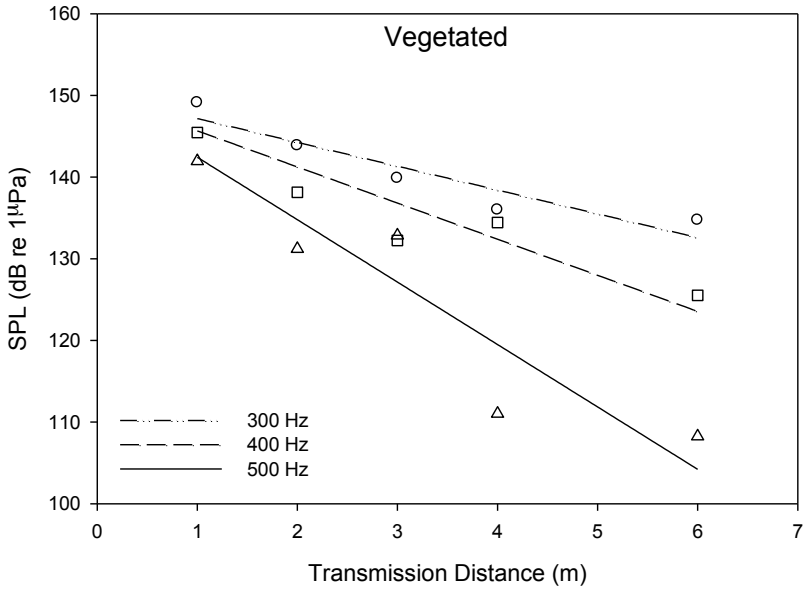

Figure 4.4. Sound pressure levels obtained for the low-frequency transmission loss experiments in a) bare and b) vegetated substrates. Sound pressure levels represent the root-mean-square average of 64 recorded waveforms. A linear model forced through the y-intercept of 150 dB re 1 µPa was fit to data for each substrate type , which represents the source level of the underwater speaker.

Figure 4.5a.

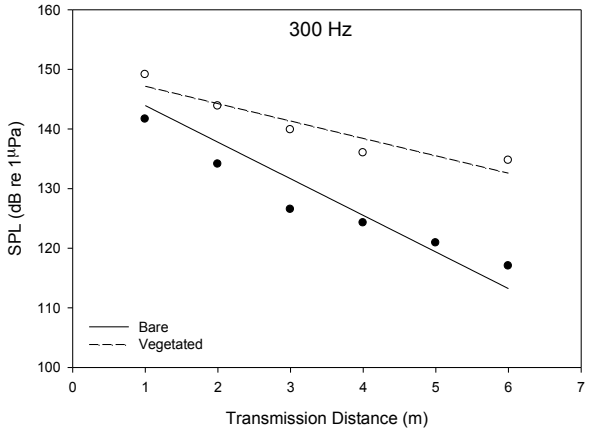

Figure 4.5b.

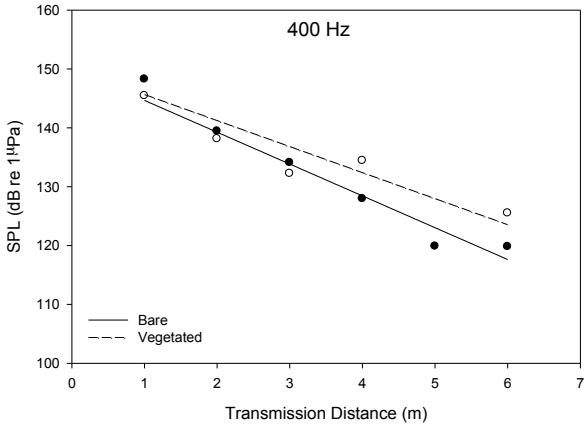

Figure 4.5c.

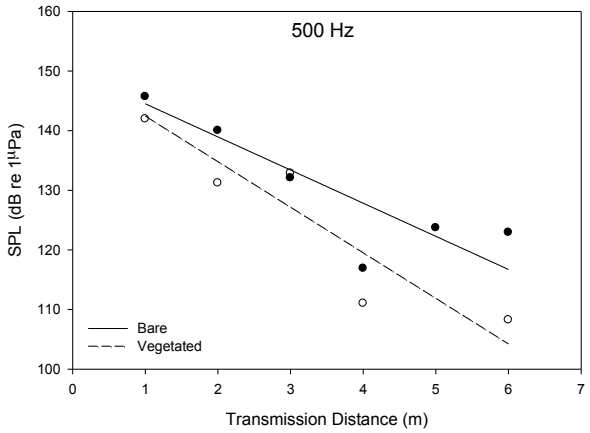

Figure 4.5. Sound pressure levels obtained for the low-frequency transmission loss experiments for a) 300 Hz, b) 400 Hz and c) 500 Hz tones. Sound pressure levels for the vegetated (empty circles) and bare (filled circles) substrates represent the root-mean-square average of 64 recorded waveforms. Data for each substrate type was fit to a linear regression model forced through the y-intercept of 150 dB re 1 μPa, which represents the source level of the underwater speaker.

Table 4.1. The detection threshold was calculated using the equation $EE = SE - 2TL + TS_E$, where *EE* is the energy flux detection threshold, *SE* is the source energy flux density, *TL* is the transmission loss and TS_E is the target strength (derived from Au et al. 2007). Previously obtained values for *EE* (33.1 dB; Au et al. 2002), *SE* (167 dB; Au et al. 1980) and TS_E (-24 dB for a 17 cm mullet; Au et al. 2007) were all used in the detection threshold calculation. All values in the table represent mean ± s.d. (n=3).

	Bare		***Halodule***		***Thalassia***	
	February	June	February	June	February	June
α (dB m^{-1})*	0.47 ± 0.31	1.24 ± 0.37	0.16 ± 0.19	3.78 ± 1.21	0.34 ± 0.12	16.5 ± 2.56
Detection Threshold (m)	60.4 ± 50.1	23.45 ± 5.49	161 ± 115	9.81 ± 2.26	61.1 ± 17.1	2.82 ± 0.341

	2-way Anova		
	Species	Season	Interaction
α (dB m^{-1})*	$p < .01$	$p < .01$	$p < .01$
Detection Threshold (m)	n.s.	$p < 0.01$	n.s.

Table 4.2. Results of the linear regression models for the low-frequency transmission loss experiments. Results of the *z* test represent statistical comparisons of the slopes for the bare and vegetated substrate combinations for each frequency. Statistical significance is represented at both the (* ; $p < 0.01$) and (+ ; $p < 0.05$) level for each comparison.

	300 Hz		**400 Hz**		**500 Hz**	
	Bare	*Vegetated*	*Bare*	*Vegetated*	*Bare*	*Vegetated*
Slope	-6.14	-2.92	-5.41	-4.42	-5.56	-7.64
r^2	0.84	0.88	0.96	0.82	0.74	0.85
z	7.45^{*}		2.42^{+}		2.44^{+}	

Table 4.3. Measurements of seagrass morphology for *Halodule wrightii* and *Thalassia testudinum*. Values represent mean ± s.d. (n = 3 for epiphyte cover, shoot density, above and below-ground biomass; n = 30 for leaf length).

	Halodule		***Thalassia***		***2-Way ANOVA***		
	February	June	February	June	Species	Season	Int.
Leaf Length (cm)	12.5 ± 3.8	13.4 ± 4.9	15.0 ± 5.3	30.7 ± 12.2	$p < 0.01$	$p < 0.01$	$p < 0.01$
Epiphyte Cover (mg DW m^{-2})	7.15 ± 7.37	1.15 ± 0.36	7.59 ± 0.68	1.45 ± 0.70	*n.s.*	$p < 0.05$	*n.s.*
Shoot Density (Shoots m^{-2})	7179 ± 117	12729 ± 304	849.0 ± 86.5	1038 ± 218.0	$p < 0.01$	$p < 0.01$	$p < 0.01$
Above-Ground Biomass (g DW m^{-2})	77.40 ± 3.73	169.9 ± 38.89	244.0 ± 20.82	417.4 ± 129.9	$p < 0.05$	*n.s.*	*n.s.*
Below-Ground Biomass (g DW m^{-2})	270.5 ± 11.77	666.5 ± 96.20	563.7 ± 127.1	1021.6 ± 224.9	$p < 0.05$	$p < 0.05$	*n.s.*

Bibliography

Allen, M. C., A. J. Read, J. Gaudet, L. S. Sayigh, 2001. Fine-scale habitat selection of foraging bottlenose dolphins *Tursiops truncates* near Clearwater, Florida. *Mar Ecol Prog Ser*. Vol 222, pp. 253-264.

Abramoff, M.D., Magalhaes, P.J., Ram, S.J. "Image Processing with ImageJ". Biophotonics International, volume 11, issue 7, pp. 36-42, 2004.

Astrup, J. 1999. Ultrasound detection in fish – a parallel to the sonar-mediated detection of bats by ultrasound-sensitive insects? *Comparative Biochemistry and Physiology Part A*. Vol. 124, pp. 19-27.

Au, W.W.L., and K.J. Snyder. 1980. Long-range target detection in open waters by an echolocating Atlantic bottlenose dolphin (*Tursiops truncatus*). *J. Acoust. Soc. Am*. Vol. 68, pp. 1077-1084.

Au, W.W.L., D.W. Lemonds, S. Vlachos, P.E. Nachtigall, H.C. Roitblat. 2002. Atlantic bottlenose dolphin hearing threshold for brief broadband signals. *J. Comp. Psychol*. Vol. 116, pp. 151-157.

Au, W.W.L., K.J. Beniot-Bird, R.A. Kastelein. 2007. Modeling the detection range of fish by echolocating bottlenose dolphins and harbor porpoises. *J. Acoust. Soc. Am*. Vol. 121, pp. 3954-3962.

Au, W.W.L. and M.C. Hastings. 2008. Princicples of Marine Bioacoustics. DOI: 10.1007/978-0-387-78365-9_1, Springer Science + Business Media, LLC. New York, NY.

Au, W.W.l., B.K. Brainstetter, K.J. Beniot-Bird, R.A. Kastelein. 2009. Acoustic basis for fish prey discrimination by echolocation dolphins and porpoises. *J. Acoust. Soc. Am.* Vol. 126, pp. 460-467.

Baltz, D. 2002. Spotted seatrout spawning requirements and essential fish habitat: a microhabitat approach using hydrophones. In Listening to Fish: Passive Acoustic Applications in Marine Fisheries (ed. R. Rountree, C. Goudey and T. Hawkins), Cambridge, MA: Massachusetts Institute of Technology. pp. 90-93.

Barimo, J. F. and Fine, M. L. 1998. Relationship of swim-bladder shape to the directionality pattern of underwater sound in the oyster toadfish. *Can. J. Zool.* Vol. 76, pp. 134-143.

Barros, N.B. and R.S. Wells. 1998. Prey and feeding patterns of resident bottlenose

dolphins (*Tursiops truncatus*) in Sarasota Bay, Florida. *Journal of Mammalogy*. Vol. 79, pp. 1045-1059.

Bell, J. D., M. Westoby, A.S. Steffe. 1987. Fish larvae settling in seagrass: do they discriminate between beds of different leaf density? J. Exp. Mar. Biol. Ecol. (111) pp. 133-144.

Boswell, K.M., M.D. Keller, J.H. Cowan Jr., C.A. Wilson. 2008. Evaluation of target strength-fish length equation choices for estimating estuarine fish biomass. *Hydrobiologia*. Vol.610, pp. 113-123.

Britton-Simmons, K., J.E. Eckman, D.O. Duggins. 2008. Effects of tidal currents and tidal stage on estimates of bed size in the kelp *Nereocystis luetkeana*. *Mar Eco Prog Ser*. Vol. 355, pp. 95-105.

Caffrey, J.M. and W. M. Kemp, 1991. Seasonal and spatial patterns of oxygen production, respiration and root rhizome release in *Potamogeton perfoliatus* L. and *Zostera marina* L. *Aquat. Bot*., Vol. 40, pp. 109-128.

Cavanaugh, K.C., D.A. Siegel, B.P. Kinlan, D.C. Reed. 2010. Scaling giant kelp field measurements to regional scales using satellite observations. *Mar Eco Prog Ser.* Vol. 403, pp. 13-27.

Connaughton, M.A., M.L. Fine, M.H. Taylor. 1997. The effects of seasonal hypertrophy and atrophy on fiber morphology, metabolic substrate concentration and sound characteristics of the weakfish sonic muscle. *J. Exp. Biol*. Vol. 200, pp. 2449-2457.

Creed, J.C. 1997. Morphological variation in the seagrass Halodule wrightii near its southern distributional limit. *Aquatic Botanty*. Vol. 59, pp. 163-172.

Dacey, J. W. H. 1981. Pressurized ventilation in the yellow waterlily. *Ecology*. Vol. 62, pp. 1137-1147.

Daysher, L.E. 1993. Evaluation of remote sensing techniques for monitoring giant kelp populations. *Hydobiologia*. Vol. 260/261, pp. 307-312.

Dayton, P.K. 1985. Ecology of kelp communities. Ann. Rev. Ecol. Syst. Vol. 16, pp. 215-245.

Duarte, C. M. 1995. Submerged aquatic vegetation in relation to different nutrient regimes. *Ophélia*. Vol. 41, pp. 87-112.

Duarte, C.M., 2002. The future of seagrass meadows. Environ. Conserv., Vol. 29, pp. 192–206.

Dunton, K.H., Tomasko, D.A., 1994. In situ photosynthesis in the seagrass *Halodule wrightii* in a hypersaline subtropical lagoon. *Mar. Ecol. Prog. Ser*. 107, 281–293.

Ferwerda, J.G., J. de Leeuw, C. Atzberger, and Z. Vekerdy, 2007. Satellite-based monitoring of tropical seagrass vegetation: current techniques and future developments. *Hydrobiologia*, Vol. 591, pp. 59–71.

Fine, M.L., J. Shrinil, T.M. Cameron. 2004. The effect of loading on disturbance sounds of the Atlantic croaker *Micropogonias undulatus*: air versus water. *J. Acoust. Soc. Am.* Vol.116, pp. 1271-1275.

Finneran, J.J., D.A. Carder, S.H. Ridgeway. 2001. Low-frequency acoustic pressure, velocity, and intensity thresholds in a bottlenose dolphin (*Tursiops truncatus*) and white whale (*Delphinapterus leucas*). *J. Acoust. Soc. Am*. Vol. 111, pp. 447-456.

Fletcher, R.S., W. Pulich Jr., and B. Hardegree, 2009. A semiautomated approach for monitoring landscape changes in Texas seagrass beds from aerial photography. *J. Coast. Res*., Vol. 25, pp. 500–506.

Fonseca, M.S. and J. A. Cahalan, 1992. A preliminary evaluation of wave attenuation by 4 species of seagrass. *Est. Coastal Shelf Sci*., Vol. 35, pp. 565–576.

Fourqurean, J.W. and J.C. Zieman. (1991). Photosynthesis, respiration and whole plant carbon budget of the seagrass *Thalassia testudinum*. *Mar. Ecol. Prog. Ser*. 69: 161-170.

Harley, C.D.G., A.R. Hughes, K.M. Hultgren, B.G. Miner, C.J.B. Thornber, L.F. Rodriguez, L. Tomanek, S.L. Williams. 2006. The impacts of climate change in coastal marine systems. *Ecology Letters*. Vol. 9, pp. 228-241.

Heck, K.L. and T.A. Thoman. 1981. Experiments on predator-prey interactions in vegetated aquatic habitats. *J. Exp. Mar. Biol. Ecol*. Vol. 53, pp. 125-134.

Heck, K.L. and T. A. Thoman, 1984. The nursery role of seagrass meadows in the upper and lower reaches of the Chesapeake Bay. *Estuaries*, Vol. 7, pp. 70–92.

Hermand, J.P., Nascetti, P., Cinelli, F., 1998. Inversion of acoustic waveguide propagation features to measure oxygen synthesis by Posidonia oceanica: Proceedings of the Oceans ’98 IEEE/OES Conference, Vol. 2, pp. 919–926.

Hermand, J.P. 2006. Continuous acoustic monitoring of physiological and environmental processes in seagrass prairies with focus on photosynthesis. In: Caiti A, Chapman NR, Hermand JP, Jesus S (eds) Acoustic sensing techniques for the shallow water environment: inversion methods and experiments. Springer, Dordrecht, p 183–196.

Holt, S.A. 2008. Distribution of red drum spawning sites identified by a towed hyrdrophone array. *Transactions of the American Fisheries Society*. Vol. 137, pp. 551-561.

Iverson, R. L., and H. F. Bittaker. 1986. Seagrass distribution and abundance in eastern Gulf of Mexico coastal waters. *Estuarine, Coastal and Shelf Science*. Vol. 22, pp. 577-602.

Jassby, A.D. and T. Platt. (1976). Mathematical formulation of the relationship between photosynthesis and light for phytoplankton. *Limnol. Oceanogr*. 21: 540-547.

Kaldy, J. E. and K. H. Dunton. 2000. Above- and below-ground production, biomass and reproductive ecology of Thalassia testudinum (turtle grass) in a shallow subtropical coastal lagoon. *Mar. Ecol. Prog. Ser*. Vol. 193, pp. 271-283.

Kemp, W.M. and L. Murray, 1986. Oxygen release from roots of the submersed macrophyte *Potamogeton perfoliatus* L.: Regulating factors and ecological implications. *Aquat. Bot*., Vol. 26, pp. 271–283.

Kinsler, L.E., Frey, A.R., Coppens, A.B., Sanders, J.V., 2000. Fundamentals of acoustics. Wiley, New York

Kirsch, K.D., J.F. Valentine, K.L. Heck. 2002. Parrotfish grazing on turtlegrass *Thalassia testudinum*: evidence for the importance of seagrass consumption in food web dynamics of the Florida Keys National Marine Sanctuary. *Mar. Ecol. Prog. Ser*. Vol. 227, pp. 71-85.

Komatsu, T., C. Igarashi, K. Tatsukawa, S. Sultana, Y. Matsuoka, and S. Harada, 2003. Use of multi-beam sonar to map seagrass beds in Otsuchi Bay on the Sanriku Coast of Japan,"*Aquat. Living resource*, Vol. 16, pp. 223-230.

Kowalski, J. L., H. R. DeYoe, T. C. Allison. 2009. Seasonal production and biomass of the seagrass, *Halodule wrightii* Aschers. (Shoal grass), in a shallow subtropical Texas lagoon. Estuaries and Coasts. Vol. 32, pp. 467-482.

Kutser, T., E. Vahtmae, C.M. Roelfsema, and L. Metsamaa, 2007. Photo-library method for mapping seagrass biomass. *Est. Coastal Shelf Sci*., Vol. 75, pp. 559–563.

Lafleur, L. D. and Shields, F. D., 1995. Low-frequency propagation modes in a liquid-filled elastic tube waveguide. *J. Acoust. Soc. Am.*, Vol. 97, pp. 1435–1445.

Lee, K. S. and K. H. Dunton. 1997. Effect of *in situ* light reduction on the maintenance, growth and partitioning of carbon sources in *Thalassia testudinum* bank ex König. J. Exp. Mar. Biol. Ecol. Vol. 210, pp. 53-73.

Lee, S.Y., C. W. Fong, R. S. S. Wu. 2001. The effects of seagrass (Zostera japonica)

canopy structure on associated fauna: a study using artificial seagrass units and sampling of natural beds. *J. Exp. Mar. Biol. Ecol*. (259) pp. 23-50.

Luczkovitch, J.J., R.C. Pullinger, S.E. Johnson, M.V. Sprague. 2008. Identifying sciaenid critical spawning habitats by the use of passive acoustics. *Transactions of the American Fisheries Society*. Vol. 137, pp. 576-605.

Major, K. M., K. H. Dunton. 2000. Photosynthetic performance in *Syringodium filiforme*: seasonal variation in light-harvesting characteristics. *Aquat. Bot*. Vol. 68, pp. 249-264.

May-Kua, M.A., P.L. Ardisson, U. Ordonez-Lopez. 2010. Morphological variation in *Thalassia testudinum* in two shallow coastal environments from the southeastern Gulf of Mexico. *Botanica Marina*. Vol. 53, pp. 449-455.

McCarthy, E.M. and B. Sabol, "Acoustic characterization of submerged aquatic vegetation: Military and environmental monitoring applications. *Proceedings of OCEANS 2000 MTS/IEEE Conference and Exhibition*, Vol. 3, pp. 1957–1961.

Medwin, H. 1977. Acoustical determinations of bubble-size spectra. *J. Acoust. Soc. Am*. Vol. 62, pp. 1041-1044.

Meleder, V., J. Populus, B. Guillamont, T. Perrot, P. Mouquet, 2010. Predictive modeling of 21 seabed habitats: case study of subtidal kelp forests on the coast of Brittany, France. *Mar Biol*. Vol. 157, pp. 1525-1541.

Mulhearn, P.J., 2001. Mapping seabed vegetation with sidescan sonar," DSTO Report No. TN-0381, Defense Science and Technology Organization, Australia.

Neely, M. B. 2000. Somatic, respiratory, and photosynthetic responses of the seagrass *Halodule wrightii* to light reduction in Tampa Bay, Florida including a whole plant carbon budget. Seagrasses: Monitoring, ecology, physiology, and management. pp. 33-48.

Nowacek, D.P. 2005. Acoustic ecology of foraging bottlenose dolphins (*Tursiops truncatus*), habitat-specific use of three sound types. *Marine Mammal Science*. Vol. 24, pp. 587-602.

Olesen, B., N. Marba, C. M. Duarte, 2004. Recolonization dynamics in a mixed seagrass meadow: The role of clonal versus sexual processes. *Estuaries*, Vol. 27, pp. 770-780.

Onuf, C. P. 1996. Biomass patterns of seagrass meadows of the Laguna Madre, Texas. *Bulletin of Marine Science*. Vol. 58, pp. 404-420.

Pasqualini, V., P. Clabaut, G. Pergent, L. Benyoussef, and C. Pergent-Martini, 2000.

Contribution of side scan sonar to the management of Mediterranean littoral ecosystems. *Int. J. Remote Sens*., Vol. 21, pp. 367-378.

Paternoster, R. R. Brame, P. Mazerolle, A. Piquero. 1998. Using the correct statistical test for the equality of regression coefficients. *Criminology*. Vol. 36, pp. 859-866.

Paul, M., A. Lefebvre, E. Manca, C.L. Amos. 2011. An Acoustic method for the remote measurement of seagrass metrics. *Estuarine, Coastal and Shelf Science*. Vol. 93, pp. 68-79.

Phillips, R.C. and E. G. Menez, 1988. Seagrasses . Smithsonian Institution Press, Washington, DC.

Povey, M. J. W., 1997. Ultrasonic Techniques for Fluids Characterization. Academic Press,London.

Riegl, B.M., R. P. Moyer, L. J. Morris, R. W. Virnstein, S. J. Purkis, 2005. Distribution and seasonal biomass of drift macroalgae in the Indian River Lagoon (Florida, USA) estimated with acoustic seafloor classification (QTCview, Echoplus). *J. Exp. Mar. Biol. Ecol*. Vol 326, pp. 89-104.

Roberts, D. G., J. Caperon. 1986. Lacunar gas discharge as a measure of photosynthesis in seagrasses. *Mar. Ecol. Prog. Ser*. Vol. 29, pp. 23-27.

Short, F.T. and H.A. Neckles, 1999. The effects of global climate change on seagrasses. *Aquat. Bot*., Vol. 63, pp. 169–196.

Quintana-Rizzo, E., D. Mann, R. Wells, 2006. Estimated communication range of social sounds used by bottlenose dolphins (*Tursiops truncatus*). *J. Acoust. Soc. Am*., Vol. 120, pp. 1671-1673.

Quintino, V., R. Freitas, R. Mamede, F. Ricardo, A. M. Rodrigues, J. Mota, A. Perez-Ruzafa, C. Marcos, 2009. Remote sensing of underwater vegetation using single-beam acoustics. *ICES Journal of Marine Science*. Vol. 67, pp. 594-605.

Ramcharitar, J., D.P. Gannon, A.N. Popper. 2006. Bioacoustics of the fishes of the Family Scianidae (croakers and drums). *Transactions of the American Fisheries Society*. Vol.135, pp. 1409-1431.

Roundtree, R.A., R.G. Gilmore, C.A. Goudey, A.D. Hawkins, J.J. Luczkovitch, D.A. Mann. 2006. Listening to fish: applications of passive acoustics to fisheries science. *Fisheries*.Vol. 31, pp. 433-446.

Schuette, J. L., M. J. Klug. 1995. Evidence for mass flow in flowering individuals of the submersed vascular plant *Myriphyllum heterophyllum*. *Plant Physiol*. Vol. 108, pp. 1251-1258.

Silva, J., Y. Sharon, R. Santos, S. Beer, 2009. Measuring seagrass photosynthesis: methods and applications. *Aquat Biol*. Vol. 7, pp. 127-141.

Stekoll, M.S., L.E. Deysher, M. Hess, 2006. A remote sensing approach to estimating harvestable kelp biomass. *Journal of Applied Phycology*. Vol. 18, pp. 323-334.

Warren, J. D., B. J. Peterson. 2007. Use of a 600-kHz Acoustic Doppler Current Profiler to measure estuarine bottom type, relative abundance of submerged aquatic vegetation, and eelgrass canopy height. *Estuarine, Coastal and Shelf Science*. Vol. 72, pp. 53-62.

Wilson, P.S. and K. Dunton, 2008. Laboratory investigation of the acoustic response of seagrass tissue in the frequency band of 0.5-2.5 kHz. *J. Acoust. Soc. Am*., Vol. 125, pp. 1951-1959.

Wilson, C.J., P.S. Wilson, C.A. Greene, and K.H. Dunton. 2010. Seagrass leaves in 3-D: Using computed tomography and low-frequency acoustics to investigate the material properties of seagrass tissue. *Journal of Experimental Marine Biology and Ecology*. Vol 35 pp.128-134.

Wood, A. B., 1930. A Textbook of Sound. Macmillan, New York, first edition.

Zieman, J. C., J. W. Fourqurean, R. L. Iverson. 1989. Distribution, abundance and productivity of seagrasses and macroalgae in Florida Bay. *Bulletin of Marine Science*. Vol. 44(1), pp. 292-311.